Tactile Perception:
Role of Friction and Texture

Lisa Skedung

KTH Royal Institute of Technology
School of Chemical Science and Engineering
Division of Surface and Corrosion Science

Stockholm 2012

Tactile Perception: Role of Friction and Texture
Lisa Skedung (skedung@kth.se)
Doctoral Thesis

Cover illustration: Schematic 3D image showing the human interaction with a stimulus (commissioned from Fredrik Dahlström, i3D).

Abstract

Tactile perception is considered an important contributor to the overall consumer experience of a product. However, what physical properties that create the specifics of tactile perception, are still not completely understood. This thesis has researched how many dimensions that are required to differentiate the surfaces perceptually, and then tried to explain these dimensions in terms of physical properties, by interconnecting human perception measurements with various physical measurements. The tactile perception was assessed by multidimensional scaling or magnitude estimation, in which methods human participants assign numbers to how similar pairs of surfaces are perceived or to the relative quantity of a specified perceptual attribute, such as softness, smoothness, coarseness and coolness. The role of friction and surface texture in tactile perception was investigated in particular detail, because typically tactile exploration involves moving (at least) one finger over a textured surface. A tactile approach for measuring friction was developed by means of moving a finger over the surfaces, mounted on a force sensor. The contribution of finger friction to tactile perception was investigated for surfaces of printing papers and tissue papers, as well as for model surfaces with controlled topography. The overarching research goal of this thesis was to study, systematically, the role of texture in tactile perception of surfaces.

The model surfaces displayed a sinusoidal texture with a characteristic wavelength and amplitude, fabricated by surface wrinkling and replica molding techniques. A library of surfaces was manufactured, ranging in wavelengths from 270 nm up to 100 μm and in amplitudes from 7 nm up to 6 μm. These surfaces were rigid and cleanable and could therefore be reused among the participants. To my knowledge, this is the first time in a psychophysical experiment, that the surface texture has been controlled over several orders of magnitude in length scale, without simultaneously changing other material properties of the stimuli.

The finger friction coefficient was found to decrease with increasing aspect ratio (amplitude/wavelength) of the model surfaces and also with increasing average surface roughness of the printing papers. Analytical modeling of the finger's interaction with the model surfaces shows how the friction coefficient increases with the real contact area, and that the friction mechanism is the same on both the nanoscale and microscale. The same interaction mechanism also explains the friction characteristics of tissue paper. Furthermore, it was found that the perceptions of smoothness, coarseness, coolness and dryness are satisfactorily related to the real contact area at the finger-surface interface.

It is shown that it is possible to discern perceptually among both printing papers and tissue papers, and this differentiation is based on either two or three underlying dimensions. Rough/smooth and thin/thick were the two main dimensions of surface feel found for the printing papers, whereas friction and wavelength were strongly related to the perceptual cues employed in scaling the model surfaces. These experimental results support the *duplex theory of texture perception*, which holds that both a "spatial sense"; used to discriminate the roughest textures from the others, and a "vibration sense"; used to discriminate among the smoother textures, are involved. The perception of what is considered rough and smooth depends on the experimental stimulus context. It is concluded that friction is important for human differentiation of surface textures below about 10 μm in surface roughness, and for larger surface textures, friction is less important or can even be neglected.

The finger friction experiments also allowed the following conclusions to be drawn: (i) The interindividual variation in friction coefficients is too large to allow direct comparison; however, the trends in relative friction coefficients for a group of participants are the same. (ii) Lipids are transferred to the test surface of study, and this lowers the friction. (iii) Many of the studies point to a characteristic frequency during sliding of about 30 Hz, which is both characteristic of the resonance frequency of skin and the expected frequency associated with the fingerprints. (iv) The applied load in surface interrogation is in fact regulated in response to the friction force.

The limits in tactile perception were indirectly researched by similarity scaling experiments on the model surfaces. Wrinkle wavelengths of 760 nm and 870 nm could be discriminated from untextured reference surfaces, whereas 270 nm could not. The amplitude of the wrinkles so discriminated was approximately 10 nm, suggesting that nanotechnology may well have a role to play in haptics and tactile perception.

**Ke*ywords:* *human skin, tactile friction, finger friction, skin friction, skin tribology, biotribology, tactile perception, haptic perception, psychophysics, haptics, surface roughness, surface texture, contact area, nanostructure, model surfaces, surface wrinkling, printing paper, tissue paper, magnitude estimation, multidimensional scaling, tactile threshold, psychophysical relations, smoothness, coolness, coarseness, softness, force sensor, skin lipids, topical formulations, skin creams.*

Sammanfattning

Taktil perception bidrar starkt till den sammantagna upplevelsen av en produkt, men hur materials olika ytegenskaper påverkar och styr perceptionen är ännu inte helt klart. Den här avhandlingen undersöker hur många och vilka egenskaper som är viktiga när känslan mellan två ytor jämförs. Tillvägagångssättet är tvärvetenskapligt där fysikaliska mätningar kopplas ihop med perceptions mätningar där människor används som instrument. Två typer av perceptionsförsök har utförts, multidimensionell skalning där försökspersoner sätter siffror på hur lika två ytor känns, samt magnitud estimation där i stället intensiteten på specifika perceptuella storheter som t.ex. upplevt lenhet, upplevd mjukhet och upplevd strävhet bedömdes. Eftersom taktil perception innebär kontakt samt relativ rörelse mellan hud och ytor, har fokus i avhandlingen varit att undersöka hur friktion och ytans struktur (ytråhet) påverkar och bidrar till den taktila perceptionen. Förutom fysikaliska mätningar på friktion och ytstruktur har värmekonduktivitet, mjukhet samt olika standard mätningar inom pappersindustrin mätts. En metod för att mäta friktion mellan ett finger och olika ytor har utvecklats för att i möjligaste mån återspegla friktionskomponenten i upplevt taktil perception. Friktionskoefficienter beräknades och jämfördes mellan alla ytor. De stimuli som har studerats är tryckpapper och mjukpapper samt modellytor, gjorda för att systematiskt undersöka hur ytstruktur påverkar perceptionen.

Tillverkningsmetoden för modellytorna valdes så att ytorna var tåliga och kunde tvättas och därmed återanvändas. Strukturen på ytorna bestod av ett vågformat mönster där våglängden varierade mellan 270 nm och 100 μm och amplituden mellan 7 nm och 6 μm. Enligt vår vetskap är det första gången som strukturer i de här skalorna har gjorts utan att samtidigt ändra andra material egenskaper.

Friktionskoefficienten minskade med ökad kvot mellan amplituden och våglängden på modellytorna samt med ytråheten på tryckpappren. En analytisk modell tillämpades på kontakten mellan ett finger och ytorna som visade att friktionskoefficienten beror av den verkliga kontaktarean. För de mycket grövre mjukpappren uppmättes inga stora skillnader i friktion förmodligen för att kontakarean mellan de olika mjukpapprena var lika. Den faktiska kontakarean visade sig också vara viktig för perceptionen av lenhet, strävhet, torrhet och svalhet.

Det visade sig vara en stor perceptuell skillnad mellan olika typer av tryckpapper och mjukpapper utifrån hur stimuli placerade sig på en taktil karta. För de tre materialen användes enbart två alternativt tre egenskaper hos materialet för att särskilja mellan alla olika par. För tryckpapper verkade en viktig dimension kunna beskrivas av alla de perceptuella och fysikaliska egenskaper som har med kontaktarean att göra, d.v.s. lenhet, svalhet, torrhet, ytråhet, värmekonduktivitet samt friktion. För att taktilt

särskilja mellan olika ytor där bara strukturen är varierade, kunde friktion och våglängden relateras till spridningen i kartan. Båda studierna stödjer *duplex theory of texture perception,* där ett spatialt sinne används för att särskilja en av de grövre ytorna från en slät, och ett vibrationssinne för att särskilja mellan olika släta strukturer. Friktionen visade sig alltså vara en viktig fysikalisk egenskap för strukturer under åtminstone 10 μm i ytråhet.

Från fingerfriktions mätningar kunde även följande slutsatser dras: (i) Stora skillnader i friktionskoefficient mellan olika personer uppmättes, men trenderna mellan olika individer var samma, vilket gör att relativa skillnader i friktion från en individ är representativa. (ii) Lipider (fingerfett) som överförs från fingret till ytan vid kontakt sänker friktionen. (iii) Frekvensinnehållet i friktionskraften varierar mellan olika ytor och den frekvenstopp som ses vid 30 Hz kan möjligtvis bero på fingrets struktur eller resonansfrekvensen på huden. (iv) Den pålagda kraften under en friktionsmätning visar sig omedvetet regleras av den friktionskraft som fingret möter under rörelse.

Hur små strukturer som kan diskrimineras har indirekt undersökts genom likhetsförsöket på modellytorna där försökspersoner skulle bedöma hur lika alla par av ytor kändes. Resultaten visade att ytorna med våglängder på 760 nm och 870 nm upplevdes olika jämfört med referens ytor utan något systematiskt mönster, medan ytan med 270 nm i våglängd inte kunde särskiljas. Amplituden på ytan som kunde diskrimineras var endast ca 10 nm, vilket indikerar att nanoteknologi mycket väl kan bidra inom haptiken och för att i framtiden kontrollera den taktila perceptionen.

Nyckelord: *taktil friktion, fingerfriktion, hudfriktion, hudtribologi, biotribologi, taktil perception, psykofysik, haptik, ytråhet, ytstruktur, ytveckning, nanostruktur, kontaktarea, modellytor, friktionskoefficient, kraftmätare, bestruket papper, obestruket papper, tryckpapper, mjukpapper, multidimensionell skalning, magnitud estimation, taktilt tröskelvärde, lenhet, mjukhet, svalhet, strävhet, hudlipider, topikala beredningar, hudkräm.*

Preface

When I started as a PhD student at the Division of Surface and Corrosion Science in September 2007, I was a complete newbie to the topic of both friction and feel, and the word perception was entirely new for me. After four years of intensive research, including planning, experimental work, analyzing data, interpreting results, reading articles, writing manuscripts, making and giving presentations, presenting results at conferences and meetings, taking courses etc., my PhD era in life is about to come to an end. What I have enjoyed most in this interdisciplinary project, the first within this topic at KTH, are the collaborations, both with the industrial partners and the Department of Psychology at Stockholm University, and the basic research questions that are nonetheless very close to applied research with industrial relevance. Through exposure at YKI, industry has really shown interest in the topic of interconnecting physical properties with tactile perception, resulting in contract work regarding finger friction measurements already being performed at YKI. I have scratched the surface in many disciplines in this project, tribology or biotribology, material science, surface and colloidal chemistry, paper chemistry, and last but not least, psychophysics. As a consequence, I now know a little about many things instead of much about little things, and this thesis is hopefully of interest to many people in different fields. This thesis summarizes what I have been working with during these four years. I hope you will enjoy reading it and learn something new about friction, texture and touch.

Lisa Skedung
Stockholm, October 2012

List of Articles

This thesis is a summary of the following articles:

Article I: **Finger Friction Measurements on Coated and Uncoated Printing Papers**
<u>Lisa Skedung</u>, Katrin Danerlöv, Ulf Olofsson, Maiju Aikala, Kari Niemi, John Kettle and Mark W. Rutland
Tribology Letters, Volume 37, Issue 2, 2010
© 2009 Springer Science+Business Media, LLC

Article II: **Tactile Perception: Finger Friction, Surface Roughness and Perceived Coarseness**
<u>Lisa Skedung</u>, Katrin Danerlöv, Ulf Olofsson, Carl Michael Johannesson, Maiju Aikala, John Kettle, Martin Arvidsson and Mark W. Rutland
Tribolgy International, Volume 44, Issue 5, 2011
© 2011 Elsevier

Article III: **Haptic Perception of Fine Surface Texture: Psychophysical Interpretation of the Multidimensional Space**
Martin Arvidsson, <u>Lisa Skedung</u>, Maiju Aikala, Katrin Danerlöv, John Kettle and Mark W. Rutland and Birgitta Berglund,
Submitted

Article IV: **Feeling Small: Exploring the Tactile Perception Limits**
<u>Lisa Skedung</u>, Martin Arvidsson, Jun Chung Young, Christopher M. Stafford, Birgitta Berglund and Mark W. Rutland
Submitted

Article V: **Tactile Friction of Controlled Fine Surface Textures: Role of Real Contact Area and Adhesion**
<u>Lisa Skedung</u>, Kenneth Duvefelt, Ulf Olofsson, Jun Young Chung, Christopher M. Stafford and Mark W. Rutland
Submitted

Article VI: **Robust Hydrophobic Surfaces Displaying Different Surface Roughness Scales While Maintaining the Same Wettability**
Petra M. Hansson, <u>Lisa Skedung</u>, Per M. Claesson, Agne Swerin, Joachim Schoelkopf, Patrick A. C. Gane, Mark W. Rutland and Esben Thormann.
Langmuir, Volume 27, Issue 13, 2011
© 2011 American Chemical Society

Article VII: **Tactile Friction of Topical Formulations**
<u>Lisa Skedung</u>, Lovisa Ringstad, Izabela Buraczewska Norin and Mark W. Rutland
Manuscript

The author's contribution to the appended articles:

I.   Major part of planning, interpretation, writing and experimental work, with exceptions of surface roughness measurements (performed by Kari Niemi at KCL, Finland), and XPS (performed by Marie Ernstsson and Mikael Sundin at YKI, Institute for Surface Chemistry, Sweden)

II.   Major part of planning, interpretation, writing and experimental work, with exceptions of surface roughness measurements (performed by Kari Niemi at KCL, Finland)

III.   Part of planning, interpretation and writing (physical measurements) and experimental work (finger friction measurements)

IV.   Major part of planning and experimental work with exceptions of MDS data analysis (performed by Martin Arvidsson at Department of Psychology at Stockholm University). Part of interpretation of results and writing.

V.   Major part of planning, interpretation, writing and experimental work with exceptions of contact modeling (performed by Kenneth Duvefelt at Machine Design at KTH)

VI.   Major part of experimental protocol development. Part of interpretation and writing.

VII.   Equal contribution by the author of this thesis and Lovisa Ringstad at YKI.

Other publications not included in the thesis:

A comparative study of the tribological behaviour of a highly viscous Naphthenic oil and Polyisobutenes
Mehdi Fathi-Najafi, Karin Persson and Lisa Skedung
NLGI Technical Paper #1007, 2010

One Appendix with results from standard paper tests of both printing papers and tissue papers is included after the appended articles.

Table of Contents

1 Introduction

Already from the moment of birth, we perceive, consciously or not, the physical world around us through our skin senses and by touching. Tactile perception is vitally important to a child's development because it is involved in early learning such as manipulating objects and distinguishing differences in texture and shape. Touching and exploring things, also delivers temperature accompanied with warmth and cold perceptions, and may also provide experiences of pain. We continue to rely and hone our tactile perception into adulthood, and it is through the senses recruited in touching that a great deal of information is communicated.

An increasing interest in tactile perception is seen from many fields, largely because of its potential commercial use. This is driven by a range of factors, for example the development of a sense of touch in robotics and haptic perception for virtual reality and remote sensing,[1,2] as well as the desire to improve the tactile aesthetics in "touch intensive" consumer products such as phones, touch-pads, conditioners, skin cream, packaging, fabrics and paper.

This thesis work, has involved collaboration with industrial partners within the printing paper and tissue paper industries, both consumer oriented, where the tactile feel affects the consumer's impression and preferences of the products. For the tissue industry, the softness feel is an important benchmark of a product, especially for toilet paper, handkerchiefs and facial tissue. Today, softness is measured by means of comparative tests performed by trained panels. These evaluations are both time and resource exacting, and therefore methods to calculate perceived softness by means of measurable physical properties would be beneficial. In the printing paper industry, the feel is important both for readers and customers who select paper. From that stems industrial interest in identifying paper properties that will affect tactile feel and can be controlled in the paper production.

The properties that control human tactile perception are still not completely understood. If the determining properties for various materials were known, then new products and surface treatments could easier be designed to deliver specific tactile perceptions, *i.e.* "perception delivery". While focus in the literature has been on relating physical properties with emotional attributes (affective),[3-7] the aim of the research presented in this thesis was to interconnect sensory attributes, such as perceived roughness, perceived softness and

perceived smoothness, to various physical properties. This is accomplished by conducted psychophysical experiments in which human participants scale various well-defined perceptual attributes applicable to sets of stimuli. Moreover, the important tactile dimensions are searched for by scaling perceived similarities of stimulus pairs followed by multidimensional scaling of the resulting similarity matrices. All samples then end up in a map of tactile perceptions, and the organization is interpreted by means of physical properties of the stimuli. For example, upon comparing the feeling of two different surfaces, what properties are similar and what properties may be discriminated? If one property is more important than any other, then that property can potentially be engineered to modify the perception.

Tactile perception necessitates contact and relative motion between the skin and the surfaces of interest. This implies that properties such as friction and surface roughness ought to be important physical properties for tactile sensing. This thesis focuses mainly on the contribution of friction and topography to the feel of both printing paper and tissue paper as well as model surfaces, in which the surface texture is systematically varied. The main research questions are summarized below:

- What is the role of friction and texture in tactile perception?
- What is the relationship between texture and friction?
- How can model surfaces with systematically controlled roughness be fabricated to cover as wide scans as possible from nanoscale and up?
- Which method is most relevant for measuring friction to be related to tactile perception measurements?
- What is the smallest texture that can be perceived in active touch?

This inter-disciplinary research project has been performed as a joint project with the Perception and Psychophysics Unit of the Department of Psychology at Stockholm University. Together, the two complementary projects constitute the Perception Delivery section within the Institute Excellence Centre CODIRECT (Controlled Delivery and Release Centre), hosted by YKI, the Institute for Surface Chemistry. Besides collaboration with the researchers in psychology, PhD student Martin Arvidsson and Professor Birgitta Berglund, collaboration with Professor Ulf Olofsson at Machine Design at KTH was established. The precisely structured model surfaces were in collaboration prepared at the National Institute of Standards and Technology (NIST) in

Washington DC. The industrial partners in the projects have been Oy Keskuslaboratorio (KCL) in Finland, a paper research institute, now merged with VTT Technical Research Centre, and Eka Chemicals in Sweden. Some work on textile fabrics are also presented in this thesis. This work was performed in collaboration with Fred Butler®, which is a company that has developed an environmentally friendly method for dry-cleaning.

The thesis starts with some background and important references to related work within the fields regarding tribology in general, skin friction, psychophysics as well as the sensory receptors that allow us to feel. The different stimuli, the characterization techniques and the developed finger friction approach are described in Chapter 3. Chapter 4 discusses the fabrication of model surfaces and Chapter 5 summarizes the main results from the finger friction measurements. As you will see, the results are not presented article by article, but rather mixed in order to be easier to follow as a reader and this also allowed an even further interpretation of the results. Both unidimensional and multidimensional psychophysical results are presented in Chapter 6. While summarizing all the results upon writing this thesis, it appeared that the real contact area seems important in many aspects of the human interaction with surfaces.

2 Background

2.1 Elementary aspects of tribology

Tribology is the study of friction, lubrication and wear[8], where the word *tribos* is from the Greek and means rubbing. When two surfaces are in contact and slide over each other, a friction force arises in the direction opposite to the relative motion. This movement can cause wear, i.e. damage to one or both surfaces, resulting in progressive loss of surface material. Both friction and wear can be reduced by adding lubricants to the system, for example oils and greases.

The friction force for dry friction is generally considered directly proportional to the applied load (1st law of friction) and independent on the apparent area of contact (2nd law of friction), first applied by Leonardo da Vinci (1452-1519), stated by Guillaume Amonton (1663-1705) and further verified by Charles-Augustin de Coulomb (1736-1806). Friction is most often described by the friction coefficient *(μ)* that relates the friction force *(F)* to the applied load *(L)*, as described by these two classical laws of friction:

$$\mu = \frac{F}{L} \tag{2.1}$$

Tribology strongly affects industrial processes, as well as our everyday life. In some situations high friction is required and in other cases low friction is desired. When skiing for example Vasaloppet, low friction, typically 0.05 N,[9] between the snow and the ski is preferable; similarly, low friction between the skin surface and the socks is an advantage when running to avoid blistering.[10] In contrast, high friction, typically 0.2-0.3 N,[9] is wanted between either a shoe or foot in contact with the ground to avoid slipping. The reason for easily slipping on the pedals when biking on a rainy day as well as by the swimming pool are due to that water can act as a lubricating film. There are four different regimes of lubrication, hydrodynamic lubrication (full film), mixed lubrication, elastohydrodynamic lubrication and boundary lubrication.[8,11] In the hydrodynamic regime, two surfaces are completely separated by a thick fluid film, whereas in boundary lubrication only a thin molecular layer (additives in the lubricant) protects the surfaces from coming in contact. The friction in a lubricated contact depends on for example sliding velocity, lubricant viscosity and film thickness.

All surfaces display some roughness or unevenness due to asperities on the surface. Surfaces that appear perfectly smooth are not perfectly smooth on an atomic scale. When two surfaces are brought together only a few of these asperities or peaks are in contact, so that the real contact area is usually much smaller than the apparent area. The number of asperities in contact increases with increasing load.

2.2   Skin friction

Biotribology, first defined in the early 1970s,[12,13] includes tribology in all biological systems, *e.g.* artificial implants and articular cartilage,[14] contact lenses,[15] hair,[16,17] personal care products[18,19] and skin,[20-22] which is considered in this thesis. Skin friction was first considered in the cosmetic industry to assess both skin care products and skin health. To paraphrase Gitis *et al.*[23] "When a person feels her or his skin with her or his finger, the resultant perception of the skin property is nothing but friction between the finger and the skin. Thus, friction measurements represent the most straightforward way to exactly mimic the person's feeling of her or his skin conditions". Upon measuring skin friction, deviations from Amonton's law have been observed,[24-26] because of the elastic properties of the skin.[27] Dry friction of a sphere sliding over the skin surface arises from two mechanisms,[22,28,29] interfacial adhesion and deformation according to:

$$F = F_{adhesion} + F_{deformation} \tag{2.2}$$

The deformation force comes from ploughing the harder asperities through the softer surface and is estimated by the following expression:[22,30]

$$F_{deformation} = \beta \left(\frac{9}{128R}\right)^{2/3} E^{*-1/3} L^{4/3} \tag{2.3}$$

where β is the hysteric loss fraction, R is the contact radius, L is the applied load and E is the effective Young's modulus, obtained from the Young's modulus and Poisson ratio *(v)* of the two surfaces in contact according to following equation:

$$E^* = \left(\frac{1-v_{skin}^2}{E_{skin}} + \frac{1-v_{probe}^2}{E_{probe}}\right)^{-1} \tag{2.4}$$

Several works find adhesion as the main contributor to skin friction.[22,31,32] Adhesion arises from attractive atomic or intermolecular forces at the asperities in contact and the total adhesion contribution to friction is a function of the contact area *(A)* and the interfacial shear strength *(τ)* associated with rupture of the adhesive forces. Thus, the adhesion contribution[22,31] can be expressed as

$$F_{adhesion} = \tau A = \tau \pi a^2 = \tau \pi \left(\left(\frac{3LR}{4E^*} \right)^{1/3} \right)^2 \tag{2.5}$$

The friction coefficient is according to *eq. 2.1*, the ratio of the friction force to applied load. Based on *eq. 2.3* and *eq. 2.5*, the friction coefficients based on deformation and adhesion, are then proportional to $L^{1/3}$ and $L^{-1/3}$, respectively. This indicates that the friction coefficient decreases with increasing load if the mechanism is adhesion driven and increases with applied load if the friction mechanism is driven by deformation. The expressions above are derived considering a solid sphere sliding on the skin, but the contribution of adhesion and friction coefficient decreasing with the load has also been found when a finger is sliding over solid surfaces,[33,34] especially at low loads. However, Masen[35] suggests that the contribution to deformation on the friction coefficient should not be ignored. Which mechanisms that contribute to friction in a skin contact are typically studied by plotting the friction coefficient for various applied loads or contact pressures. The curves obtained are usually non-linear at low loads showing a decrease in friction coefficient with load[17,25,30] or contact pressure,[36] and the friction coefficient can be described by a negative power function according to *eq. 2.6*. For the high load regime (load > 1 N), it has also been reported that the relation between the friction force and applied load is linear; but with a non-zero intercept,[37,38] due to the deformation of the finger at low loads.[37]

$$\mu = \frac{F}{L^n} \tag{2.6}$$

Skin friction has been measured, mainly *in vivo*, by sliding or rotating a probe of various materials of stationary skin, predominantly measured on the forearm.[39,40] Friction has been studied as a function of age,[41-43] anatomical site,[26,41,43] gender,[41] hydration,[41,44,45] as well as hydration in combination with various lubricants.[24-26,46-48]. These studies report that hydrated skin displays higher friction compared to dry skin. Some attempts have been made to

6

correlate skin friction with skin feel in the cosmetic area,[48,49] mainly as an effect of moisturizers.

A second type of skin friction measurement employs actively moving a finger over a stationary surface as when exploring a surface, a more pertinent approach to measure friction to be linked to tactile perception. Recently, a number of studies have emerged, where friction is measured while moving a fingertip[5,33,37,38,50-57] or arm[58,59] over a surface. Moreover, a couple of these studies have combined finger friction measurements and sensory evaluation.[5,54-57,60] Friction measurements between an index finger and different car interior materials and aluminum samples with different roughness have been performed by Liu *et al.*[57] where both measured surface roughness and friction correlated with the "rough-smooth" and "grippy-slippery" perceptions. A new study by Schreiner *et al.*[60] could not correlate perceived slipperiness with finger friction based on measurements on three polymer surfaces, and they therefore conclude that tribological attributes of human skin is of limited value when it comes to haptic perception. Finger friction has also been considered when studying grip.[20,38,50,61,62] One interesting finding is that the friction force encountered when manipulating objects controls the grip force.[63-65]

In a contact where at least one of counter-surfaces is elastic, for example rubber or skin, and the real contact area may approach the apparent contact area as the elastic material can deform over the surface asperities.[66] This is often discussed in combination with an observed decrease in friction with increasing surface roughness.[33,34,38,67,68] Rougher counter-surfaces thus result in lower real contact area with fewer amounts of asperities contributing to interfacial adhesion, and therefore lower friction. However, Tomlinsson *et al.*[37] found that finger friction increases with increasing roughness. Derler and Gerhardt[20] discuss in a recent review that in an adhesion-dominated regime friction decreases with increasing roughness, whereas in a deformation-dominated regime, friction increases with increasing roughness up to a plateau. Although several experimental studies of tactile friction have reported the relation between friction coefficient and surface roughness, only little attention has been paid to systematically study the role of texture or surface roughness in tactile friction.[37,56,69,70] There are no systematic studies on friction and roughness of fine-textured surfaces, with feature sizes reaching down to the nanometer scale. Reasons for not having studied this issue in depth yet may be due to the issues of manufacturing,

characterizing and measuring such structures that are large enough and allow repeated interrogation with a finger.

Moisture or hydration of skin has shown to increase the skin friction coefficient.[21,33,34,58,68,71-75] Two different mechanisms discussed in the literature that increases friction due to moisture results from that water on the surfaces may form capillary bridges with the finger that increases adhesion and therefore also friction,[34,76] or that water absorption decreases the Young's modulus of skin and makes the surface more smooth resulting in an increase in contact area.[22,71] When measuring tactile friction, large differences between subjects are often observed, a phenomenon probably due to variations in moisture.[21,24,74]

In this thesis work, friction coefficients are measured by moving a finger over the surfaces of interest using load sensors, where the friction coefficients are calculated according to Amonton's law and compared between all stimuli.

2.3   The skin

The skin is a large multilayered organ covering the entire body, composed of the epidermis, dermis and subcutaneous fat tissue. The outer layer (10-20 μm) of epidermis is called stratum corneum (SC), arranged in a brick and mortar structure as corneocytes (bricks) embedded in a lipid lamellar intercellular matrix (mortar).[77]   The arrangement of ceramides, fatty acids and sterols (mainly cholesterol) within this matrix[78] work as an effective barrier between the body and the environment. Disruption of this lamellar barrier can increase the transepidermal water loss and consequently affect hydration of skin and cause skin dryness.[79] Besides protecting the body from water loss and from foreign substances entering the body, tactile information is mediated through sensory receptors embedded in the skin, see paragraph below.

The skin covering the palms of the hands and soles of the feet are different from other parts of the body. For example, these parts are glabrous (hairless), contain a system of papillar ridges and comprise only eccrine sweat glands and no sebaceous glands like the other parts of the body. Sebaceous glands secrete sebum, a waxy/oily secrete containing fatty acids, glycerides, hydrocarbons and alcohols.[80] Eccrine sweat contains 98-99 % water and the rest is both inorganic and organic components such as anions, cations, ammonia, amino acids, urea and glucose. It is the apocrine sweat glands, localized around the nipples,

armpits and genital regions, that may form an odor when the secrete comes in contact with bacteria on the skin.[80]

Each person has a unique fingerprint, invariable after they have been developed in 16th fetal week.[81] These finger ridges have a height of about 100 μm, and a spatial separation (wavelength) of approximately 450 μm,[5,82] as confirmed by my finger imprint shown in **Figure 2.1**B. The biological function of fingerprints is not to aid personal identification, but rather to increase friction to improve grip.[83] This is why finger ridges sometimes are called "friction ridges". The finger ridges have a high density of sweat glands (eccrine), about 150-350 per cm,[34] and can be seen in **Figure 2.1**A as white dots if looking carefully. The sweat pores allow water or moisture to be secreted which aid increasing friction.[24] Spurr[84] discusses that excess water can escape into the valleys to avoid lubrication of the skin surface. It may be a physiological reason that lipids are not secreted by sweat glands on the finger ridges, since that most probably would oppose the friction effect of moisture. On the other hand, some research suggests that the primary role of the fingerprints is instead to improve tactile perception,[82,85-87] based on that compared with flat skin, fingerprints reduce contact area by a factor of one-third. Thus, in an adhesion-dominated contact like human skin, finger ridges would decrease friction.
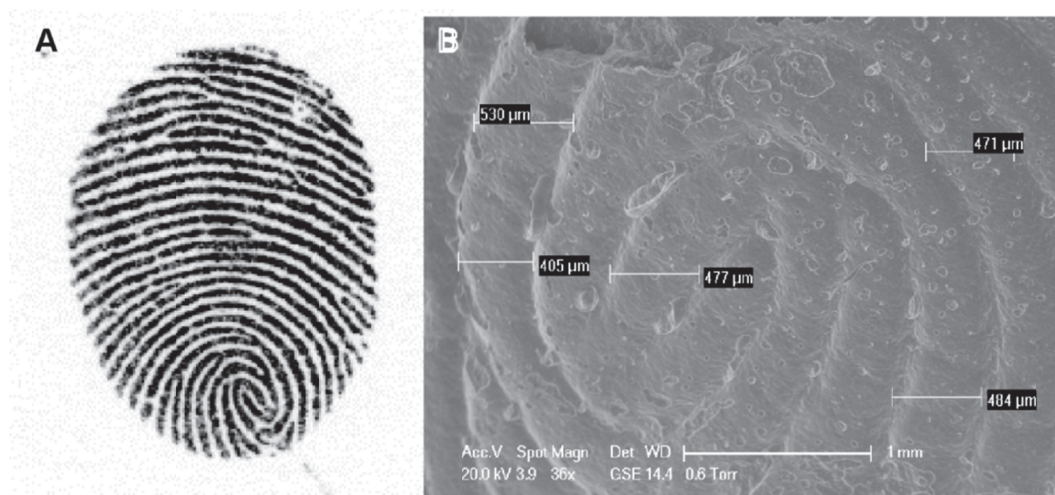

Figure 2.1 (A) My fingerprint. Sweat glands can be seen as white small dots on the finger ridges (in black) (B) Scanning Electron Microscope image of a finger imprint (dental mold), giving an idea of the wavelength of the finger ridges.

2.4 Sensory receptors in the skin

Many kinds of sensory receptors are embedded in the skin. They are triggered by various kinds of stimulation which give rise to the perceptions of touch, pressure, vibration and cold, but also of many more complex and suttle perceptions such as tickle, itching, wetness, irritation, stinging, etc. Receptor signals convey the sensory information via afferent nerves in the spinal cord to the brain. How the resulting mental perceptions are actually created is a mystery. As illustrated in **Figure 2.2**, the receptors are either free nerve endings (nociceptors), which give rise to pain sensations (high threshold), or encapsulated as are the thermoreceptors as well as the four distinct mechanoreceptors. The latter respond to mechanical stimuli or deformations of the skin:[1] Meissner Corpuscles, Merkel disks, Ruffini endings and Pacinian Corpuscles.
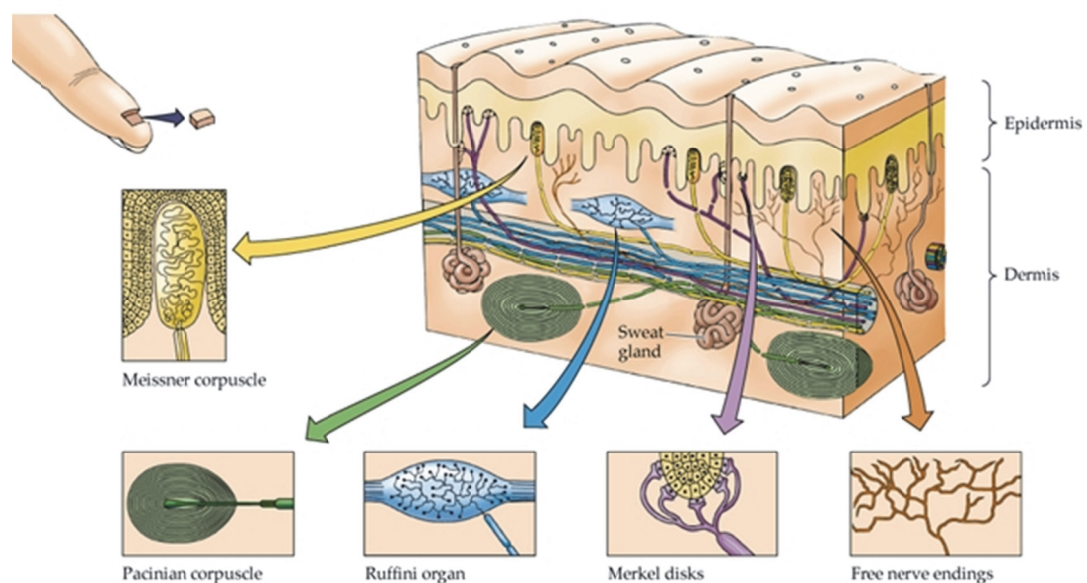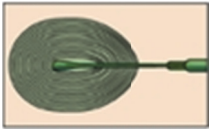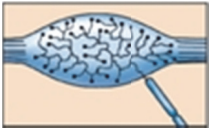
Figure 2.2. *Illustration of mechanoreceptors and free nerve endings embedded in the skin. Used with kind permission from Purves et al: Neuroscience, Second Edition, Sinauer Associates, Inc., Sunderland, MA, 2001.*[88]

Each of these mechanoreceptors is connected to specialized nerve endings, either fast-adapting (FA) or slowly-adapting (SA). A further sub-categorization is based on the size of the receptive field, either small (I) or large (II).[89-91] Fast-adapting implies that the receptors need *dynamic* stimuli in order to maintain activity, whereas a small well-defined receptive field implies *spatial acuity*. The functions of each tactile unit are still not completely understood, but FAI and

SAI units are sensitive to deformation (static touch). Conversely, the FAII and SAII units need movement (dynamic touch) or changes in deformation to stay activated because of fast adaptation. The characteristics of the four distinct mechanoreceptors are summarized in **Table 2.1**.[1,64,90] The density of receptors decreases with age. For example, Meissner's corpuscles, which are the most abundant type of receptor in the glabrous skin of a fingertip, decreases from about 24 per mm^2 to about 6 per mm^2 by the age of 75.[1,92,93]

Table 2.1 The four mechanoreceptors and their response sensitivity.[88,90,94-96]

Mechanoreceptor		Adaptation rate	Receptive field	Sensitivity
Meissner corpuscle		Fast (FA)	Small (I)	Movement or deformation changes Motion, grip control (3-40 Hz)
Merkel disks		Slow (SA)	Small (I)	Deformation Spatial structure, shape (2-16 Hz)
Pacinian corpuscle		Fast (FA)	Large (II)	Movement or deformation changes Fine textures through vibrations (40-500Hz)
Ruffini organ		Slow (SA)	Large (II)	Lateral deformation of skin Skin stretch (100-500 Hz)

2.5 Tactile and haptic perception

There are two forms of tactile perception, passive tactile perception (cutaneous perception) and active tactile perception (kinaesthetic perception).[97,98] Cutaneous perception is a result of mechanical deformations of the skin when statically touching a surface. The information is limited in static touch, and to apprehend the whole object, exploratory movement is necessary.[99,100] Kinaesthetic perception is generated from movements of an arm, shoulder, hand or finger. Movement generates the kinaesthetic perceptions linked to the cutaneous perceptions, and since the participants freely explore the surfaces in this thesis work, *haptic perception* is the actual subject of scientific study in this thesis. Nevertheless, I still use tactile perception as the concept for what is investigated, because it is a more common word to a broader audience and is readily associated with human skin.

2.6 Psychophysics

Psychophysics is the scientific study of the relation between stimulus (physics) and sensation (psychology).[101] A good description of the methods, theories and applications of modern and classical psychophysics can be found in the book *Psychophysics - The Fundamentals,* written by Gescheider.[101] The founder of the term "psychophysics" was the German scientist Gustav Theodor Fechner who published *Elements of Psychophysics* in 1860, where he described research that relates physical stimuli to how they are perceived. All our senses are studied in psychophysics: vision, hearing, taste, smell and touch (or the senses of the skin), and there are three basic types of experiments: determination of absolute thresholds, discrimination thresholds and unidimensional scaling of quantity. In absolute threshold experiments, the smallest amount of stimulus intensity to produce a sensation (or be detected) is investigated, whereas discrimination thresholds are the smallest amount of difference in stimulus intensity that can produce a sensation (or be detected). The actual physical stimulus is considered the input to the sensory system and the output is the sensation. Thus, these traditional threshold methods state a perception threshold in units of a stimulus intensity where the output is just detected (or not) or discriminated (or not).

The output of a sensory system such as perceived brightness, odor, warmth or loudness,[102] can be measured as quantities by the aid of various scaling methods.[103] In such experiments, the *perceived quantity* (above threshold of a stimulus) is measured and presented as a function of *stimulus intensity*, which

gives a psychophysical function of magnitude. Steven proposed a power law, relating this sensation magnitude *(Ψ)* (perceived quantity) with the stimulus intensity *(Φ)* according to:

$$\Psi = k\phi^n \tag{2.7}$$

where *n* is the power exponent and *k* is an arbitrary constant. This relation became more exerted than the classical Fechner-Weber law (*Ψ = k logΦ*) when scaling methods became more regularly used.[101] Traditional psychophysical functions often show logarithmic human responses between physical intensity and sensory magnitude, for example the perceived loudness; a response of the human ear, is proportional to the logarithm of sound intensity and perceived brightness; a response of the human eye, implies a logarithmic relationship with physical luminance.[101]

There are many scaling techniques to measure perceptual quantities (sensory magnitudes), but the direct ratio scaling methods, particularly magnitude estimation is most useful and widely used and also the method employed within this thesis work. In magnitude estimation experiments, participants assign numbers to their perceived quantities of the presented stimuli. Therefore, one assumption of the method is that humans can make numerical judgments of quantities on perceptual continua, *e.g.* degree of softness.

2.6.1 Unidimensional psychophysics

Most studies on tactile perception are unidimensional, investigating single perceptual attributes[6] such as perceived softness,[104-106] slipperiness[60,107] and perceived roughness, the latter is by all means the most extensively studied tactile perception.[97,108-113] Perceived roughness and the role of mechanoreceptors in roughness perception have been researched using artificial surfaces: linear gratings, [109,114,115] raised dots[116-118] or sandpaper,[119] where the spatial separation, the feature size and width have been varied. For spatial densities at the millimeter scale, the gap between the surface features seems important for the roughness perception, whereas the width of the features has a smaller effect.[97,115]

Perceived roughness with smaller features has also been investigated, in order to study the *duplex model of texture perception*,[99,120-123] originally proposed by David

Katz.[99] Depending on the sizes of the elements on the surfaces, a texture can either be a macro texture (features larger than 100 µm and/or spatial separations > 200 µm) or a micro texture (features smaller than 100 µm and/or spatial separations <200 µm). This *duplex model* suggests that different mechanisms contribute to the perception of a micro texture (fine surface) and a macro texture (coarse surface). The perception depends on a "spatial sense" for discernment of coarse textures and a "vibration sense" for fine-textured surfaces.

2.6.2 Spatial resolution of the fingertips

Mainly two methods to evaluated spatial resolution of skin have been employed. In a "two-point threshold" assessment, participants judge whether one or two points are felt on the skin,[97,124] conversely, when estimating a "point-localization threshold", participants judge whether a second stimulus is applied to the same or different spot as the first stimuli presented. This latter threshold is about 1-2 mm on the fingertip and lower compared to two-point threshold. The spatial acuity is highest of the fingertips probably due to the high density of sensory receptors, and lowest on the back.[97]

The duplex theory of texture perception indicate that spatial separations above 200 µm can be discriminated by static touch (just pressing down the finger), whereas smaller separations need movement and are detected by vibrations.[99,120-123] Lamotte and Whitehouse[125] showed that the detection threshold of a raised dot with a diameter of 550 µm was 2.1 µm in height on an otherwise smooth surface.[125] Miyaoka *et al.[119]* found a tactile threshold between 1 µm and 3 µm in particle sizes (fine abrasive paper) using a two-alternative, forced-choice procedure where participants judged which out of two presented surfaces that felt rougher. The literature still lacks research on the limitations in active touch. In this thesis work, a method of similarity scaling was employed for the model surfaces with spatial separations ranging from nanometer up to 100 micrometer to investigate the tactile limits, without asking for a specific attribute or if a pattern was felt or not.

2.6.3 Multidimensional psychophysics

In order to get a comprehensive picture of tactile perception, researchers have also tried to map the dimensions of the tactile space using multidimensional scaling (MDS).[126-133] The purpose is to find the number of underlying dimensions or specific properties that affect the ability to discriminate among surfaces and also what these dimensions are. In contrast to unidimensional scaling, the participants are not told what attribute to think of, but rather to scale perceived similarities or dissimilarities of presented pairs of stimuli on a common scale, for example, a scale from 0% to 100% similarity. All possible combinations of pairs within one set of stimuli are presented, and are given a scale value based on how similar the two stimuli feel. After all pairwise comparisons from a large group of participants, about 20, the similarity data is averaged in a matrix and analyzed according to the selected model for MDS. In this thesis, the judged similarities are measures of psychological distance, where a pair that is perceived similar has a short psychological distance. These psychological distances are then visually presented in a map with the number (n) of dimensions that best represents the data.[134,135]

As an illustration of the MDS analysis, inspired by Lyne *et al*,[130] I here present the map obtained (**Figure 2.3**) upon performing MDS on a matrix of flight distances[136] between cities in Europe. As can be seen, the map obtained resembles the actual map well.
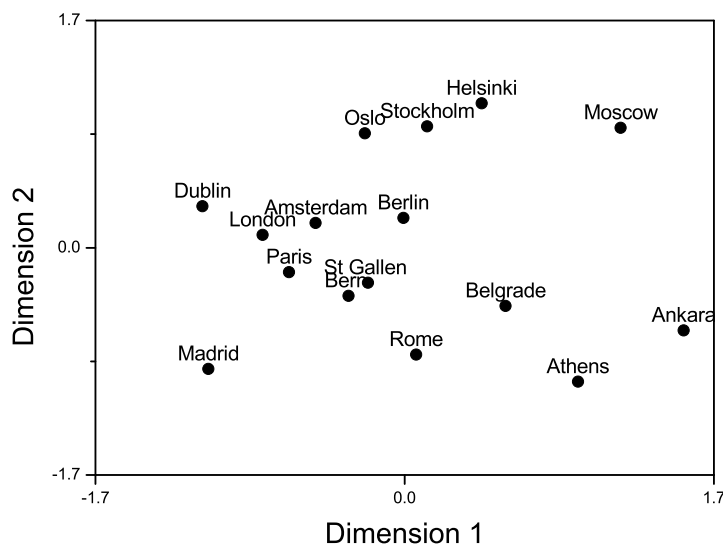

Figure 2.3 Two-dimensional map obtained when analyzing a matrix consisting of flight-distances between cities in Europe using multidimensional scaling.

In this example, a two-dimensional solution was selected and the dimensions are interpreted as north/south and east/west, because that makes sense in this specific case. A tactile map can be obtained in the same way, analyzing a matrix of perceived dissimilarities (tactile distances). The closer two surfaces are located in a tactile map the more similar they are perceived.

The multidimensional studies reported in the literature, typically, find between two and four dimensions for tactile perception, but the actual number seems unclear. Okamoto *et al.*[137] review research on tactile dimensionality and they find five dimensions in total: macro roughness, fine roughness, hardness/softness, coldness/warmness and friction. In addition, they assume that the sticky/slippery and moist/dry dimensions are parts of the friction dimension. The interpretations of the dimensions are typically made by fitting adjective rating scales into the tactile space[126,127,129] or by relating the perceptual dimensions to physical measurements.[128,130,131]. In general, the dimensions obtained are interpreted as perceptual dimensions. Furthermore, with the exception of fabrics[133] and tissue,[130] most MDS studies have focused on objects or different materials rather than a set of similar surfaces from the same material.

In the present thesis, an attempt is made to map the tactile space for two important consumer materials; printing paper and tissue paper, as well as model surfaces. The underlying dimensions (important dimensions) are searched for by relating physical measurements to the coordinates of the multidimensional tactile maps. Besides Lyne *et al.*,[130] the studies within this thesis are among the first to correlate physical quantities with the perceptual outcome of a multidimensional study on a set of surfaces from the same family group. Both unidimensional and multidimensional psychophysical results, and some experimental details, are presented in Chapter 6.

3 Methodology

In this chapter, the different stimuli are designated and the techniques used to characterize these stimuli in terms of texture, thermal conductivity and elemental composition are briefly described. Moreover, the developed and extensively used tactile approach to measure finger friction is explained.

3.1 Stimuli

The printing papers and tissue papers were supplied by the industrial partners, KCL and EKA, respectively. They were selected to cover a wide range of products from industry.

3.1.1 Printing paper

The 21 printing papers, listed in **Table 3.1**, are classified with a paper grade, based on the pulp, treatment and/or end use. Uncoated papers are mainly used as copy papers and in newsprint, wood-free (chemical pulp) coated papers are usually used in advertising materials and high-quality books and magazines, and coated papers with mechanical pulp are normally used in magazines, catalogues and in advertising materials. Seven of the papers were uncoated (in bold in **Table 3.1**) and 14 papers were coated, either made from mechanical or chemical pulp (wood-free) with a grammage (weight) from 45 g/m^2 up to 130 g/m^2. The coated papers are further subcategorized based upon the extent of their finishing; Gloss > Silk > Matt; or amount of coating; MWC > LWC and MFC. A supercalendered paper is uncoated but has been smoothened to obtain more similar properties of a coated paper.

Table 3.1 *The 21 printing-paper stimuli sorted in alphabetical order, together with their respective paper grade and grammage. Wood-free means that the papers are made from chemically treated pulp. The seven uncoated papers are shown in bold.*

Paper sample	Paper grade	Grammage (g/m²)	R_a surface roughness (µm)
LWC 45	Light-weight coated	45	1.96±0.05
LWC 60	Light-weight coated	60	1.75±0.04
MFC 48	Machine-finished coated	48	2.55±0.04
MFC 60	Machine-finished coated	60	2.38±0.04
MWC 100	Medium-weight coated	100	1.28±0.03
MWC 60	Medium-weight coated	60	1.54±0.03
News 45	**Newsprint**	**45**	**4.03±0.07**
SC-A 48	**Supercalendered (virgin fibres)**	**48**	**2.00±0.05**
SC-A 60	**Supercalendered (virgin fibres)**	**60**	**1.91±0.03**
SC-B 45	**Supercalendered (recycled fibres)**	**45**	**2.12±0.04**
SC-B 60	**Supercalendered (recycled fibres)**	**60**	**2.20±0.04**
WFC-Gloss 100	Wood-free coated	100	1.24±0.03
WFC-Gloss 115	Wood-free coated	115	1.23±0.03
WFC-Gloss 130	Wood-free coated	130	1.25±0.02
WFC-Gloss 70	Wood-free coated	70	1.34±0.03
WFC-Matt 100	Wood-free coated	100	1.70±0.05
WFC-Matt 70	Wood-free coated	70	1.66±0.05
WFC-Silk 115	Wood-free coated	115	1.54±0.05
WFC-Silk 130	Wood-free coated	130	1.59±0.04
WFU 100	**Wood-free uncoated**	**100**	**3.85±0.05**
WFU 60	**Wood-free uncoated**	**60**	**3.91±0.05**

3.1.2 Tissue paper

The tissue papers obtained are also divided into three groups: bathroom tissue, absorbent tissue and facial tissue, and listed Table 3.2. Adsorbent tissue contains wet strength resins in order to not fall into fragments upon contact with a liquid. On the other hand, bathroom tissue has to decompose upon contact with water and no wet strength resin is added. The tissue samples are made of different pulps; the tissue samples T1, T3, T5 and T8 are made from kraft pulp (chemical pulp) and CTMP (chemo-termo-mechanical pulp), tissue T6, T7, T11, T12, T14 and T15 from softwood and eucalyptus pulp and T2, T4, T9, T10, T13, T16 and T17 from recycled newsprint or office waste. Eucalyptus pulp gives a high bulk, important for tissue softness. A through-air-dried (TAD) sample, where the water has been removed by high temperatures instead of being pressed away onto a cylinder, also contains a higher bulk. Perceived softness is the most important attribute within the tissue industry and it is generally divided into surface softness and bulk softness.[106,130,138] It is generally the creeping process that gives tissue bulk and softness; however the TAD process and addition of debonders that lower the strength between fibers to the pulp, often result in even bulkier and softer tissue papers.

Table 3.2. *The 17 tissue paper stimuli, divided into absorbent tissue, bathroom tissue and one sample of facial tissue.*

Tissue sample	Information
T1	Absorbent tissue. Contains WSR. Kraft pulp and CTMP
T2	Absorbent tissue. Contains WSR. Recycled pulp
T3	Absorbent tissue. Contains WSR. Kraft pulp and CTMP. TAD
T4	Absorbent tissue. Contains WSR. Recycled pulp (newsprint)
T5	Absorbent tissue. Contains WSR. Kraft pulp and CTMP. Embossed.
T6	Facial tissue. Some WSR. Softwood and eucalyptus kraft pulp.
T7	Bathroom tissue. Softwood and eucalyptus kraft pulp.
T8	Absorbent tissue. Contains WSR. Kraft pulp and CTMP. TAD
T9	Bathroom tissue. Recycled pulp (newsprint)
T10	Bathroom tissue. Recycled pulp (office waste)
T11	Bathroom tissue. Softwood and eucalyptus kraft pulp. TAD.
T12	Bathroom tissue. Softwood and eucalyptus kraft pulp.
T13	Absorbent tissue. Contains WSR. Recycled pulp (newsprint)
T14	Table napkin. No WSR. Softwood and eucalyptus kraft pulp.
T15	Bathroom tissue. Softwood and eucalyptus kraft pulp.
T16	Bathroom tissue. Recycled pulp (office waste)
T17	Bathroom tissue. Recycled pulp (newsprint)

3.1.3   Paper standard tests

Standard printing-paper and tissue-paper tests were performed by the industrial partners according to different ISO protocols and standard tests. These results are given in Appendix I (included at the end, after the appended articles). These tests were all performed in a controlled environment of 50 % relative humidity and 23 °C. The measured properties that will be discussed further in this thesis are grammage for the printing papers (ISO 536:1995), and the corresponding measure in tissue industry called basis weight (ISO 12625-6), given in g/m². In addition, tensile stiffness *(TS)* for the tissue papers, obtained from the maximum slope of the tensile force versus tensile stretch curve, given in kN/m, will be considered.

Bulk softness[106,130] is calculated from the tensile stiffness according to:

$$Bulk\ softness = 99TS^{-0.36} \tag{3.1}$$

Surface softness was measured by Eka Chemicals, using a rebuilt record player (**Figure 3.1**), first developed by Hollmark.[106] A needle, acting as a "synthetic fingertip", is sliding on the tissue paper. The signal that depends on the surface texture of the tissue is logarithmically amplified to exaggerate peaks and filter

out fine details.[106] The smoothness number (*LENA*-value) is then calculated by dividing the number of peaks with the mean amplitude. Since this *LENA*-value depends on the surface texture, it can be seen as a measure of the surface roughness of the tissue samples.
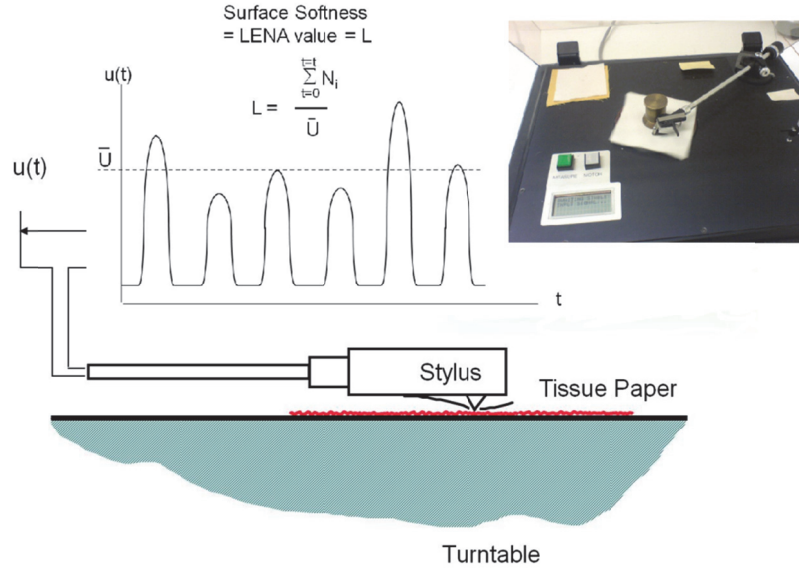

Figure 3.1 *Rebuilt record player used by Eka Chemicals to measure surface softness of tissue paper.[106]*

Combined softness is calculated from the geometrical mean of *TS*, measured in both the machine direction and cross direction, and the *LENA*-value, measured on both the smooth and rough side, according to:

$$Combined\ softness = 61TS^{-0.22}LENA^{0.31} \tag{3.2}$$

3.2   Experimental techniques

3.2.1   Characterization of texture

A non-contacting **laser profilometer** (NanoFocus µScan), was used to measure surface roughness of the printing papers (Article I-III). A laser beam emitted from a point light source is focused on the surface through an objective lens that moves rapidly up and down to adjust focus (where the maximum light intensity occurs). These movements are recorded and represent the surface profile. The vertical resolution of the confocal sensor is typically 20 nm and the

spatial resolution, which depends on the adjustable step length and scanning speed, was about 0.2 μm in this work.

The topography of the wrinkled model surfaces were measured using a **stylus profilometer** (Taylor Hobson Form Talysurf PGI 800), a contacting technique (Article IV-V). A diamond stylus tip was drawn 1.1 mm over the surface in a direction perpendicular to the wrinkle orientation. The vertical resolution is a few nanometers, and the horizontal resolution depends on the radius of the tip, which was 2 μm in this work.

The nanoscale-textured model surfaces, both wrinkled and particle surfaces could not be resolved in the above mentioned techniques. These were instead imaged and characterized with an **atomic force microscope** (AFM)[139] with a much smaller tip radius compared to the stylus instrument (Article IV-VI). Briefly, a sharp tip, i.e. cantilever, scans over a surface, either in contact mode or tapping mode® (Veeco Instrument). A laser is deflected from the back of the cantilever onto a mirror and subsequently into a photodetector. As the tip traces various surface features, its upward and downward movement shifts the beam between upper and lower photodiode components, creating voltage differences that move a piezoelectric scanner in the z-direction to keep the feedback constant (constant force/deflection or oscillation amplitude). It is the movement of the scanner that renders height information.

The texture of a surface is normally made up of both waviness and roughness (higher frequency). Often the waviness is filtered away by using a cut-off wavelength. Irregularities with a wavelength greater than this value will not be considered. Primary roughness parameters (*P*) are named as an *R*-parameter after any cut-off filtering. There are a number of different roughness parameters that describe the topography of a surface, and they are generally divided into four groups; amplitude, spatial, hybrid and functional parameters.[140]

Two standard parameters, R_a and R_q, were used to characterize the surface roughness of the printing papers. The standard cut-off values when characterizing a printing paper is 5 μm (lower limit) and 10 mm (upper limit). R_a is the arithmetic average deviation of surface heights z of all points x from the center line of the test surface of length L:

$$R_a = \frac{1}{L} \int_0^L z(x)\, dx \tag{3.3}$$

Mathematically the center line is defined in such a way that the sum of the z values is zero. R_q, also called root-mean-squared roughness (*RMS*), is defined as the square root of the mean value of the squares of the distances z of all points x from the center line L:

$$R_q = \sqrt{\frac{1}{L} \int_0^L z^2(x)\, dx} \tag{3.4}$$

The amplitude of the wrinkled-textured surfaces was estimated from the R_z parameter (ten-point height), the average absolute value of the five highest peaks *(P)* and the five lowest valleys *(V)*:

$$R_z = \frac{(P1+P2...P5)-(V1+V2...V5)}{5} \tag{3.5}$$

A good parameter to estimate the wrinkle wavelength was the *S*-parameter that gives the average spacing of local peaks in the profile. In addition, λ_a was estimated from the AFM profiles.

$$S = \frac{S1+S2...S_n}{n} \tag{3.6}$$

Furthermore, an **optical microscope** (Zeiss Axioplan) has been employed, mainly to estimate the surface wavelengths and possible wear of the wrinkled model surfaces, as well as to characterize phase structures in the topical formulations.

3.2.2 Characterization of thermal conductivity

Thermal conductivity was measured with a HotDisk (HotDisc AB, Sweden), based on the Transient Plane Source (TPS) technique.[141] A current is applied to a thin film sensor (HotDisc 7280 with radius of 14.67 mm in this work), which serves as both the heat source and thermometer. The thermal conductivity is obtained by monitoring the temperature increase, which is highly dependent on the thermal transport properties of the surrounding material, as a function of time. Thermal conductivity was measured on the printing papers by KCL and used in Article III.

3.2.3 Characterization of elemental composition

X-Ray Photoelectron Spectroscopy (XPS), also known as ESCA (Electron Spectroscopy for Chemical Analysis) provides quantitative chemical information such as elemental composition, chemical states and amount of different functional groups for the outermost 2-10 nm surface layer. The surface is placed in ultra-high vacuum and exposed to well-defined irradiation of x-ray energy, resulting in emission of photoelectrons. The kinetic energy of these emitted electrons is used to calculate the binding energy, which can be related to the chemical state of bonding.

In this work, XPS was used to investigate a possible transfer of lipid material to the surfaces upon stroking, and thus high-resolution carbon spectra were curve-fitted, showing chemical shifts in the carbon signals due to different functional groups between carbon and oxygen; there are four types of carbon peaks, C1-carbon (carbon with no bonds to oxygen, C-C, C=C, C-H), C2-carbon (carbon with one bond to oxygen, C-O, C-O-C), C3-carbon (carbon with two bonds to oxygen, O-C-O, C=O) and C4-carbon (carbon with three bonds to oxygen, O-C=O, C(=O)OH).[142] Filter paper served as a good model for paper since it consists only of cellulose, and only a low amount of C1-carbon is present. Lipids on the other hand contain mainly C1-carbon.

3.3 Finger friction

A tactile approach to measure friction has been developed, consisting of continuously recording the *friction force* and *applied load* (normal force) as a finger is moving over a surface mounted on a force sensor. Finger friction measurements were first evaluated on a set of printing papers (Article I-III), using a three-component piezoelectric force sensor, and then employed on model surfaces (Article IV-V) and tissue paper. The approach used in these dry contacts was further elaborated into lubricated contacts (Article VII) upon measuring finger friction of different topical formulations. In this latter study, finger friction measurements were performed with a ForceBoard™ (Industrial Dynamics AB).

3.3.1 Force sensors

The three-component piezoelectric force sensor (Kistler 9251A), fixed between two parallel steel plates (**Figure 3.2**), contains piezoelectric crystals that convert mechanical load into electrical signals. The charges generated are proportional to the load applied, and are converted into voltage by a charge amplifier (Kistler 5038A3). To get the output signal in Newton instead of voltage, the force sensor was calibrated in the three directions (F_x, F_y and F_z), by placing standard weights (0.1 - 0.5 kg) on the top plate while continuously recording the output voltage signal. Scale factors were obtained from the inverse of the slope of the voltage versus loading force plot. As a check, calibration was also tested for lighter weights (10 g, 20 g and 50 g), to verify the linearity of the lower range of forces applied in tactile friction measurements. Three forces were recorded upon stroking at a sampling rate of 100 Hz with a LabVIEW system.
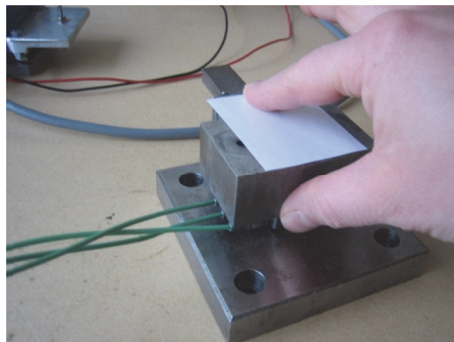

Figure 3.2 The finger friction device consisting of a piezoelectric force sensor attached between two parallel steel plates.

The ForceBoard™[143] is equipped with two load cells, one horizontal and one tangential, consisting of strain gauges in a Wheatstone bridge configuration. A mechanical load is converted into voltage signals that are amplified and proportional to the applied load. Forces are sampled at 100 Hz using DAQFactory software.

3.3.2 Finger friction measurements

Friction coefficients were calculated as the ratio of friction force and applied load according to *eq. 2.1*. A standard measurement for dry friction was 15 stroking cycles, however; the friction coefficient was calculated as the average of the first three stroking cycles since participants tended to make an estimation about the surface feel after only a couple of stroking cycles. The average applied load of all finger friction measurements performed by the respondent was 1.1 ± 0.2 N (mean ± SD). This corresponds to an apparent contact pressure of 13 kPa or 3 kPa, considering the diameter of the apparent contact area to be 10 mm or 20 mm, respectively. This average applied load of 1 N was in agreement with the reported optimum contact load when detecting tactile stimulus.[144] It should be noted that the standard deviation of load within one measurement was larger than between measurements, although the load was intended to be kept constant. Each of the 14 different participants (Article II) used their preferred load from 0.2 N up to 5.2 N, but with an average of the group of 1.3 N. The approximated stroking speeds for all measurements were approximately 10 – 60 mm/s, where a speed of 20 – 30 mm/s was normally applied by the respondent. The output data is a text file of columns with the time and respective forces and MATLAB scripts have been written in order to facilitate the different analyses of the friction measurements. The main benefit using the script is that many files can be analyzed simultaneously and the results such as the average friction coefficients, applied load, change in friction coefficient with time and average friction force are summarized in an excel-file. **Figure 3.3** shows typical curves of the two forces and the corresponding friction coefficients, both before and after removal of the turning points associated with changing direction of the finger. The forward strokes (away from the body) are negative and the backward strokes (towards the body) are positive. The friction coefficients are obtained using both the positive and negative arms of the curve.
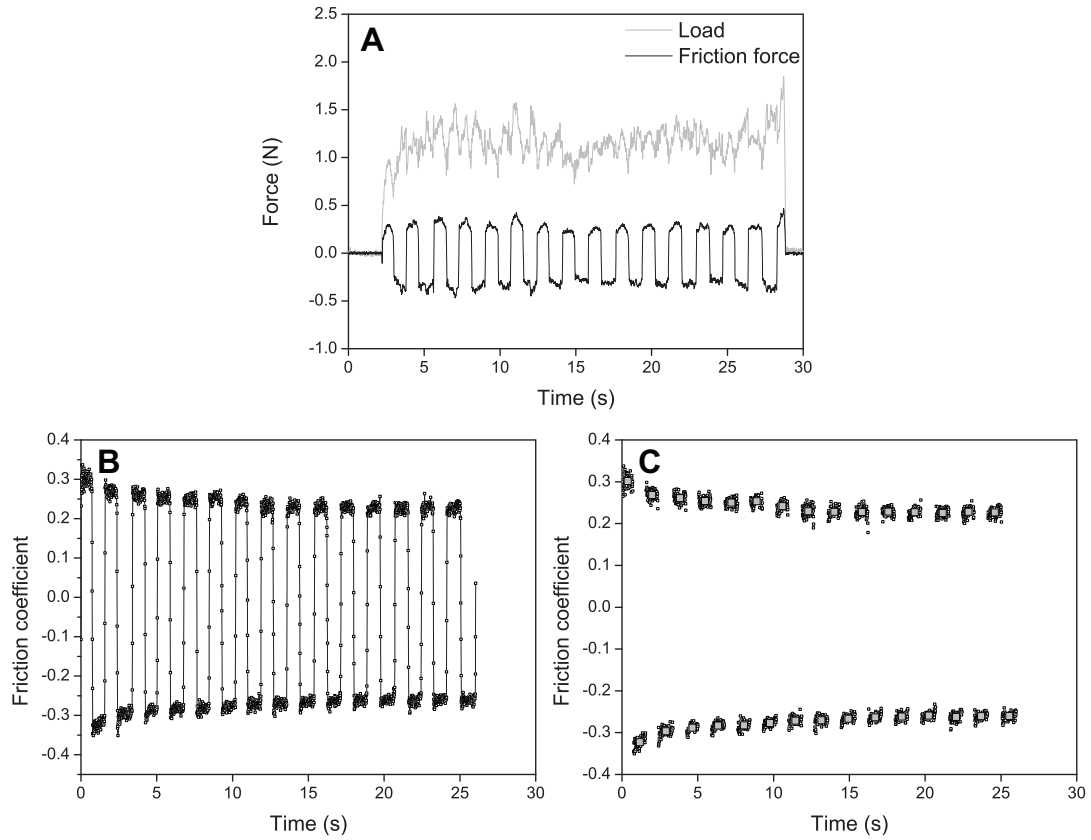
Figure 3.3 Forces and friction coefficients sampled from one measurement (15 stroking cycles) of the printing paper News 45 (**A**) Friction force and load versus time (**B**) Friction coefficient in each sampling point after adjustment of the time (**C**) Friction coefficients after removal of the turning points and the average friction coefficient of each stroke (grey square).

Results and Discussion

The main results of this thesis are summarized in the following chapters. Chapter 4 describes the outcome of the fabrication of model surfaces, and Chapter 5 includes many aspects of the physical measurements with much focus on the finger friction measurements. If you are only interested in the perception part, you can go straight to Chapter 6, but if you continue reading you will see that the physical measurements display some interesting results in themselves.

4 Fabrication of model surfaces with controlled texture

Two approaches were engaged to fabricate model surfaces with the aim of investigating the role of texture or surface roughness in tactile friction as well as tactile perception. Firstly, silica particles of various sizes were deposited onto glass surfaces using the Langmuir-Blodgett technique[145] (Article VI). Secondly, surface wrinkling[146,147] was employed, that generated large enough surfaces to allow one finger moving over the surface, a wide library from nm up to sub-millimeter in wrinkle wavelength and the surfaces could be reused (Article IV and V).

4.1 Particle surfaces

Negatively charged silica particles (30, 60, 90, 200, 800 and 4000 nm) could be deposited onto glass surfaces using Langmuir-Blodgett (LB) deposition after physical modification with a cationic surfactant, hexadecyltrimethylammonium bromide (CTAB). Besides allowing electrostatic attraction to the negatively charged glass surface, this amphiphilic surfactant allows the modified silica particles to stay on the water subphase in the LB trough. A protocol developed by Lee *et al.*[148] and Tsai *et al.*[149] was somewhat modified, for details see Article VI. The silica particles were dissolved in chloroform that evaporates quickly upon spreading onto the water surface. The smaller particle sizes, 30 nm to 90 nm, were filtered before spreading on the water subphase in order to remove aggregates that were formed during the preparation steps. Directly after evaporation each particle, with associated surfactant, has a large mean particle area. However, upon moving barriers over the water surface, this mean area is continuously decreasing until the particles are closely packed in a monolayer. The glass surface, already lowered into the water upon spreading the particles,

was moved upwards through this monolayer as the surface pressure was kept constant, resulting in particle deposition onto the glass surface. The surfactant molecules (organic material) were removed in a sintering step, leaving only the silica particles on the surface. The resulting closed packed monolayers for all particle sizes are displayed in **Figure 4.1**.
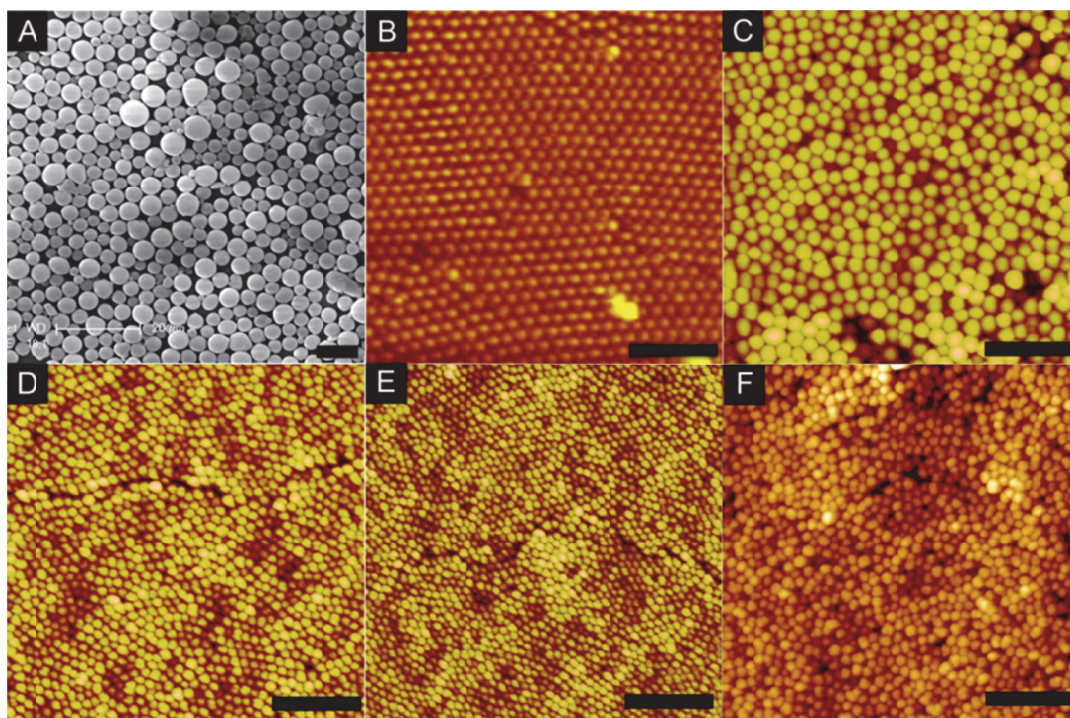

Figure 4.1 *Closely packed monolayer films of silica particles, deposited using the Langmuir-Blodgett technique (**A**) 4000 nm, scale bar 10 µm (**B**) 800 nm, scale bar 10 µm (**C**) 200 nm, scale bar 1.25 µm (**D**) 90 nm, scale bar 0.75 µm (**E**) 60 nm, scale bar 0.5 µm (**F**) 30 nm, scale bar 0.25 µm. The images were obtained with an atomic force microscope (**B-F**) and scanning electron microscope (**A**). Image from Article VI,[150] reprinted with permission © 2011 American Chemical Society.*

An AFM-based wear test was developed to test the stability of the particle monolayer since robust surfaces were demanded for the tactile applications. This test involved reciprocally moving an AFM tip in contact mode over the particle layers at a very high contact pressure (about 2 GPa). The layer was considered robust if the layer was not damaged. Both time (5 − 30) min and temperature (450 - 700) °C was explored, and the optimum sintering conditions found was 30 min at 600 °C. Differences in stability of surfaces sintered at 550 °C and 600 °C for a time period of 30 min are illustrated in **Figure 4.2**.
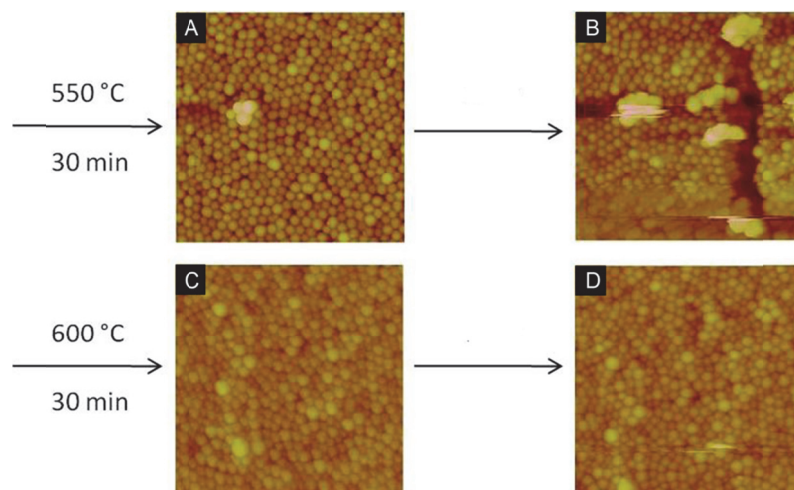
Figure 4.2 *Robustness test of particle films after different sintering times and temperatures by scratching a cantilever tip reciprocally at high contact pressure using an atomic force microscope. Image from Article VI, reprinted with permission,[150] © 2011 American Chemical Society.*

Although conditions that appeared to give robust surfaces were found, successive loss of silica nano particles in tactile exploration could not be completely guaranteed. This consideration together with the rather limited roughness (R_a) span obtained, from 3 nm up to 90 nm, resulted in a second approach to fabricate model surfaces.

4.2   Wrinkle-textured surfaces

This approach is based on *surface wrinkling* that is induced by applying a mechanical stress to a bilayered system with a higher elastic modulus of the top layer.[146,151-153] This buckling instability has been utilized to measure the elastic modulus of thin polymeric films,[151,154-156] as well as a novel method to fabricate patterned surfaces.[147,152,157-159] The procedure of surface wrinkling is schematically illustrated in **Figure 4.3**. A specimen (75 mm × 25 mm) of prepared polydimethylsiloxane (PDMS) was mounted into a strain stage[154] and strained uniaxially from length L to ΔL (or stretched as written in the figure). The strained PDMS was then exposed to either ultraviolet ozone (UVO) irradiation or oxygen plasma (OP) treatment, which oxidize the top layer of the PDMS into a stiffer film. Consequently, this upper part attained a higher elastic modulus compared to the thicker substrate.[152,160] Upon subsequently releasing the strain, *i.e.* placing the sample under axial compression, surface wrinkles were formed spontaneously perpendicular to the direction of strain due to the mismatch in elastic modulus between the stiffer top layer and softer substrate.
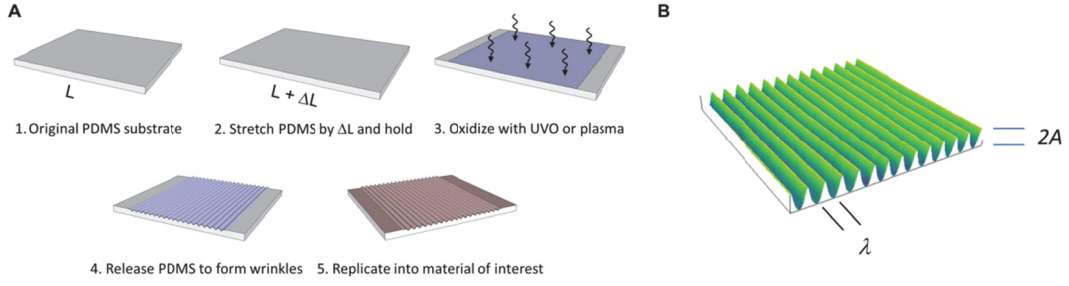
29

Figure 4.3 (A) Schematic illustration of surface wrinkling (B) 3D image, obtained with the stylus profilometer, of a wrinkled surface (WS11) showing the two entities that vary, wrinkle wavelength (λ) and amplitude (A)

The wrinkle wavelength obtained is the optimum wavelength that minimizes the strain energy of the system,[146,161] and this equilibrium wavelength can be expressed as[161,162]

$$\lambda = 2\pi h_f \left(\frac{(1-v^2)E_f}{3(1-v^2)E_s} \right)^{1/3} \tag{4.1}$$

where h_f is the film thickness, E the elastic modulus and v the Poisson's ratio; s denotes the substrate and f the film. Both h_f and E_f increases with increasing treatment time, and therefore the wrinkle wavelength could be systematically altered by employing different treatments times.[146,152] UVO treatment typically produced wavelengths in the order of tens to hundreds of micrometers, and OP typically in the sub micrometer range. On the other hand, the wrinkle amplitude *(A)* could be varied by employing different compressive strains (ΔL/L), since the amplitude depends on the compressive strain *(ε)* according to[152,162,163]

$$A = h_f \left(\frac{\varepsilon}{\varepsilon_c} - 1 \right)^{1/2} \tag{4.2}$$

where ε_c denotes the critical strain needed for onset of wrinkling.[161,162] However, cracks can also be formed if the strain is too high or the exposure time too long,[152,164] due to the brittleness of the surface layer. For the purpose of the end use of these surfaces, it was intended to avoid such cracks. Thus, optimization of both exposure times and critical strains was needed in order to get as wide a library of surfaces as possible.

Each wrinkled PDMS-specimen was replicated into a durable, cleanable surface replica using a UV-curable adhesive polymer (NOA81; Norland optical adhesive). Untreated PDMS-specimens were also replicated, representing surfaces with no systematic sinusoidal texture, hereafter called blank surfaces (BS).

The exposure times and compressive strains for the wrinkled surfaces are listed **Table 4.1**, together with the resultant wavelengths and amplitudes. The obtained wavelengths ranged from 270 nm up to 100 μm and the amplitudes from 7 nm up to 6 μm. This library of surfaces was then used to study the role of texture in tactile perception (Article IV) and tactile friction (Article V).

Table 4.1 Measured wavelengths and amplitudes of the wrinkle-textured model surfaces (WS), together with the exposure times and strains that were used to obtain the wrinkles. The numbering of the surface names is from the smallest to largest wavelength fabricated in this study. The surfaces WS1-WS3 were replicated from OP-treated PDMS, while the surfaces WS4-WS17 were replicated from UVO-treated PDMS.

Surface	Wavelength (μm)	Amplitude (μm)	Exposure time (min)	Applied strain (%)
WS1	0.270±0.040	0.007±0.001	1	6
WS2	0.760±0.050	0.013±0.003	1.5	3.5
WS3	0.870±0.050	0.022±0.005	2.5	3
WS4	17.5±1.0	1.2±0.1	20	60
WS5	17.6±1.0	1.2±0.1	20	48
WS6	20.5±0.9	1.6±0.1	30	40
WS7	25.0±1.1	3.1±0.3	40	55
WS8	25.1±1.2	2.1±0.2	40	35
WS9	31.2±1.4	2.4±0.3	50	25
WS10	34.0±2.4	4.0±0.5	50	34
WS11	37.4±2.6	4.5±0.4	60	35
WS12	39.9±2.9	3.3±0.3	60	20
WS13	42.9±2.6	3.6±0.3	60	25
WS14	46.5±2.6	4.0±0.2	75	20
WS15	70.7±2.9	1.9±0.1	90	14
WS16	90.0±4.3	3.4±0.3	120	10
WS17	98.8±5.9	6.0±0.6	120	12

5   Finger friction results

A tactile (or haptic) approach to measure friction has been developed in order to study the role of friction in tactile perception. These finger friction measurements are included in all articles besides Article VI and the main results are summarized in this chapter. The four images in **Figure 5.1** will be used throughout the rest of this thesis to indicate which stimuli that is considered. Data are presented as means and standard deviations and correlations are presented as Pearson correlation coefficients (r).
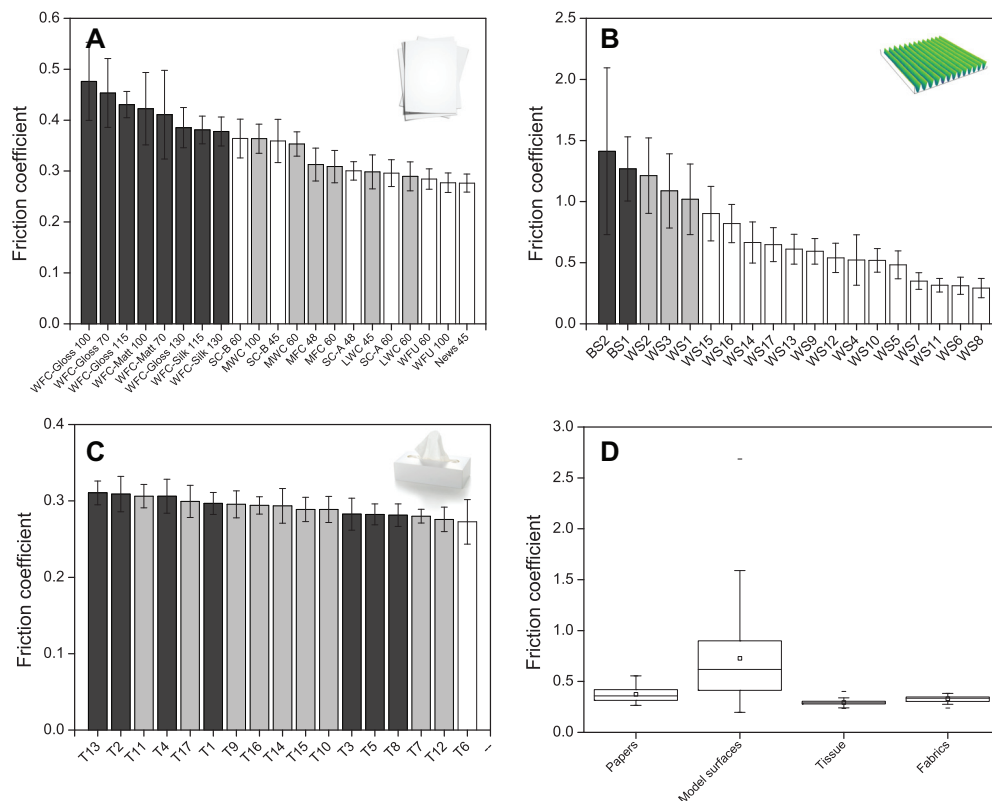

Figure 5.1 Images used throughout Chapter 5 and Chapter 6 to indicate which set of stimuli that is considered.

5.1   Differences in finger friction within a single stimuli set

Figure 5.2A displays the average friction coefficients, averaged over the first three stroking cycles, sorted in decreasing order for the 21 printing papers (n = 4), 19 wrinkled model surfaces (n = 6) and 17 tissue papers (n = 9). The friction coefficients range between 0.276 and 0.476 for papers, 0.292 and 1.41 for the model surfaces and 0.273 and 0.311 for tissue. A comparison of the friction coefficients for the different stimuli groups, as well as fabrics (wool, acetate, cotton and polyester), are shown in a box plot in **Figure 5.2**D. The model surfaces show the greatest friction coefficient with an average of 0.73, followed by paper (0.38), fabrics (0.33) and tissue (0.29). The model surfaces also show greatest variations in friction coefficient within the group, displayed by a large range in **Figure 5.2**D. This illustrates the danger of referring to "a material" without taking into account the differences within a group of materials.

The printing papers group naturally according to the paper grade. The WFC papers show the highest friction coefficient and the uncoated papers (newsprint and WFU) display the lowest, with coated mechanical papers grouped together, and the SC-papers place intermediate. The SC-B papers, containing recycled fibers, show higher friction than the SC-A papers made of virgin fibers.

Figure 5.2 Average finger friction coefficients (mean ± SD), sorted in decreasing order for printing papers (**A**), model surfaces (**B**) and tissue papers (**C**). Note the differences in scale on the y-axis. A comparison between the materials is illustrated by a box plot (**D**), showing the respective mean (small square) and median (line) inside the box, representing the upper and lower quartile. The whiskers symbolize the maximum and minimum values that are not extreme outliers. The colors, dark grey, light grey and white, only have significance within each figure, representative of different sub-groups; wood-free coated papers, coated papers from mechanical pulp and uncoated papers: blank surfaces, nanoscale surfaces and microscale surfaces: absorbent tissue, bathroom tissue and personal care tissue, respectively.

Out of the model surfaces, the blank surfaces (BS) with no systematic pattern, display the highest friction coefficients, followed by the nanoscale surfaces and further microscale pattern surfaces. These results show that friction measurements with the piezoelectric force sensor can discriminate a set of similar surfaces such as printing papers of different paper grades and patterned surfaces ranging in wavelength from nanometer to sub millimeter in terms of finger friction. However, no large differences in friction were obtained for the various tissue samples or textile fabrics.

5.2 Friction coefficient decreases with increasing roughness

There is a trend that the friction coefficient decreases with increasing surface roughness of the printing papers, as revealed by **Figure 5.3**, although the correlation is weak (r = 0.72). *News 45* is the roughest paper of the stimuli set, and also displays lowest friction. This decreasing trend was assumed to depend on the real contact area,[33,34,53,165] where rougher papers are expected to have a smaller number of contact points with a finger and therefore lower friction. As can be seen in **Figure 5.3**B, the friction appears independent of the weight of the paper. Hence, the friction coefficient seems to be linked to the surface and not the bulk of the paper, which is reasonable.
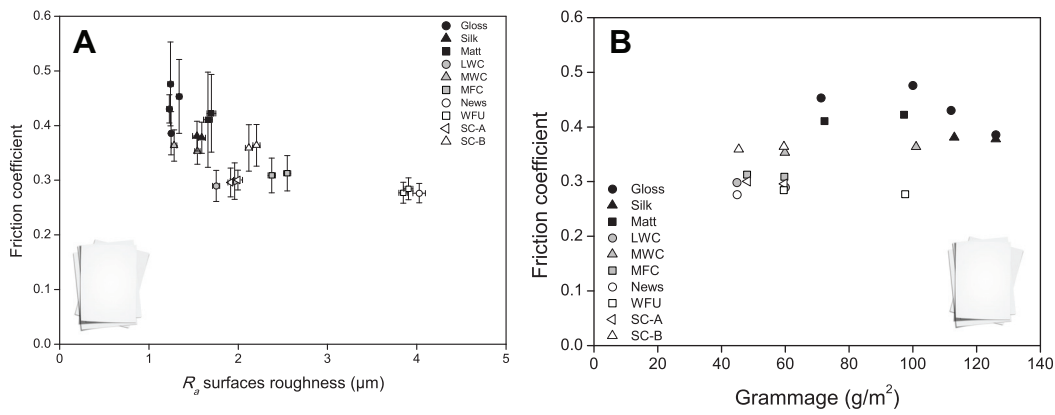

Figure 5.3 *Friction coefficient versus R_a surface roughness (**A**) and paper grammage (**B**). The symbols (same in both figures) display the different paper grades. Data are presented as mean ± SD. Article I[165]*

Although friction is reasonably explained by the surface roughness (R_a), the effect of coating type and amount of coating cannot be completely ruled out. Generally, WFC papers and MWC papers, which display the highest friction coefficients in this study, contain higher coat weight than LWC and MFC papers. Also, the SC-B papers that show higher friction coefficient than SC-A, consist of a higher filler content. Therefore, it is possible that the amount and composition of the coating and the fillers in the paper and also chemicals in the pulp, can give rise to more specific interfacial interactions which affect for example the adhesion and therefore also the friction. No detailed information was available on the type or amount of coating of the commercial papers used, and therefore the investigation of any influence of paper surface chemistry is not considered in this thesis.

The role of surface texture in tactile friction was further addressed by fabricating model surfaces of the same material and varying solely wrinkle wavelength and amplitude. The finger friction coefficient is plotted versus the wrinkle wavelength in **Figure 5.4**A. The friction coefficient decreases with increasing wavelength up to about 30 μm and then it starts to increase again, first thought to be due to an adhesion contribution at low wavelengths and a deformation component at higher wavelengths. A somewhat similar trend was noted with the wrinkle amplitude, down to about 2 μm; above that no correlation between friction and amplitude is seen (**Figure 5.4**B). If instead the ratio of amplitude and wavelength (A/λ) is considered a characteristic length scale,[157] an interesting relation with the friction coefficient appears (**Figure 5.4**C). The results imply that the friction coefficient decreases with increasing aspect ratio, *i.e.* either with increasing amplitude or decreasing wavelength. Since the surfaces are made from the same material, the observed differences in friction presumably depend on the real contact area.
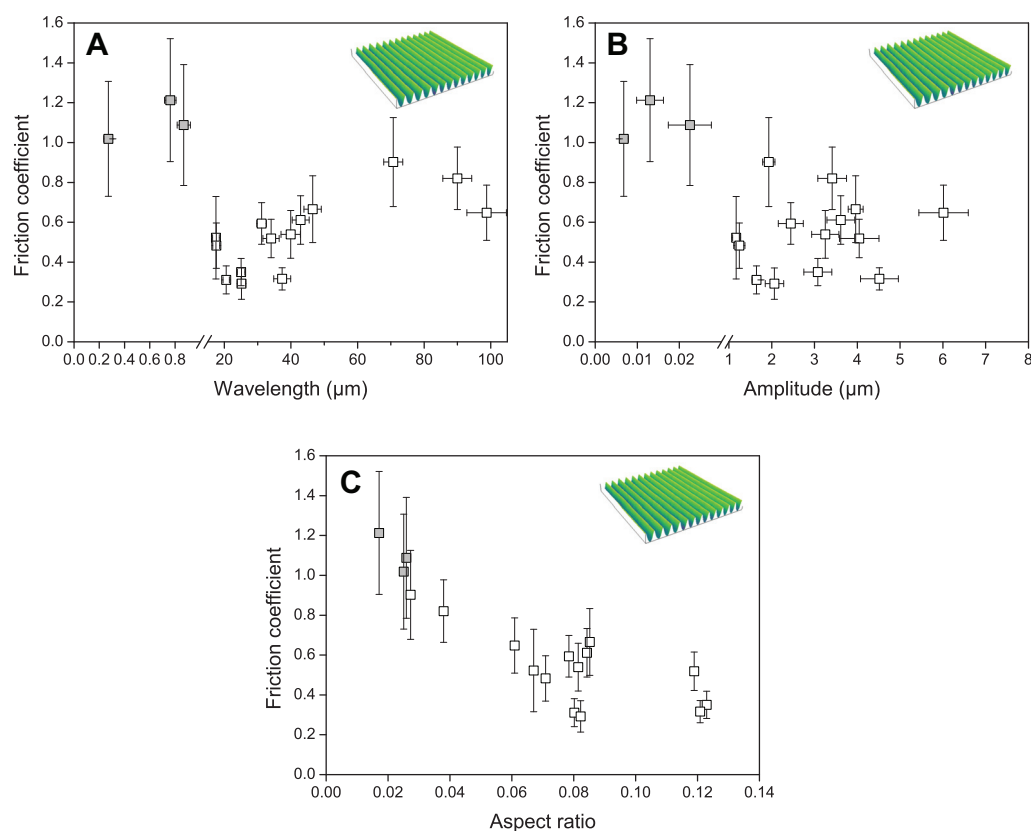

Figure 5.4 *Finger friction coefficient versus wrinkle wavelength (**A**), amplitude (**B**) and aspect ratio (**C**). The nanoscale surfaces (WS1-WS3) are displayed as filled symbols and microscale surfaces (WS4-WS19) as unfilled symbols. Not the break in the x-axis scale in **A** and **B**. Data are presented as mean ± SD. Article V[166]*

5.3 Contact modeling - friction is a function of real contact area

An analytical model was employed to investigate if the role of aspect ratio on friction is due to differences in real contact area. The analytical model used, introduced by Westergaard,[167] assumes a contact between an elastic half-space and a rigid wavy surface with a characteristic wavelength and amplitude. It is valid to approximate this as a contact between a wavy surface and a flat elastic finger, since the wavelength of the finger ridges is much greater than that of the wrinkled surfaces (**Figure 5.5**). One single contact, *i.e.* one wrinkle, is evaluated and considered to be representative of the contact ratio for the whole contact.
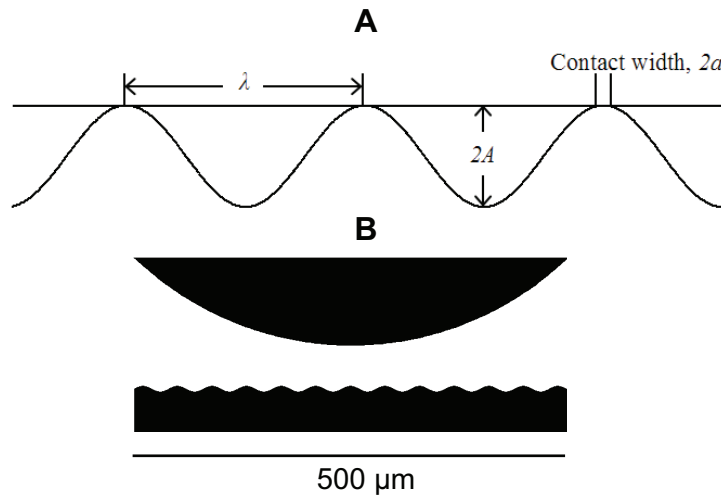

Figure 5.5 (A) Schematic illustration of the assumed contact used to approximate the contact ratio between a flat elastic finger and the wrinkled surfaces with a characteristic wavelength (λ) and amplitude (A). The contact ratio is defined as 2a/λ and when 2a equals to λ, complete contact occurs. (B) Comparison of one approximated finger ridge and surface WS12 with a wavelength and amplitude of 40 μm and 3.3 μm, respectively.

The employed model[167] expresses the ratio of the real to the apparent contact area according to:

$$\frac{2a}{\lambda} = \frac{2}{\pi} \sin^{-1} \left(\frac{\overline{p}}{p^*} \right)^{1/2} \tag{5.1}$$

where a is half the width of a singular contact, λ is the wrinkle wavelength, $\overline{p}$ is the actual surface pressure, approximated with *eq. 5.2*, and p^* is the pressure needed for full contact (*eq. 5.3*). The pressure needed for full contact depends on the effective Young's modulus E^* for the materials (*eq. 5.4*) and the amplitude and the wavelength of the surface.

$$\bar{p} = \frac{L}{\pi r^2} \tag{5.2}$$

$$p^* = \pi E^* \frac{A}{\lambda} \tag{5.3}$$

$$E^* = \left(\frac{1 - v_{finger}^2}{E_{finger}} + \frac{1 - v_{surface}^2}{E_{surface}} \right)^{-1} \tag{5.4}$$

The values used to calculate the contact ratios are shown in **Table 5.1**. The Young's modulus of the finger was given a value of 0.2 MPa, and the Poisson ratio a value of 0.4, values in agreement with reported values in the literature,[82,168,169] and chosen so that no surface gave 100 % contact ratio. Dandekar *et al.*[168], reported an epidermal modulus of 0.18 MPa for a human fingertip and Maeno *et al.*[82] estimated the Young's modulus of the epidermis to be 0.14 MPa, whereas the softer dermis and subcutaneous tissue showed values of 0.08 and 0.034 MPa, respectively. The Young's modulus and Poisson ratio of the wrinkled surfaces were provided by the supplier of the UV-curable adhesive.

Table 5.1 *Parameters used in the analytical model to estimate the contact ratio between a finger and the wrinkled model surfaces.*

	Values
E_{finger}	0.2 MPa
$E_{surface}$	1,379 MPa
v_{finger}	0.4
$v_{surface}$	0.4
Load	1 N
Apparent contact diameter	10 mm
Contact pressure	0.0127 N/mm²

The finger friction coefficient is plotted versus both the aspect ratio and the estimated contact ratio for the various surfaces in **Figure 5.6**, as a 3D scatter plot. As can be seen, the aspect ratio and contact ratio are inversely related to each other, and the friction coefficient decreases with increasing aspect ratio (as discussed before) and increases with the contact ratio, also depicted in **Figure 5.6**B. Therefore, this model suggests that differences in finger friction are due to different contact ratios or real contact areas, a key parameter directly related to the adhesion mechanism of friction. The finger is allowed to have greater contact area if the spatial separations are greater or the heights of the wrinkles are lower. It is interesting to note that the nanoscale surfaces follow the same trend as the microscale surfaces. Based on this result, we assume that the friction behavior on the printing papers is also due to the real contact area.
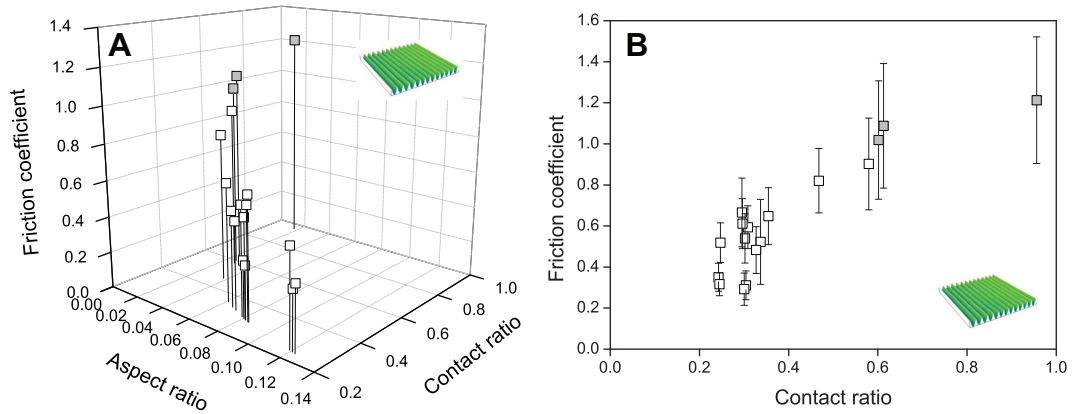

Figure 5.6 (A) 3D scatter plot of friction coefficient versus aspect ratio (amplitude/wavelength) and estimated contact ratio (B) Friction coefficient versus estimated contact ratio for the different wrinkled-textured model surfaces. Data are presented as mean ± SD. Article V[166]

Unfortunately, surface roughness on the tissue samples has not been measured in a way that can be compared with the printing papers or model surfaces; however, by eye one can see that they are much rougher. These rougher tissue surfaces seem to display a roughness scale where the friction coefficient is independent of the roughness. It might be that the real contact area is similar between a finger and all the 17 tissue stimuli, and therefore the adhesion contribution to friction for all tissue papers does not vary considerable, resulting in that analogous friction coefficients are obtained.

5.3.1 Real contact area important also for thermal conductivity

The physical measure of thermal conductivity also bears an interesting relation to the surface roughness, as can be seen in **Figure 5.7**. In Section 5.3, a relationship between friction and real contact area was established and it reasonable that thermal conductivity is also dependent on the real contact area. More contact points allows more heat to be transferred.
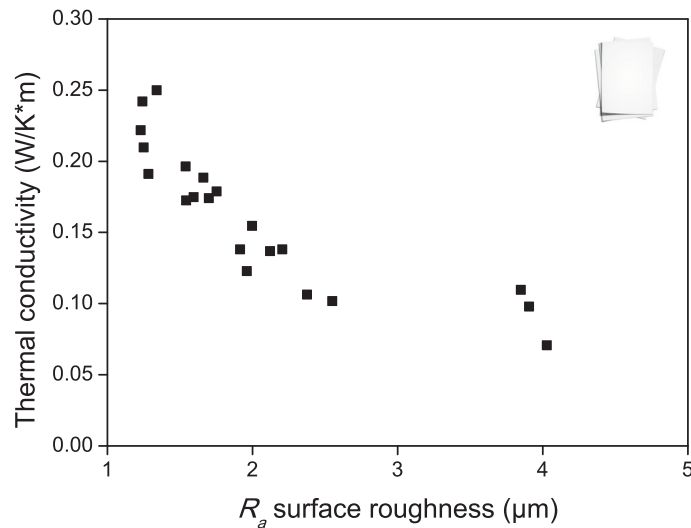

Figure 5.7 *Thermal conductivity plotted versus the R_a surface roughness for the 21 printing papers, indicating that thermal conductivity, just like finger friction, depends on the real contact area of fine textures.*

5.4   Similar trends but large individual variations in friction coefficients

Several participants performed finger friction measurements on a selection of eight papers (Article II) to investigate if measurements performed by a trained experimenter can be considered representative of a larger population. As can be seen in **Figure 5.8**, the same trends in friction were obtained when taking the average of the group (Article II) and compare that with the results from the first study (Article I). The WFC papers (Gloss and Matt) display the highest friction and the uncoated papers the lowest (News, WFU and SC-A). An additional observation is that there were large deviations between the 14 participants, consistent with other studies where different people have measured finger friction on various substrates.[53,57] For example, considerable differences in friction coefficients among 12 subjects were found by Derler *et al*.[53], which was due to different states of hydration. Hence, the variations in this study may well be explained by different skin hydration states of the

participants. This is just speculative, since the moisture content of the finger tips was not measured.
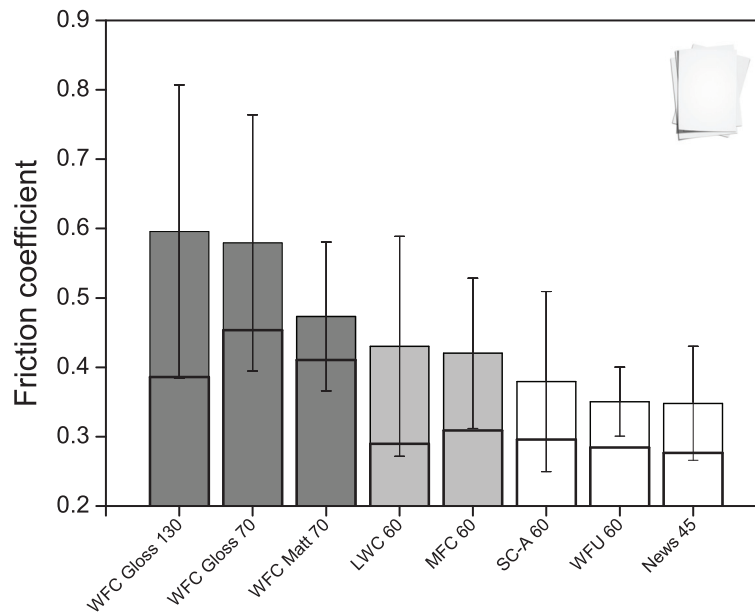

Figure 5.8 *Average friction coefficients (mean ± SD) of eight selected papers, measured by 14 participants. The results from the previous study with one experimenter (Article I) are shown as transparent columns with thicker black border line. The wood-free coated papers (dark grey) display the highest friction. Article II[170]*

The results show that finger friction measurements by one individual are representative of a larger population, if considering relative comparison of friction coefficients within a set of surfaces. However, comparison of exact values of friction coefficients obtained by two different persons should be avoided.

5.5   Load is regulated by the friction force encountered

An interesting and unexpected finding that came out of this study is that the participants regulated the *applied load* in response to the perceived friction even though they were instructed to use a constant preferred load. Higher friction papers resulted in a lower force applied as depicted in **Figure 5.9**. In contrast, higher loads could be applied, if a low friction was encountered. This suggests that there is some optimum friction regime that is comfortable upon feeling a surface and that allows the finger to smoothly slide over the surface. These adjustments in load, that most probably occur unconsciously, show that humans are very sensitive in responding to friction signals. This can be related

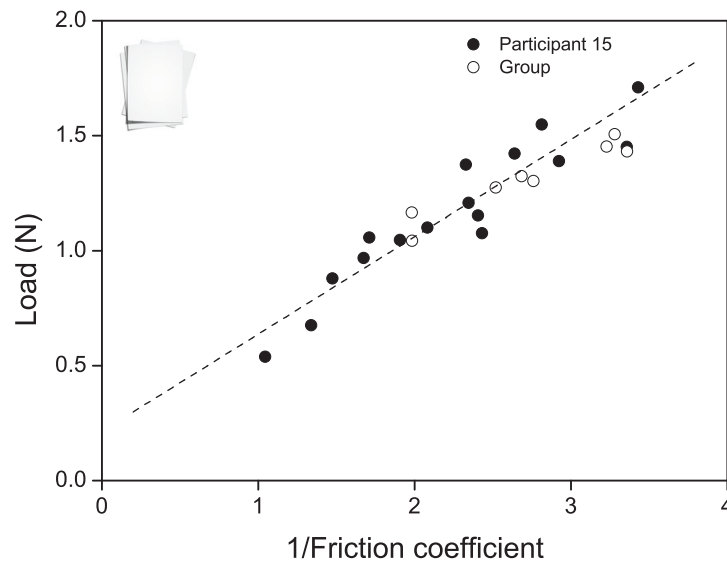to previous studies on grip showing that humans adjust the load based on friction to optimize grip.[63,64]

Figure 5.9 *Applied load versus the inverse of the friction coefficient obtained from all measurements of participant number 15 (n = 16) and also the average of the group. This shows that the load that was supposed to be kept constant is actually varied depending on the friction coefficient. The linear fit (r = 0.94) has a slope of 0.42, corresponding to some optimum friction force for surface interrogation. Article I*[165]

5.6   Decrease in friction due to transfer of lipids

An observed decrease in friction coefficient during repeated stroking (one measurement) on printing paper is discussed in Article I. Considering the difference in average friction coefficient between the last and first stroking cycle, the decrease varied from 20 % to 42 %, where the greatest decrease is seen during the first couple of strokes. Generally, the smoother coated papers display a greater decrease compared to the rougher uncoated papers, except SC-B. This phenomena of decreasing friction during repeated sliding or contact with a human finger has been reported elsewhere for paper[51,171] and other materials.[34] This decrease in friction is discussed in terms of moisture being transferred to the porous paper[51] and transfer of lipid material.[34] A decrease in friction has also been observed over the first contacts on paper-to-paper friction,[172,173] where the decrease has been associated with progressive damage of the paper surface.[173]

To further investigate the decrease in friction observed on the printing papers, the change in friction coefficient over the 15 stroking cycles is evaluated for all

friction measurements performed within this thesis work and compared in **Figure 5.10** by means of a box plot. The average change for each material is considered as a comparison, although differences within each material group exist. In an additional experiment, changes in friction were compared between a finger and a steel ball and elastomer ball on a selection of five papers; these results are also presented in **Figure 5.10**. As can be seen, all materials stroked by a human finger show an average decrease in friction, whereas a steel ball and elastomer ball give a rise in friction coefficient over time. Whereas the increase in friction coefficient may be due to wear, the decrease is most probable due to deposits like sweat and lipids from the human finger. This seems highly probable in view of the fact that humans leave latent fingerprints on surfaces that are touched.[80] A set of experiments were performed in order to further study the cause of this change in friction over time, as described in Article I.
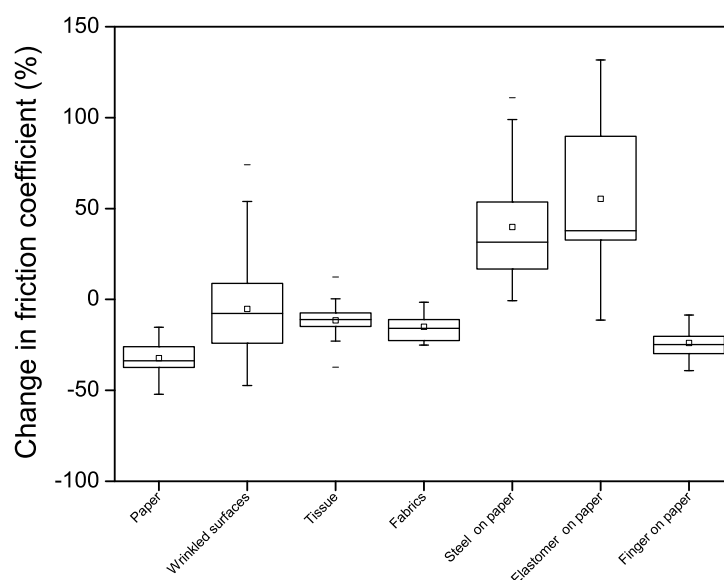

Figure 5.10 *Comparison of changes in friction coefficient for the different materials within this thesis work, measured by one individual. The box plot shows the respective mean (small square) and median (line) inside the box, representing the upper and lower quartile. The whiskers symbolize the maximum and minimum values that are not extreme outliers. All materials that have been stroked with a human finger exhibit an average decrease in friction coefficient over 15 stroking cycles, whereas a paper surface stroked with a steel ball or elastomer ball display an increase instead.*

A filter paper stroked with a finger 15 times back and forth as in the finger friction measurements, were studied with XPS, and compared with the signal of an untouched filter paper. High-resolution carbon spectra are depicted in **Figure 5.11**, showing an increase in the C1-signal from 6 % for clean filter

paper to 37 % for stroked filter paper. Additional low amounts of N, Si, Na and S were found, which is consistent with bio deposits from the finger such as salt and proteins. This increase in the C1-carbon signal strongly indicates that lipid material is transferred from the finger to the surface upon stroking in finger friction measurements, and it seems highly probable that this lipid material can act as a lubricant film and lower the friction. However, the origin of these lipids is not entirely clear. It is known that fingerprint ridge deposits from the hands come from eccrine sweat glands, *i.e.* secreted sweat that does not contain any fatty acids.[80] Sebaceous glands however, located on all parts of the body besides the palms of the hands and soles of the feet contain fatty acids and hydrocarbons. Therefore, deposits from washed hands should not contain sebaceous material.[174-176] Instead of lipids secreted from the sweat glands, it may be epidermal lipids[175] from stratum corneum cells that end up on the surface together with sweat deposits from eccrine sweat glands. On a smoother surface, more lipids are likely to be deposited due to a larger real contact area, enhancing the effect of lubrication. This can help explain why smoother papers show a larger decrease in friction compared to the rougher papers.
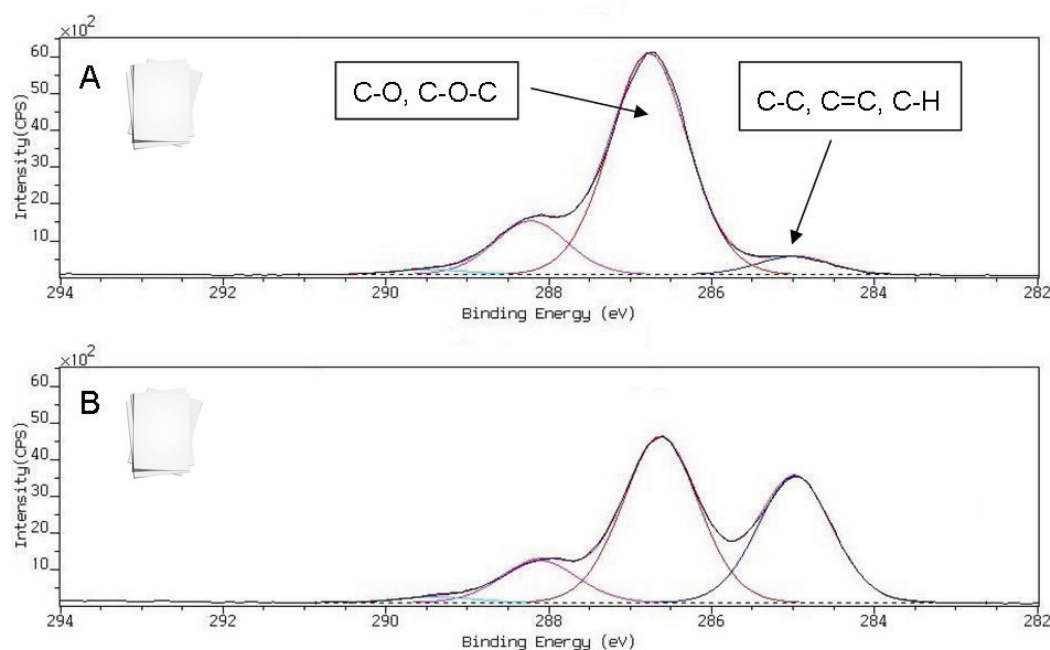

Figure 5.11 *Curve fitted high-resolution carbon spectra (C 1s spectra) for (**A**) virgin filter paper used as a reference sample and (**B**) after stroking the filter paper surface 15 times with the index finger as in the finger friction measurements. An increase in the C1-carbon (C-C,C=C, C-H) from 6% (**A**) to 37% (**B**) of the total carbon signal, as well as a decrease in the C2-carbon (C-O, C-O-C) is detected after stroking the finger. This increase in C1-carbon is possibly originating from hydrocarbon chains in skin lipids. Article I.[165]*

Figure 5.12 depicts three repeated finger friction measurements on the same paper sample of *WFC Matt 100*. As can be seen, the friction coefficient decreases during the first strokes on a new sample, and then it flattens out. The following two measurements (each performed after a pause of 30 s) on the same sample do not show the decrease. When changing to a new sample, the friction starts with a high value again, following by a fast decrease. The same trend is also observed for the three other papers tested: *WFC Silk 130*, *SC-B 60* and *WFC Gloss 100*. Lipids in a latent fingerprint stay on the surfaces at least for 24 hours[80], as a result the lubricating properties remain for the second and third measurements in **Figure 5.12**.
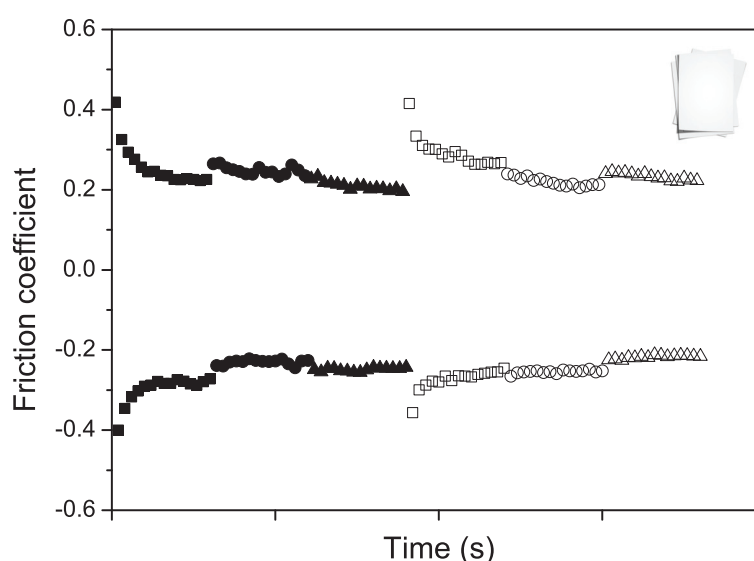

Figure 5.12 Black symbols: three finger friction measurements on the same paper sample (WFC-Matt 100) with a waiting time of 30 seconds between each measurement. White symbols: a new WFC-Matt 100 paper is measured three times. A considerable decrease is only observed during the first couple of strokes on a new paper sample. Each measurement (15 cycles) ranged about 25 seconds. Article I.[165]

The glands are continuously secreting sweat;[34] however, it is not always perceptible. Thus, lipids are deposited together with water which makes up 98-99 % of the sweat content.[80] If there is an absorbing material like printing paper, tissue paper and textiles as used within this work, the moisture should be absorbed into the surface; otherwise water stays on the surface and then contributes to an increase in friction. The model surfaces are not porous, suggesting that sweat can stay on the surface, and therefore work against the lubrication mechanism with lipids. Actually, a slight increase is first observed in the friction coefficient of model surfaces, possibly due to moisture from the finger, following by a decrease (moisture evaporates). Finally, a larger real

contact are should result in that more lipids and moisture are transferred from the finger to the surface. For that reason we see a lower decrease in friction for tissue and fabrics that are macroscopically rough. It is therefore concluded that the reason for the observed friction decrease is the transfer of lipid material, the greater the contact area the greater the lubricating effect. However, this mechanism is competing with the effect of moisture being secreted from the sweat glands that can increase friction.

5.7 Frequency content in friction force

Fast-Fourier-Transform analysis (FFT) of the friction force and normal force indicates that there are two types of sliding, showing different bandwidths or dynamics in the amplitude spectrum, as can be seen in **Figure 5.13**, when comparing the inset figures in A and B (more dynamics) with the insets in C and D (less dynamics).
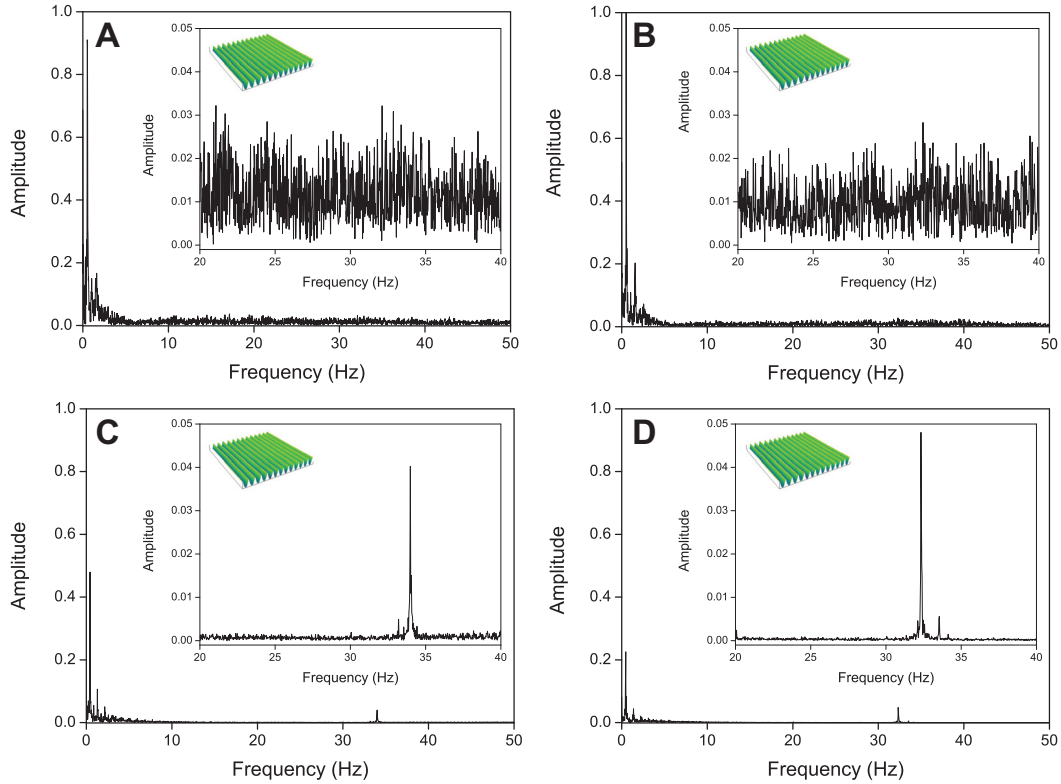

Figure 5.13 *Frequency content of the friction force of four different surfaces: (**A**) WS1, (**B**) WS3, (**C**) WS8 and (**D**) WS9. The insets are magnifications from 20 Hz to 40 Hz. More dynamics are present in the friction force of the nanoscale surfaces (**A** and **B**). Article V[166]*

A greater bandwidth (*more dynamics*) was obtained for the surfaces with lowest aspect ratio, *i.e.* the blank surfaces (BS1 and BS2), nanoscale textures (WS1-WS3) and the surfaces with largest wavelengths (WS15-WS17). This suggests that the textures which give rise to a high real contact area with a finger and consequently higher friction, as discussed in Section 5.3, show more dynamics in the forces to a greater extent. Stick-slip was noted on the very same surfaces, suggesting that the greater bandwidth of the frequency content in the friction force emerge from stick-slip. In contrast, the textures with higher aspect ratio show less bandwidth in the amplitude spectrum. It is speculated that this

dynamics may be connected to how the surfaces are perceived when touching them, where more dynamics most probably are associated with a more unpleasant feeling.

Interestingly, a frequency peak at 30 ± 1 Hz is observed for all surfaces, as can be seen in **Figure 5.14**. Since the peak appears on all surfaces, independent of the wrinkle wavelength (**Figure 5.14**A), it may be that the origin of this peak is due to the finger ridges. Dividing the stroking speed (approximated to be 25 mm/s) with the frequency peak of 30 Hz, results in a wavelength of 800 μm, about the same length scale as the finger ridges. This frequency also corresponds to the resonance frequency of the skin,[177] and given the similarity of the numbers it may be that there is an evolutionary relationship between the fingerprint spacing and this parameter.

The same frequency analysis was performed on the friction measurements with different participants (Article II) on eight selected printing papers. The average frequency peak for each participant is displayed in **Figure 5.14**B. The frequency peak ranges from 27 Hz up to 36 Hz, but here the participants could vary the speed and it is not clear whether the frequency variations reflect differences in fingerprints or in speed or a combination of both.
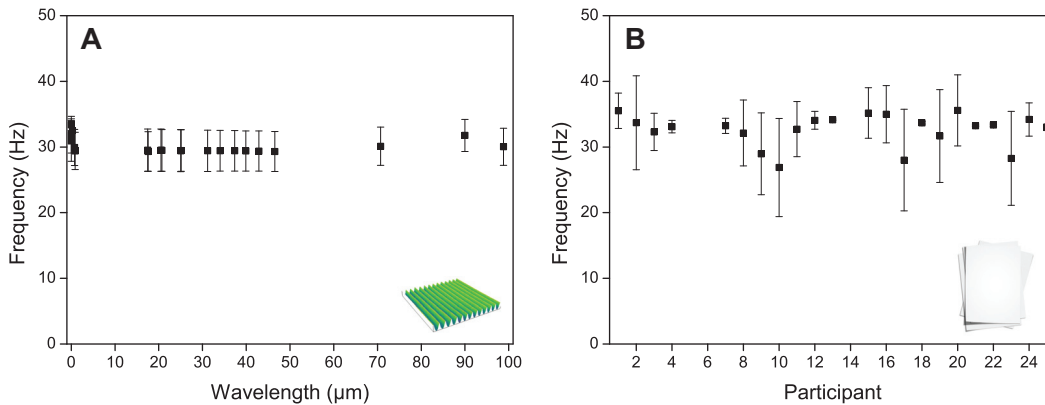

Figure 5.14 *The main frequency peak, obtained from frequency analysis of the friction force, versus wrinkle wavelength (**A**) and participant number (**B**).*

5.8   Stability of wrinkled surfaces

Two sets of patterned surfaces were replicated. It was decided to use one set of surfaces whereas the second set was kept in reserve in case something happened to one of the surfaces. The surfaces were checked in an optical microscope regularly. After all friction measurements and tactile exploration, each surface had been touched between 850 and 1600 times including cleaning after each handling procedure. **Figure 5.15** illustrates wear of the surfaces, primarily encountered in the middle of the surface where people mainly felt. The material that ended up in the valleys was assumed to originate from deposits from the finger; however, analysis with Confocal Raman on the worst contaminated surface (WS4), indicated that the material in the valleys actually are wear from the surfaces, since both the peak and the valley gave rise to the same Raman signals as shown in **Figure 5.15**D-E. During Raman analysis some organic material caused fluorescence, most probably deposits from the finger left on the surface. As revealed upon comparison of all microscopy images, the surfaces exhibiting the lowest aspect ratios contain less material in the valleys.
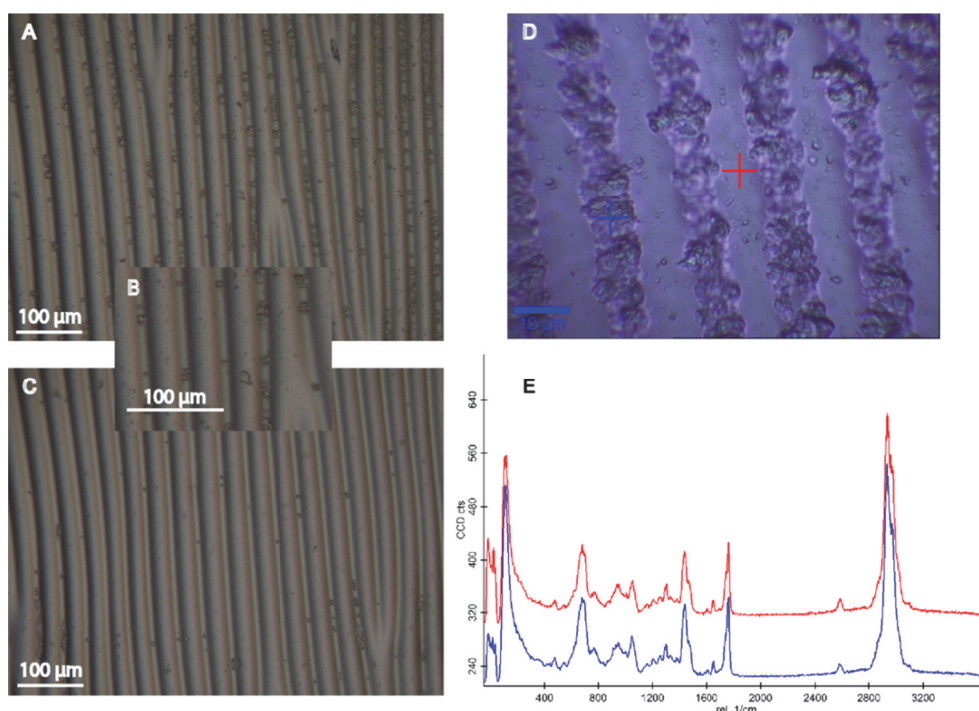

Figure 5.15 Optical microscope images of surface WS12, showing more wear in the middle of the surface (*A* and *B*) compared to the edges (*C*). (*D*) Confocal Raman image of surface WS4 (the surface with most material in the valleys) showing that the debris is tare from the surfaces, concluded from identical confocal Raman signal spectra (*E*) on and between the wrinkles. The magnification is 10x (*A*-*C*)

5.9   Tactile friction of liquid crystalline phases

The tactile friction approach was further extended by means of using finger friction measurements to study frictional behavior of topical formulations (Article VII). Although considerable research has been devoted to evaluate the tribological properties of skin creams using AFM,[18,178-180] or rotational probes on the skin,[47-49] as discussed in Section 2.2, less attention has been paid to measuring friction upon moving fingers over a skin treated area, in which the friction encountered should resemble the friction perceived, *i.e.* tactile friction. As a first approach to studying the feasibility of detecting differences in these lubricated contacts, model skin creams with considerably different tactile properties were studied. In these measurements friction was measured between an index finger and formulation applied onto a model skin substrate (Vitro-Skin®, IMS Inc.).[181-183] As a check of finger status, a reference measure on an untreated part of the model skin was always performed prior to the actual measurement.

Three formulations; lamellar (A), cubic (B) and reversed hexagonal (C), were prepared to represent different liquid crystalline phases from the ternary monoolein-sodiumoleate-water system[184] shown in **Figure 5.16**.
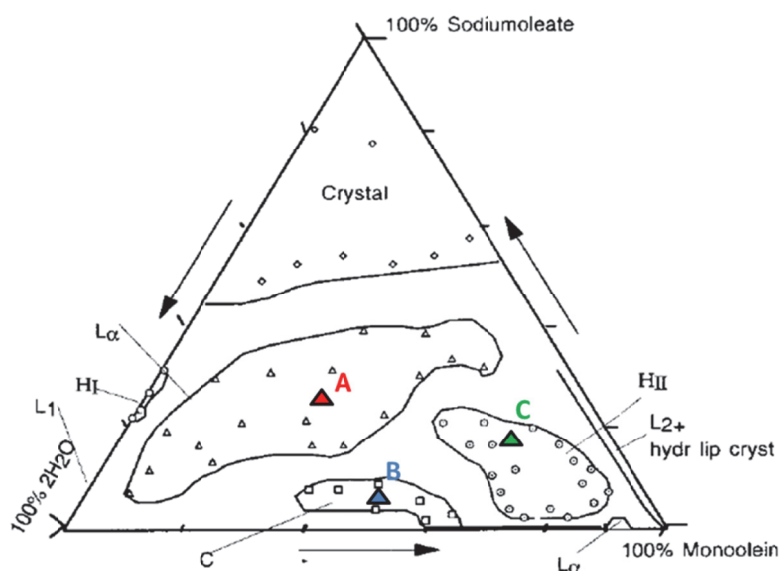

Figure 5.16 *Ternary phase diagram for the monoolein-sodiumoleate-water system[184], with formulation A (28%:27%:45%, w/w/w), B (48%:7%:45%, w/w/w) and C (64%:16%:20%, w/w/w) shown as red, blue and green, respectively, representing three different liquid crystalline phases: lamellar phase, cubic phase and reversed hexagonal phase. Adapted with permission,[184] copyright (2001) American Chemical Society. Article VII*

Finger friction was measured directly after spreading with a gloved finger (allowing more even film thickness) as well as after 2.5 min, 6 min and 20 min, to see if changes in friction could be obtained with time due to water evaporation. Evaporation experiments indicated that Formulation B and C undergo phase transitions, based on the amount of water that evaporates. The friction coefficients obtained are displayed in **Figure 5.17**. Formulation A showed a lamellar structure from the beginning and was still in the lamellar phase after 20 min, and no change in friction was seen over time. For Formulation B, on the other hand, a dramatic reduction in friction coefficient was already observed 2.5 min after application, accompanied by a phase transition from cubic (isotropic) to a mixture of reversed hexagonal, lamellar and isotropic phases. For Formulation C, reversed hexagonal phases became more abundant within a minute after application, followed by a transition to a mixed phase with isotropic regions, where the isotropic region increased with time (**Figure 5.18**C). This probably explains why a decrease in the friction coefficient was observed for Formulation C between 6 min and 20 min (**Figure 5.17**).

The actual phase structures at each measured point of time were verified by optical microscopy, see **Figure 5.18**. Thus, it appears that different liquid crystalline phases give different friction; cubic > reversed hexagonal > lamellar. Moreover, changes in friction over time are accompanied with phase transitions associated with water evaporation. According to the author's perception, the three phases exhibit considerable different tactile properties: the cubic phase feel sticky, the reversed hexagonal phase greasy whereas the lamellar phase, which has a similar structure to the outer layer of skin, has a softer feel. Reversed hexagonal and cubic phases are not traditionally used in skin creams, however, they have shown interesting topical delivery properties for pharmaceutical components to the skin and mucosa.[185-187]
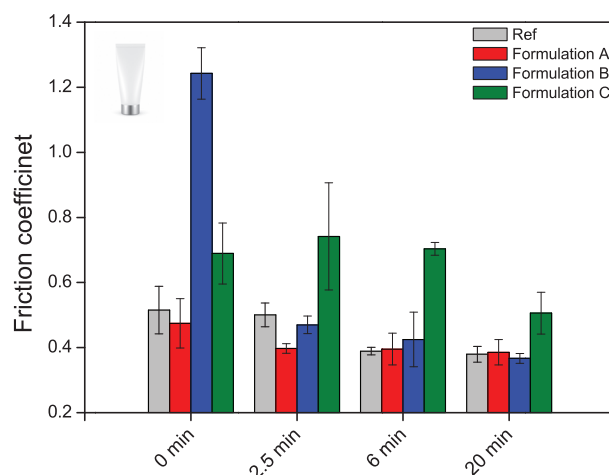
Figure 5.17 *Friction coefficients measured between an index finger and model skin after application of formulations of different liquid crystalline phases; lamellar phase (A), Cubic phase (B) and mainly reversed hexagonal phase (C), at different times; immediately after application and spreading (0 min), as well as after 2.5 min, 6 min, and 20 min. Data is presented as mean ± SD. Changes in friction over time are associated with phase transitions upon water evaporation. Article VII*
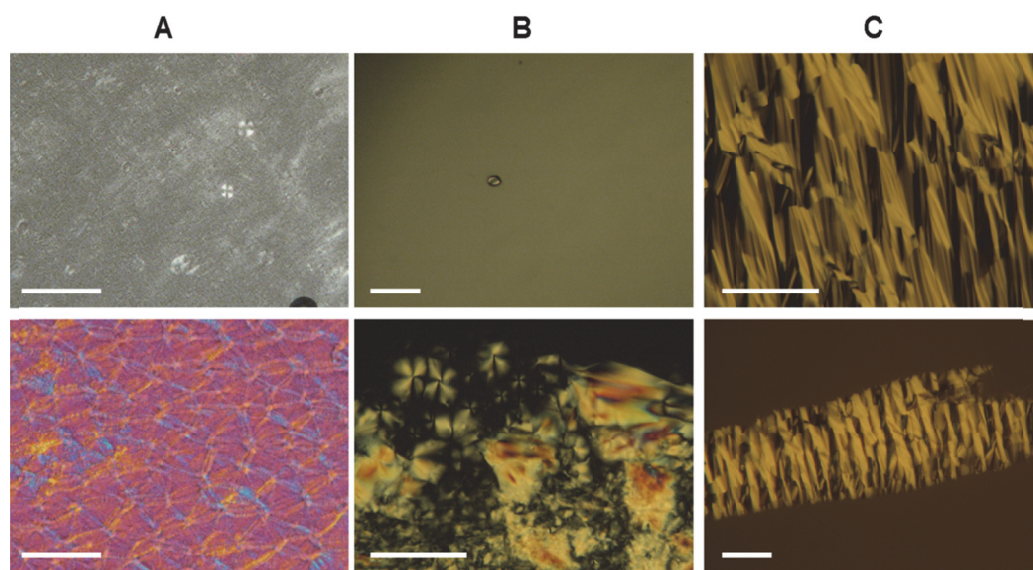

Figure 5.18 *Optical microscopy images of formulation A, B and C directly after spreading on a cover glass (first row) and after exposure to the surrounding environment for 6 min (formulation B) and 20 min (formulation A and C) (second row); The magnification is 10x or 20x and the scale bar is 100 μm. Article VII*

Furthermore, the friction coefficient of the references decreased with time as water evaporated from the hydrated model skin, a result in concordance with the literature for human skin.[21,34,71] Besides model cream formulations, Article VII also deals with finger friction measurements on commercial topical formulations containing different humectants, and the interesting reader is referred to the appended manuscript.

6 Tactile perception

This chapter starts with a brief description of the method of magnitude estimation, *i.e.* intended for scaling perceptual quantities, followed by a summary of the main unidimensional psychophysical results. Further, the method of similarity scaling is described and the multidimensional perception results are discussed. All perception experiments, summarized in **Table 6.1**, were conducted according to the guidelines from the Ethical Committee for Social Science Research at Stockholm University. **Figure 6.1** shows a participant during an experimental session of similarity scaling on the model surfaces.

Table 6.1 *Summary of the unidimensional (ME) and multidimensional (MDS) perception experiments (the author of this thesis was considerably involved in the experiments shown in bold).*

Experiment	Attributes	Number of stimuli	Number of estimations*	Participants	Article
ME printing paper	**coarseness**	**8**	**56**	**10 women and 14 men 22-29 years old**	**II[170]**
ME printing paper	smoothness coolness dryness thickness	21	504	10 women 21-47 years old	III[188]
ME tissue paper	smoothness softness thickness bulkiness	17	408	14 women 19-41 years old	
MDS model surfaces	**Perceived similarity**	**18**	**201**	**20 women 21-32 years old**	**IV[189]**
MDS printing paper	Perceived similarity	21	289	20 women 20-37 years old	III[188]
MDS tissue paper	Perceived Similarity	17	200	20 women 19-41 years old	

*per participant

Figure 6.1 *Photograph of one of the participants, estimating perceived coarseness on printing papers.*

6.1   Magnitude estimation

Scaling of perceptual attributes was performed using magnitude estimation.[101] Participants assigned numbers that corresponded to their perceived relative quantities of various perceptual attributes.[6] No modulus was defined, and the participants were allowed to set their own scale relative to the first stimulus presented.[101] Higher perceived quantity corresponds to a higher number. If a stimulus was assigned the number of "20" and the next stimulus was perceived twice as much, the number assigned should be "40". Conversely, a stimulus perceived as half of the quantity of "20" would get a number of "10". The stimuli were presented in random orders, with 6 or 7 repetitions per stimulus. The participants and perceptual attributes for each experiment are summarized in **Table 6.1**. The average scale values were calculated as geometric means (*eq. 6.1*). Before this calculation, the scale values of each participant were transformed to control for interindividual differences in the use of numbers in their own numerical scale. The grand mean of every participant's set of scale values was set equal to the grand mean of all participants scale values by multiplying each set of the individual scale values for a stimulus with the necessary factor. The geometric means of the normalized estimates were then obtained from the following equation:

$$Geometric\ mean\ =\ exp\left[\frac{1}{n}\sum_1^i ln\ x_i\right] \tag{6.1}$$

where x is the magnitude estimates of perceived quantities and n is the number of estimations.

53

6.2 Unidimensional psychophysical relationships

The role of texture in surface feel of printing papers is illustrated by four psychophysical relationships in **Figure 6.2**, where surface roughness, R_a, constitutes the common physical measure. The four perceptual scales compared are smoothness, coarseness, coolness and dryness. In the four diagrams, the fit of curves have been done merely as a guide to the eye. It appears that all the four perceptual quantities are related to the actual contact between the finger and the paper surface. The "physically smoothest" papers, *i.e.* those with the lowest R_a-value, were also perceived as "perceptually smoothest" (**Figure 6.2**A), associated with that no asperities was felt on the surface. In contrast, the "physically roughest" papers (highest R_a-value) were perceived as coarser (**Figure 6.2**B). The greater values for perceived smoothness (up to 120) as compared to perceived coarseness (up to 15) indicate that surfaces of printing papers are indeed smooth, rather than coarse. Smoothness and roughness have normally been considered as opposites perceptually, but the different scales obtained here for smoothness and coarseness (viewed as perceptual synonym to roughness), indicate that these two attributes are not bipolar, but rather two separate, but reversely associated, and strongly complimentary perceptual scales. Moreover, "physically smoother" papers were also perceived as cooler, see **Figure 6.2**C. A larger real contact area with more contact points allows a higher heat transfer rate from the fingers, which will result in a cooler perception. Finally, the "physically smoother" printing papers were also perceived as lower in dryness (**Figure 6.2**D). In this case it may be speculated that a higher real contact area provides an increased ability to wick moisture away from the finger, which would result in a less dry perception. The relationships presented above between perceptual attributes and average surface roughness (R_a), indicate that R_a is a relevant measure of surface roughness for irregularly rough surfaces like printing paper.

If surface roughness were to be measured on a set of newly designed printing papers, it would be possible to estimate their relative quantities of the perceptual attributes of smoothness, coarseness, coolness and dryness, based solely on the physical measure of R_a.
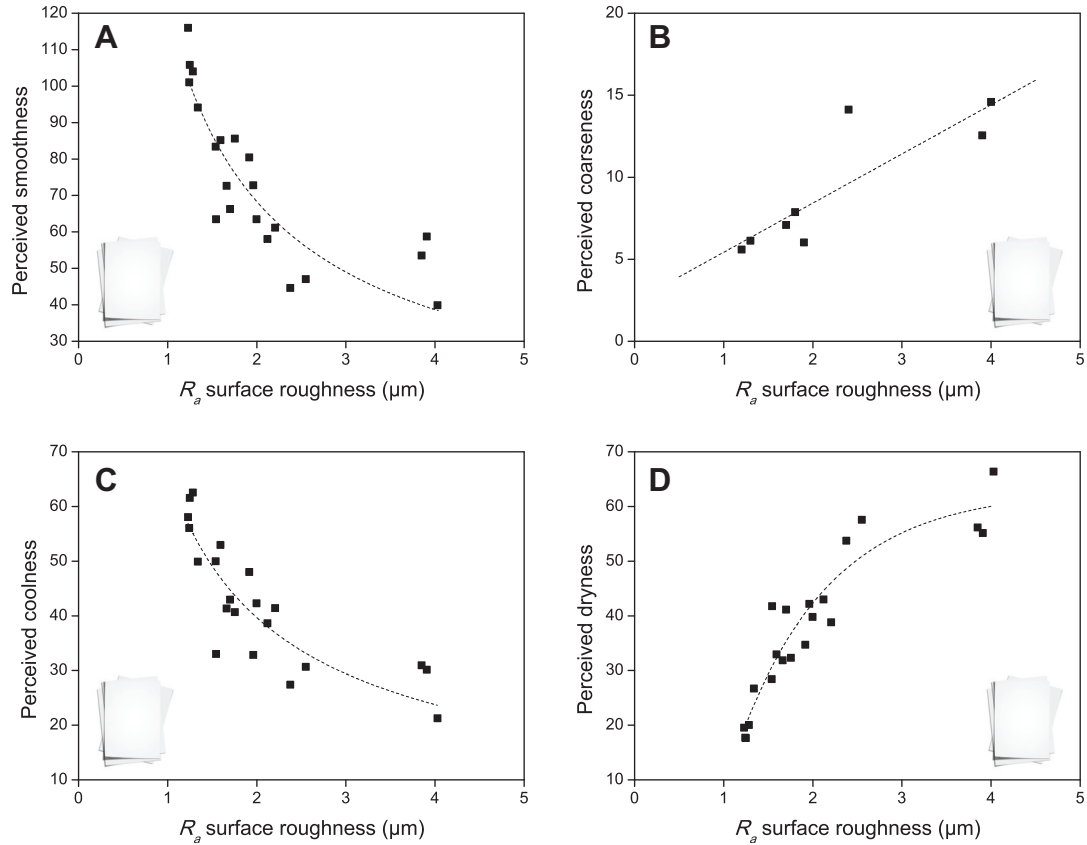
Figure 6.2 *Psychophysical relations on printing papers between magnitude estimates; smoothness (**A**), coarseness (**B**), coolness (**C**) and dryness (**D**), and the physical measure of average surface roughness (R$_a$) The fitted power functions and linear fit are a guide for the eye.*

For tissue paper, no relationships between the measured perceptual attributes and texture (LENA-value) or finger friction could be established. However, the only stimulus sample of facial tissue paper (T6) was perceived as most smooth, and it displayed both the lowest finger friction coefficient and the highest LENA-value. Facial tissues are often treated with softeners or lotions, which might be the reason why this particular tissue sample differs from the other ones. The highest and significant (p<0.05) correlation was found between perceived bulkiness and basis weight (r=0.96), see **Figure 6.3**A. Please note that it was the Swedish concept "skrymmande", and not the English word "bulkiness" that was scaled. These two concepts may be understood somewhat differently as regards their meanings. The perception of softness is a fundamental quality parameter of tissue paper,[138] and high degrees of softness is the main characteristic strived for. In this study, perceived softness was inversely correlated with perceived bulkiness (r=0.93), as shown in **Figure 6.3**B. In addition, perceived softness decreases with increasing basis weight (r=-

0.85) and tensile stiffness (r=-0.83), but increases with the physical measure of "combined softness" (r=90) (**Figure 6.3**C), calculated according to *eq. 3.2* in Section 3.1.3, that combines tensile stiffness and surface softness (LENA).[106] This result once more demonstrate that the physical measure of softness (*eq. 3.2*)[106] in fact can be used to predict perceived softness of tissue paper.
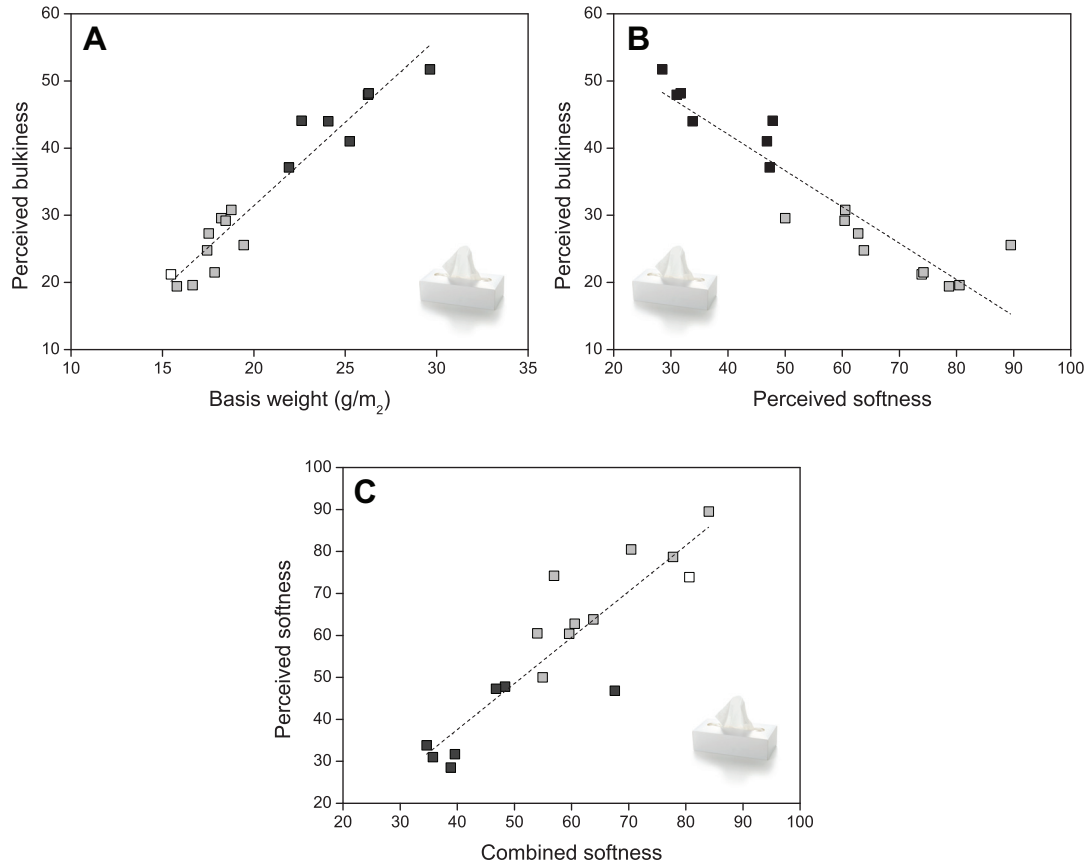

Figure 6.3 *Psychophysical relations between perceived bulkiness and basis weight (**A**) perceived softness and combined softness (**C**), and in (**B**), the relation between perceived bulkiness and perceived softness is shown. There is a distinct perceptual difference between absorbent tissue (black filled symbols) and bathroom tissue (grey filled symbols; the unfilled symbol represents facial tissue).*

6.3 Similarity scaling

Three experiments on MDS of similarity matrices have been performed and are summarized in **Table 6.1**. All possible pairs of stimuli, composed in a matrix, were compared as well as a number of test/retest pairs. The model surfaces were reused and cleaned with acetone and lint-free tissue after every comparison, whereas the paper sample of the printing and tissue papers were never re-used. The participants were blindfolded and scaled perceived similarities, between pairs of samples, from 0% (completely different) to 100% (identical). The experimental time was divided into 25-min sessions with small breaks for each participant. Perceived similarities (s) were organized in a matrix and transformed to dissimilarities (100 – s), so that surfaces perceived as similar would end up close to each other on the tactile map. The dissimilarity matrices were submitted to individual differences scaling (INDSCAL-program), a procedure that delivers a multidimensional solution "calibrated" for interindividual differences.[134,190]

Tactile maps were obtained by multidimensional scaling of the dissimilarity matrices. The number of relevant dimensions is first evaluated from the stress plot, where the stress or "goodness-of-fit" is plotted versus the number of dimensions. Stress values describe the degree of correspondence between the empirical interdistances and the interdistances in the MDS configuration; a stress value of zero means perfect fit. The stress plots for the three kinds of stimuli are shown in **Figure 6.4**: printing papers, model surfaces and tissue papers. As can be seen, the stress-plots are highly similar, and also resemble stress-plots in the scientific literature.[126,128] The rather high stress values obtained (they are generally lower than 0.15) in the three experiments depends on task difficulty due to the fact that surfaces of the same kind of material were evaluated. Normally, the number of dimensions at which an "elbow" occurs is considered relevant; however, such elbows are rarely that obvious. Therefore, dimensionality decisions should be supported by an intelligible interpretation of the organization of the stimuli in the map. In all three experiments, a two-dimensional and three-dimensional solution both appears to represent the dissimilarity data well.
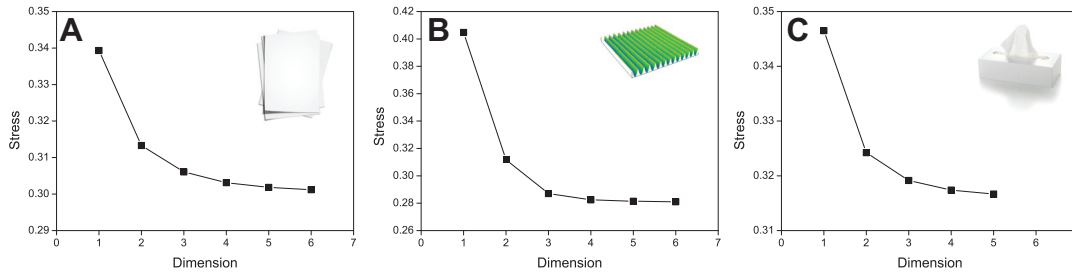
*Figure 6.4 Stress plots for the dissimilarity data of printing paper (**A**), model surfaces (**B**) and tissue paper (**C**). The three plots indicate either a two-dimensional or three-dimensional solution to all similarity data.*

To ensure reliability of individual similarity scales and concordance among the participant's similarity scales, test-retest reliability was determined. The average first set of scale values of similarity were compared to the average second set of scale values of similarity. In all three experiments, the test-retest reliability was good for the similarity matrices: r=0.98 for the printing papers (n=59), r=0.92 for the tissue papers (n=46) and r=0.91 for the model surfaces (n=48).

6.4 Tactile spaces and interpretation of underlying dimensions

The results regarding the printing papers are derived from Article III[188] and regarding the model surfaces from Article IV.[189] The tissue results are not yet summarized in a manuscript.

6.4.1 Rough/smooth and thin/thick dimensions of printing papers

The three-dimensional solution of INDSCAL was selected and interpreted for the printing papers, as presented in **Figure 6.5**. In this space, papers of the same paper grade end up close to each other, indicating that the participants were sensitive in discriminating between different grades of paper. Furthermore, a clear difference was perceived between the coated and the uncoated papers, and the SC-A papers with virgin fibers were perceived as more similar to the coated papers, whereas the SC-B papers with recycled fibers were perceived similarly to the uncoated papers. For all paper stimuli, the three-dimensional map looks like a "V", where one side is formed by the uncoated papers and the two rougher coated MFC papers. The other side of the "V" consists of the coated papers, from coated mechanical at the bottom up to the highly finished WFC papers at the top.
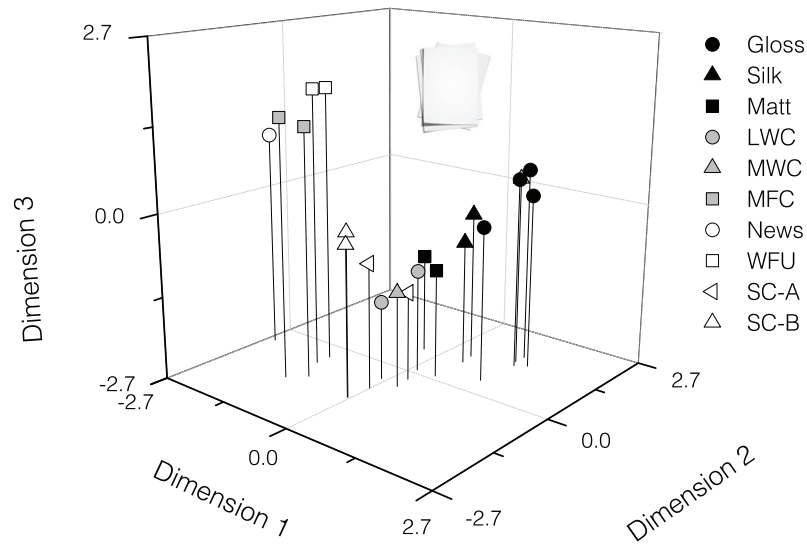
Figure 6.5 *Tactile map resembling perceived dissimilarities of the 21 printing papers. Article III[188]*

After a first screening of the distribution in the tactile map, measured physical properties, as well as measured unidimensional perceptual attributes, for the same stimuli, were rotated into the map. This was to search for the underlying dimensions of the tactile space, or to identify the paper properties that were used by the participants to feel differences.

Four physical properties (finger friction, R_a surfaces roughness, thermal conductivity and grammage, as well as four unidimensional perceptual scales (coolness, smoothness, thickness and dryness), were rotated into the three-dimensional tactile map of printing papers, using PREFMAP.[134] It should be noted that the physical properties obtained from paper standard tests were tested for as well, but these could not explain the spread of the paper samples in the tactile map (**Figure 6.5**). To increase the clarity of these results, the physical properties and perceptual attributes, contributing to the interpretation of the tactile map, are plotted separately in the two 2-dimensional planes of **Figure 6.6**. The positions of the physical and perceptual vectors suggest that dimension 1 is a smoothness/roughness dimension, in concordance with the interpretation of important tactile dimensions in the scientific literature.[126-129,132] Since smoothness, coolness, dryness and the physical measures of thermal conductivity, finger friction and R_a surface roughness are describing the spread of the data in dimension 1; it may be that this *rough/smooth* dimension is related to the real contact area upon haptically touching the paper surfaces, as

discussed in Section 6.2. Upon discriminating one physically rough paper from a smooth paper, perceived roughness, or the feeling of the asperities on the surfaces, appeared to be the important cue. However, in discriminating among the physically smooth papers, encountered friction, perceived smoothness or perceived coolness were used as cues. It may actually be the vibrations in the finger, because of haptic feeling, that allows papers to be distinguished from one another; thus, supporting the *duplex theory of texture perception* in that both a coarse sense (spatial sense) and vibratory sense are simultaneously involved in discrimination of printing-paper surfaces. This happened despite all the textures were much finer than what is generally considered as coarse textures.[120] Hence, the perception of what is rough and what is smooth seems to depend on the experimental context. Dimension 2, or the second underlying dimension in **Figure 6.5**, seems to be related to the grammage or thickness of the papers. The third dimension is interpreted as a distinctiveness dimension, originating from the highly distinguishable and recognizable paper surfaces that assumes high in this dimension.
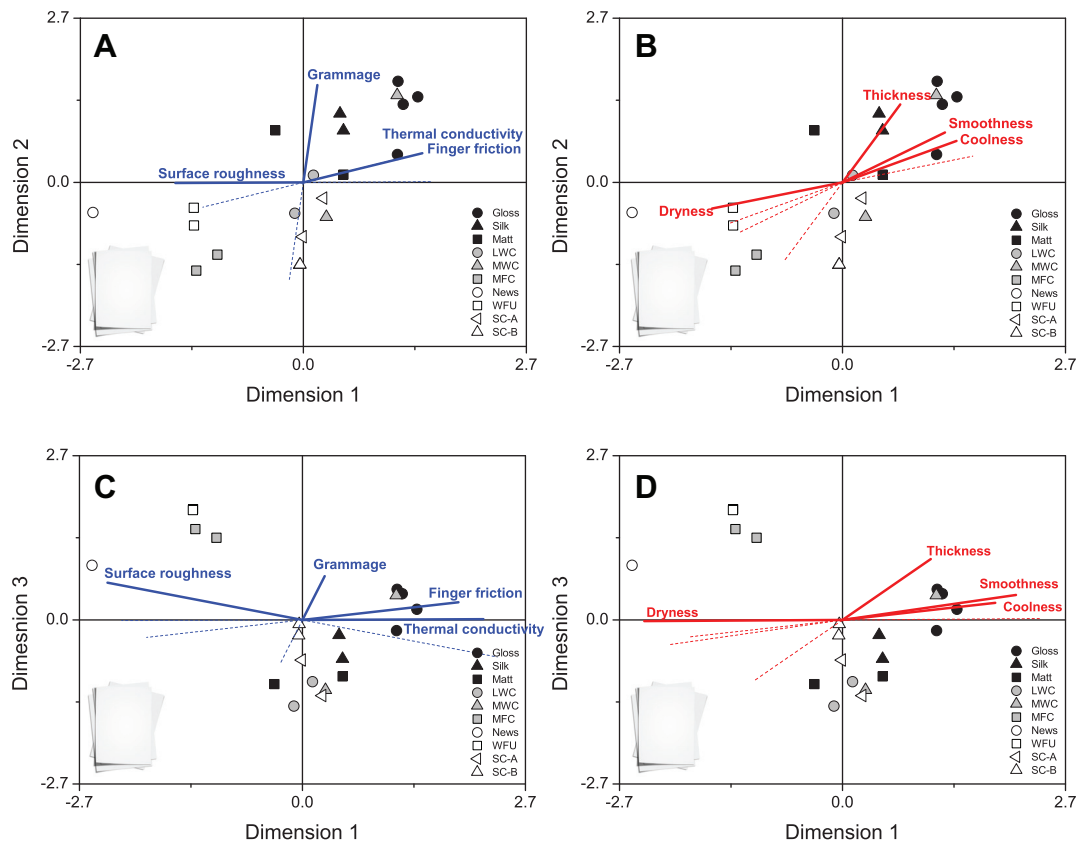

Figure 6.6 *Three-dimensional MDS solution presented as separated two-dimensional plots. Physical-property scales (in blue) and perceptual-attribute scales (in red) are rotated in the same space using PREFMAP. Article III[188]*

60

6.4.2 Surface discrimination possible at the nanometer scale

The most interesting finding, in the tactile map of the model surfaces (**Figure 6.7**A), is that the surface with 270 nm wavelength (WS1) was not distinguished from the blank surfaces, whereas those of 760 nm (WS2) and 870 nm (WS3) were. A "discrimination threshold" was thus indirectly obtained as a result by employing similarity scaling. This allowed exploration of the tactile perception limits *without* asking for a specific attribute, as is the case in more traditional threshold experiments.[119] The amplitude of the discriminated 760 nm surface was only 13 nm, showing that a human finger with its coarse structure is capable of dynamically detecting surface structures on the nanoscale.

As can be seen in **Figure 6.7**, the distribution of the model surfaces in the tactile map is highly reminiscent of the finger friction versus wavelength plot, suggesting that the participants use friction and wrinkle wavelength as the two main cues in their scaling of similarities.
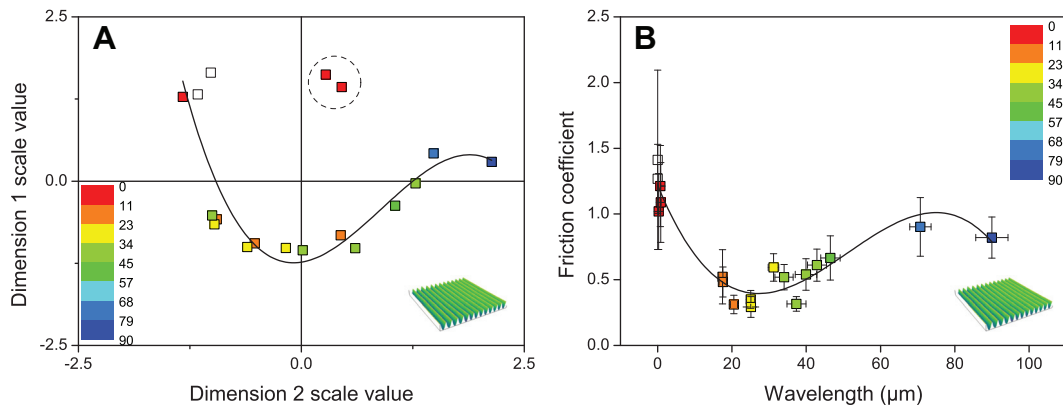

Figure 6.7 (A) Two-dimensional tactile space of perceived dissimilarities of 18 model surfaces. (B) Finger friction coefficient versus wrinkle wavelength. The color mapping is based on wrinkle wavelength from the smallest wavelength (red) to larger wavelengths (blue). The unfilled symbols are blank unwrinkled surfaces. The two surfaces within the circle are WS2 and WS3, showing that they are discriminated from the two blank surfaces as well as surface WS1.

To further interpret the two dimensions, dimension 1 is plotted versus the finger friction coefficient and dimensions 2 versus the wrinkle wavelength, as depicted in the two "psychophysical" plots in **Figure 6.8**. Sigmoid functions are fitted to these data which can be interpreted as two perceptual "sensor" regimes; one with high sensitivity (slope) and one with sensor saturation.
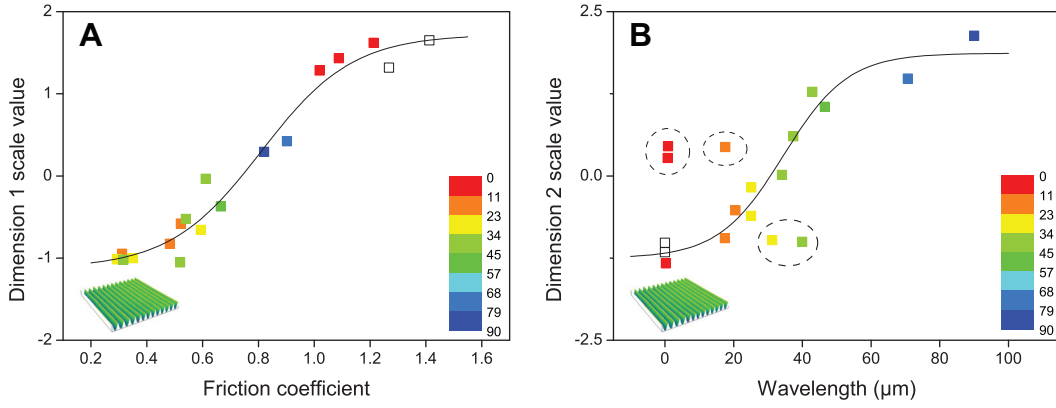
Figure 6.8 Comparison of perceptual dimensions and physical properties: (**A**) dimension 1 scale value versus friction coefficient and (**B**) dimension 2 scale value versus wrinkle wavelength. The fitted sigmoidal psychophysical functions are drawn as a guide for the eye (surfaces in circles are excluded from fitting).The color mapping is based on wrinkle wavelength, from the smallest wavelength (red) to larger wavelengths (blue). The unfilled symbols are blank unwrinkled surfaces.

In **Figure 6.8**A, the sensitivity is suggested to be determined from the loading range that can be applied during probing. Assuming the existence of an optimal friction force as reported in Section 5.5, the friction coefficients of 0.2 and 1.6 which correspond to sensor saturation, equate to applied loads of 2 N and 0.3 N, respectively. The lower load corresponds to roughly the minimum force required to maintain contact between surface and finger during sliding. The higher load corresponds to maximum deformation of the finger and to where the finger encounters difficulties to slide smoothly over the surface due to resultant stick-slip phenomena. Further, dimension 1 is suggested to be associated with the slow-adapting mechanoreceptors.

In contrast, the human sensor of dimension 2 appears to be associated with the fast-adapting mechanoreceptors. The finger surface will be struck by the top of a wrinkle with a frequency given by $f = v/\lambda$, where v is the probing speed and λ the wrinkle wavelength. Taking a wrinkle wavelength where the sensor appears optimized (40 μm), and assuming a sliding speed of 10 mm/s, the resulting frequency is 250 Hz; this value corresponds to the optimal haptic sensing of vibration frequency of the Pacinian Corpuscles, involved in fine texture perception.[95,191] Thus, wrinkle wavelengths of the order of tens of microns are optimal for exciting vibrations close to this optimal frequency and the possibility of varying the finger speed extends the sensitivity range (and likely also contributes to scatter). Regarding the larger or smaller wavelengths, closer to the "saturation levels", the discrimination based on vibrations excited in the finger seems unlikely.

6.4.3 Softness important perceptual attribute for tissue paper

Both the two-dimensional and three-dimensional solutions of the multidimensional scaling of the perceived similarities among tissue papers are shown in **Figure 6.9**. As can be seen, there is a distinct perceptual difference between the bathroom tissue and absorbent tissue papers, where these two groups are located on two opposite sides in the tactile map. The main dimension 1 represents well perceptual softness. The three tissue samples (T3, T8 and T11) that were produced with TAD (through-air-drying) and the embossed tissue sample (T5) are low in dimension 3. This suggests that the participants were also sensitive to differences in TAD-paper and tissue produced with traditional drying steps accomplished by a Yankee cylinder. The three TAD papers are the three thickest papers in mm (caliper) in the experimental set of tissue samples. Dimension 2 is weakly correlated with perceived smoothness (r=0.51), and therefore, it is suggested that for tissue paper, the main dimension 1 is softness, usually called "bulk softness" within industry, and the second dimension is more close "surface softness". Obviously these two kinds of softness are differentiated by the haptic procedure used: that is to feel by crumpling the sample in the hands of feel by surface stroking (against a flat background). The third dimension is interpreted as a thickness dimension, which may correspond to the English concept of bulkiness, since the TAD process gives bulkier tissue papers.
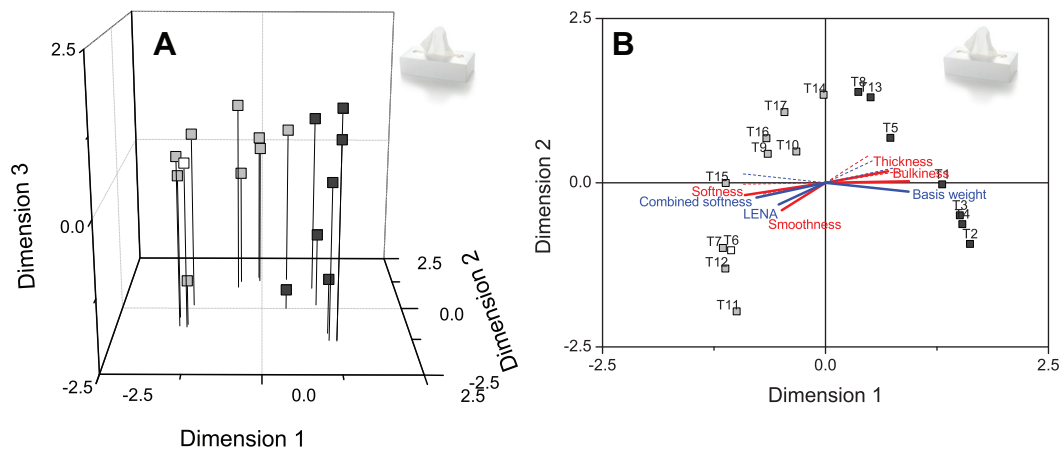

Figure 6.9 *Three-dimensional (**A**) and two-dimensional (**B**) tactile maps obtained from perceived dissimilarities of 17 tissue papers. Physical properties and perceptual attributes are rotated and fitted to the data in the same multidimensional space, using PREFMAP. There is a distinct perceptual difference between absorbent tissue (black filled symbols) and bathroom tissue (grey filled symbols; the unfilled symbol represents facial tissue).*

7 Conclusions

The main aim of this thesis was to investigate the role of friction and texture in tactile perception of printing papers, tissue papers and model surfaces. The interdisciplinary approach was to combine physical measurements with perception measurements to identify perceptual dimensions in the tactile space: the long term view is to be able to deliver tactile perception on material surfaces. The major findings within this PhD thesis are summarized as follows:

- Surface wrinkling can be used to fabricate robust, cleanable textured-surfaces, ranging from nanoscale to microscale, allowing the surfaces to be reused.

- A tactile approach to measure finger friction has been established, and differences in friction coefficients were obtained among the model surfaces and the printing papers, but not among the tissue papers.

- On fine-textured surfaces with an average surface roughness of at least 6 μm, like the printing papers and the model surfaces, the friction coefficient increases with the real contact area at the finger-surface interface. A larger real contact area allows more interfacial adhesion and consequently higher friction.

- The real contact area also seems important in tactile perception of the printing papers, for which the perceptual attributes of smoothness, coarseness, coolness and dryness are systematically related to the average surface roughness (R_q). It is, thus, possible to predict relative quantities of each of these four perceptual attributes based solely on the physical measure of surface roughness.

- The contact area adhesion effect most probably also explains why only small distinctions in the finger friction coefficients are obtained for the coarse-textured tissue papers. However, differences may be obtained upon measuring finger friction on various surface treated tissue papers, like the facial tissue sample in this thesis work, due to different lubricating properties.

- Both friction and texture appear to be important physical properties used to differentiate the surface perceptions, as shown directly for the model surfaces and through the rough/smooth dimension for the printing papers, where all physical-property and perceptual-attribute scales, related to the real contact area, described the spread of data.

Thus, friction and texture are important for tactile differentiation of the fine-textured surfaces, but for roughness larger than about 10 μm, friction is no longer used as cue for discrimination.

- In order to change or deliver specific tactile perceptions to surface feel, much can be achieved by changing the texture on at least fine-textured surfaces.

- We find that both a spatial sense and a vibration sense are used in distinguishing between surfaces in tactile perception. The spatial sense is used to distinguish the roughest textures from the others, whereas the vibration sense is used to distinguish among the smoother textures. What is considered rough and smooth depends on the experimental context.

- For tissue, softness appeared to be the most important dimension. Perceived softness is associated with the physical measure of softness that combines the measures of tensile stiffness and surface smoothness. Thus, relative quantities of perceived softness for a new set of tissue papers can be estimated from these two physical measures.

- Lipids are transferred from the finger to the surface during interrogation and work as a lubricant and lower friction, mainly on the first couple of strokes. Again the real contact area seems important, since the physically smoother papers show a greater decrease during the finger friction measurements, allowing more lipids to be transferred.

- A characteristic frequency of 30 Hz was identified in the friction force; it corresponds both to the resonance frequency of the skin and the frequency expected if considering the fingerprint structure.

- If friction coefficients are compared among a set of surfaces, average friction coefficients from single individuals are representative of a larger population; however, the interindividual variation is large and comparison of the friction coefficients obtained from different individuals should therefore be avoided.

- Although perceived pleasantness was not measured in this thesis, it is suggested that the most preferable and pleasant surface to touch is not the smoothest one; this suggestion is based on the result that smoother surfaces that were perceived cooler, displayed higher friction and stick-slip to a greater extent than less smooth surfaces.

- The applied load in surface interrogation is unconsciously regulated in response to the friction force. There appears to be an optimal friction force around 0.4 N that allows the human finger to smoothly slide on the surface.

- It is possible to measure differences in moisture content of hydrated model skin. The friction coefficient decreases as moisture is evaporated from the model skin.

- Different liquid crystalline phases show differences in tactile friction, where a cubic phase (sticky feel) show highest friction, followed by a reversed hexagonal phase (greasy feel) and a lamellar phase (soft feel). Transitions from one phase to another because of water evaporation can be followed with the friction measurements.

- Last but not least, the amplitude of the wrinkles that could be differentiated from unwrinkled blank surfaces was approximately 10 nm, demonstrating that human tactile discrimination extends into the nanoscale, and that nanotechnology may well have a role to play in haptics and tactile perception.

8 Future work

One aim of this perception delivery project was to understand tactile perception in terms of measurable physical properties, and preferably be able to use these identified physical measures to estimate tactile feel. In this thesis work, psychophysical relationships on the printing papers between perceived attributes; smoothness, coarseness, coolness and dryness, and surface roughness have been established. It would be interesting to take a set of new developed or designed papers, and from the roughness measures estimate the ranking of the different papers by means of perceived smoothness, coarseness, coolness and dryness. These estimated rankings could then be compared with perceived rankings performed by participants on the same set of papers to see if the rankings based on the physical measures and perception data correspond. To me, this is really what these psychophysical models or relationships can be used for within industry, especially in early stage development, when screening new-developed products. In the same way, softness perceptions of new developed tissue paper could be evaluated based on physical measures of tensile stiffness and surface softness.

It is speculated in this thesis that the smoothest textures which allow a greater real contact area are maybe not the most pleasant and preferable ones to touch. This assumption is based on that the smoother surfaces are perceived as cooler, display higher friction and occurrence of stick-slip, as well as more bandwidth in the amplitude spectrum when analyzing the frequency content in the friction force. It would be interesting to measure exactly which surface textures and friction responses that are preferred and comfortable to touch. Of course the optimum texture depends on what the product is, but it would be possible to make educated guesses as to which textures to aim for to maximize a positive tactile feel. Again, preference scaling could be used, in combination with simultaneous finger friction measurements to see exactly how the friction response relates to preferences.

In the same way as the physical properties and perceptual attributes have been rotated into the established tactile maps, preferences could be mapped as well. The vector of preferences would then tell towards which direction of samples and physical properties and psychological attributes that people prefer. The aim of the paper industry and tissue industry may be to design a new paper, beyond what exists on the market today, aiming for manipulating physical properties towards the direction of the preference factor.

Since we conclude that both a spatial sense and a vibration sense are used to distinguish surfaces from one another, it would be interesting to actually measure the vibrations induced upon interrogation with all stimuli investigate in this thesis, using for example an accelerometer.[96] To study how vibrations in the finger relate to the oscillations in the friction force as well as the surface texture could provide a deeper understanding of the human interaction with surfaces.

Some preliminary studies measuring macroscopic adhesion have been made, considering adhesion as the negative load during pull-up of the finger on the force sensor. The correspondence between adhesion force and perceptions of for example stickiness of skin creams could be evaluated, as well as the correlation between finger friction and perceptions of spreadability, greasiness and skin softness. If there are correlations, finger friction measurements can be used as an objective method to measure perceptions associated with skin cream application and function.

The effect of surface chemistry has not been addressed in this thesis other than that the effect of surface chemistry of the printing papers could not be completely ruled out, and the topical formulations with different liquid crystalline phases. It would be worthwhile studying the role of surface chemistry in both tactile friction and perception. A simple start might be to use surfaces such as those in Article VI which are either hydrophilic or hydrophobic.

Friction showed to be important upon discriminating tactile feel of fine-textured surfaces. It would be interesting to see how much the friction response varies with different relative humidity, which may imply that tactile perception and preferences of surface textures vary depending on the country you live.

9 Acknowledgements

First, I would like to express my greatest gratitude to my supervisor *Mark Rutland* and former co-supervisor *Katrin Danerlöv*. Your different qualifications really complemented each other, making me feel completely satisfied with the supervision. Thank you for taking on me in this interesting and challenging project and for allowing me to work independently. *Mark*, thanks for all inspiration and efforts (speciellt när det brann i knutarna) during these four years and *Katrin*, although Mark and I made a great team on our own when you decided to change career, we have really missed you!

An enormous appreciation goes to "my" psychologists, *Martin Arvidsson* and *Birgitta Berglund*, at the Department of Psychology at Stockholm University. Thanks for introducing me in the field of psychophysics. It has been a privilege to collaborate with you! *Birgitta*, a huge thank you for proof-reading parts of this thesis!

Thanks to *Ulf Olofsson* for being the co-supervisor after my maternity leave and for making me feel welcome in the corridors at Machine Design and allowing me to use the Kistler sensor to measure finger friction.

All people within *CODIRECT* are acknowledged for contributing to an interesting and pleasant forum to work in. Special thanks to *Ulla Elofsson* and *Mikael Kjellin* for managing the Centre, and to the industrial partner representatives *John Kettle* and *Maiju Aikala* from KCL and *Arne Andersson* at Eka Chemicals. It was really nice working with you!

I also extend my thanks to *Jun Chung Young* and *Christopher Stafford* at the National Institute of Standards and Technology (NIST) in Washington DC for hosting me during two effective weeks in April 2010. The surfaces you helped me fabricate have been like my babies.

10 References

1. Grunwald, M. *Human Haptic Perception: Basics and Applications.* Birkhäuser Basel, 2008.
2. Dahiya, R. S., Metta, G., Cannata, G. and Valle, M. Guest Editorial special issue on robotic sense of touch. *Ieee Transactions on Robotics* **2011**, 27(3), 385-388.
3. Chen, X., Shao, F., Barnes, C., Childs, T. and Henson, B. Exploring Relationships between Touch Perception and Surface Physical Properties. *International Journal of Design* **2009**, 3(2), 67-76.
4. Barnes, C. J., Childs, T. H. C., Henson, B. and Southee, C. H. Surface finish and touch - a case study in a new human factors tribology. *Wear* **2004**, 257(7-8), 740-750.
5. Childs, T. H. C. and Henson, B. Human tactile perception of screen-printed surfaces: self-report and contact mechanics experiments. *Proceedings Of The Institution Of Mechanical Engineers Part J-Journal Of Engineering Tribology* **2007**, 221(J3), 427-441.
6. Guest, S. *et al.* . The development and validation of sensory and emotional scales of touch perception. *Attention Perception & Psychophysics* **2011**, 73(2), 531-550.
7. Nagamachi, M. Kansei engineering - a new ergonomic consumer-oriented technology for product development. *International Journal Of Industrial Ergonomics* **1995**, 15(1), 3-11.
8. Hutchings, I. M. *Tribology: friction and wear of engineering materials.* Edward Arnold, 1992.
9. Jacobson, S., Hogmark, S. and Karlebo. *Tribologi: friktion, smörjning och nötning.* Liber Utbildning, 1996.
10. Dai, X. Q., Li, Y., Zhang, M. and Cheung, J. T. M. Effect of sock on biomechanical responses of foot during walking. *Clinical Biomechanics* **2006**, 21(3), 314-321.
11. Hamrock, B. J., Schmid, S. R. and Jacobson, B. O. *Fundamentals of Fluid Film Lubrication.* Taylor & Francis, 2004.
12. Dowson, D. A tribological day. *Proceedings Of The Institution Of Mechanical Engineers Part J-Journal Of Engineering Tribology* **2009**, 223(J3), 261-273.
13. Dowson, D. Bio-tribology. *Faraday Discussions* **2012**, 156, 9-30.
14. Dowson, D. New joints for the Millennium: wear control in total replacement hip joints. *Proceedings of the Institution of Mechanical Engineers Part H-Journal of Engineering in Medicine* **2001**, 215(H4), 335-358.
15. Holly, F. J. and Holly, T. F. Advances in ocular tribology. *Advances in Experimental Medicine and Biology* **1994**, 350, 275-283.
16. Mizuno, H., Luengo, G. S. and Rutland, M. W. Interactions between Crossed Hair Fibers at the Nanoscale. *Langmuir* **2010**, 26(24), 18909-18915.
17. Bhushan, B., Wei, G. H. and Haddad, P. Friction and wear studies of human hair and skin. *Wear* **2005**, 259, 1012-1021.
18. Bhushan, B. Nanotribological and nanomechanical properties of skin with and without cream treatment using atomic force microscopy and nanoindentation. *Journal of Colloid and Interface Science* **2012**, 367(1), 1-33.
19. Sivamani, R. K., Wu, G. C., Gitis, N. V. and Maibach, H. I. Tribological testing of skin products: Gender, age, and ethnicity on the volar forearm. *Skin Research And Technology* **2003**, 9(4), 299-305.
20. Derler, S. and Gerhardt, L. C. Tribology of skin: Review and analysis of experimental results for the friction coefficient of human skin. *Tribology Letters* **2011**, 1-27.
21. Pasumarty, S. M., Johnson, S. A., Watson, S. A. and Adams, M. J. Friction of the Human Finger Pad: Influence of Moisture, Occlusion and Velocity. *Tribology Letters* **2011**, 44(2), 117-137.
22. Adams, M. J., Briscoe, B. J. and Johnson, S. A. Friction and lubrication of human skin. *Tribology Letters* **2007**, 26(3), 239-253.
23. Gitis, N. and Sivamani, R. Tribometrology of skin. *Tribology Transactions* **2004**, 47(4), 461-469.
24. Comaish, S. and Bottoms, E. The skin and friction: deviations from Amonton´s law, and the effects if hydration and lubrication. *British Journal of Dermatology* **1971**, 81(1), 37-43.
25. El-Shimi, A. In vivo skin friction measurements. *Journal of the Society of Cosmetic Chemists* **1977**, 28, 37-51.
26. Koudine, A. A., Barquins, M., Anthoine, P. H., Aubert, L. and Lévêque, J. L. Frictional properties of skin: Proposal of a new approach. *International Journal of Cosmetic Science* **2000**, 22(1), 11-20.
27. Pailler-Mattei, C. and Zahouani, H. Study of adhesion forces and mechanical properties of human skin in vivo. *Journal of Adhesion Science and Technology* **2004**, 18(15-16), 1739-1758.

28.   Bowden, F. P. and Tabor, D. *Friction and lubrication of solids*. Oxford University Press 1954.

29.   Dowson, D. in *Bioengineering of the skin: skin surface imaging and analysis* (eds Klaus-Peter Wilhelm *et al.*) CRC Press, Boca Raton, 1997.

30.   Greenwood, J. A. and Tabor, D. The friction of hard sliders on lubricated rubber: The importance of deformation losses. *Proceedings of the Physical Society* **1958**, 71(6), 989-1001.

31.   Wolfram, L. J. Friction of skin. *Journal of the Society of Cosmetic Chemists* **1983**, 34(8), 465-476.

32.   Kwiatkowska, M., Franklin, S. E., Hendriks, C. P. and Kwiatkowski, K. Friction and deformation behaviour of human skin. *Wear* **2009**, 267(5-8), 1264-1273.

33.   Derler, S., Gerhardt, L. C., Lenz, A., Bertaux, E. and Hadad, M. Friction of human skin against smooth and rough glass as a function of the contact pressure. *Tribology International* **2009**, 42(11-12), 1565.

34.   Dinc, O. S., Ettles, C. M., Calabrese, S. J. and Scarton, H. A. Some parameters affecting tactile friction *Journal of Tribology-Transactions of the Asme* **1991**, 113(3), 512-517.

35.   Masen, M. A. A systems based experimental approach to tactile friction. *Journal of the Mechanical Behavior of Biomedical Materials* **2011**, 4(8), 1620-1626.

36.   Derler, S., Süess, J., Rao, A. and Rotaru, G. M. Influence of variations in the pressure distribution on the friction of the finger pad. *Tribology International*, Article in press, http://dx.doi.org/10.1016/j.triboint.2012.1003.1001.

37.   Tomlinson, S. E., Lewis, R. and Carre, M. J. The effect of normal force and roughness on friction in human finger contact. *Wear* **2009**, 267, 1311-1318.

38.   Tomlinson, S. E., Lewis, R. and Carré, M. J. Review of the frictional properties of finger-object contact when gripping. *Proceedings Of The Institution Of Mechanical Engineers Part J-Journal Of Engineering Tribology* **2007**, 221(J8), 841-850.

39.   Sivamani, R. K., Goodman, J., Gitis, N. V. and Maibach, H. I. Coefficient of friction: tribological studies in man - an overview. *Skin Research And Technology* **2003**, 9(3), 227-234.

40.   Veijgen, N. K., Masen, M. A. and Van Der Heide, E. A novel approach to measuring the frictional behaviour of human skin in vivo. *Tribology International* **2012**, 54, 38-41.

41.   Cua, A. B., Wilhelm, K. P. and Maibach, H. I. Frictional properties of human skin: Relation to age, sex and anatomical region, stratum corneum hydration and transepidermal water loss. *British Journal of Dermatology* **1990**, 123(4), 473-479.

42.   Asserin, J., Zahouani, H., Humbert, P., Couturaud, V. and Mougin, D. Measurement of the friction coefficient of the human skin in vivo - Quantification of the cutaneous smoothness. *Colloids And Surfaces B-Biointerfaces* **2000**, 19(1), 1-12.

43.   Elsner, P., Wilhelm, D. and Maibach, H. I. Frictional properties of human forearm and vulvar skin: Influence of age and correlation with transepidermal water loss and capacitance. *Dermatologica* **1990**, 181(2), 88-91.

44.   Loden, M., Olsson, H., Axell, T. and Werner Linde, Y. Friction, capacitance and transepidermal water loss (TEWL) in dry atopic and normal skin. *British Journal of Dermatology* **1992**, 126(2), 137-141.

45.   Naylor, P. F. The skin surface and friction. *The British journal of dermatology* **1955**, 67(7), 239-246.

46.   Highley, D. R., Coomey, M., DenBeste, M. and Wolfram, L. J. Frictional properties of skin. *Journal of Investigative Dermatology* **1977**, 69(3), 303-305.

47.   Prall, J. K. Instrumental evaluation of the effects of cosmetic products on skin surfaces with particular reference to smoothness. *Journal of the Society of Cosmetic Chemists of Japan* **1973**, 24(11), 693-707.

48.   Nacht, S., Close, J. A., Yeung, D. and Gans, E. H. Skin friction coefficient - changes induced by skin hydration and emollient application and correlation with perceived skin feel. *Journal of the Society of Cosmetic Chemists* **1981**, 32(2), 55-65.

49.   Loden, M., Olsson, H., Skare, L. and Axell, T. Instrumental and sensory evaluation of the frictional response of the skin following a single application of 5 moisturizing creams. *Journal of the Society of Cosmetic Chemists* **1992**, 43(1), 13-20.

50.   Lewis, R., Menardi, C., Yoxall, A. and Langley, J. Finger friction: Grip and opening packaging. *Wear* **2007**, 263, 1124-1132.

51.   Gee, M. G., Tomlins, P., Calver, A., Darling, R. H. and Rides, M. A new friction measurement system for the frictional component of touch. *Wear* **2005**, 259, 1437-1442.

52.   Gerhardt, L. C., Schiller, A., Muller, B., Spencer, N. D. and Derler, S. Fabrication, characterisation and tribological investigation of artificial skin surface lipid films. *Tribology Letters* **2009**, 34(2), 81-93.

53.   Derler, S., Schrade, U. and Gerhardt, L.-C. Tribology of human skin and mechanical skin equivalents in contact with textiles. *Wear* **2007**, 263, 1112-1116.

54.   Chen, X., Barnes, C. J., Childs, T. H. C., Henson, B. and Shao, F. Materials' tactile testing and characterisation for consumer products' affective packaging design. *Materials & Design* **2009**, 30(10), 4299-4310.

55.   Darden, M. A. and Schwartz, C. J. Investigation of skin tribology and its effects on the tactile attributes of polymer fabrics. *Wear* **2009**, 267, 1289-1294.

56.   Bobjer, O., Johansson, S. E. and Piguet, S. Friction between hand and handle - effects of oil and lard on textured and non-textured surfaces - perception of discomfort. *Applied Ergonomics* **1993**, 24(3), 190-202.

57.   Liu, X., Yue, Z., Cai, Z., Chetwynd, D. G. and Smith, S. T. Quantifying touch-feel perception: tribological aspects. *Measurement Science & Technology* **2008**, 19(8)

58.   Gerhardt, L.-C., Strassle, V., Lenz, A., Spencer, N. D. and Derler, S. Influence of epidermal hydration on the friction of human skin against textiles. *Journal Of The Royal Society Interface* **2008**, 5(28), 1317-1328.

59.   Gerhardt, L.-C., Lenz, A., Spencer, N. D., Münzer, T. and Derler, S. Skin-textile friction and skin elasticity in young and aged persons. *Skin Research And Technology* **2009**, 15(3), 288-298.

60.   Schreiner, S., Rechberger, M. and Bertling, J. Haptic perception of friction—correlating friction measurements of skin against polymer surfaces with subjective evaluations of the surfaces' grip. *Tribology International* **2012**, Article in press, 10.1016/j.triboint.2012.1008.1017.

61.   Carre, M. J., Tomlinson, S. E., Collins, J. W. and Lewis, R. An assessment of the performance of grip enhancing agents used in sports applications. *Proceedings Of The Institution Of Mechanical Engineers Part J-Journal Of Engineering Tribology* **2012**, 226(J7), 616-625.

62.   Fuss, F. K. and Troynikov, O. Anisotropic friction of rugby ball surfaces. *Proceedings Of The Institution Of Mechanical Engineers Part J-Journal Of Engineering Tribology* **2012**, 226(J7), 608-615.

63.   Cadoret, G. and Smith, A. M. Friction, not texture, dictates grip forces used during object manipulation. *Journal of Neurophysiology* **1996**, 75(5), 1963-1969.

64.   Westling, G. and Johansson, R. S. Responses in glabrous skin mechanoreceptors during precision grip in humans *Experimental Brain Research* **1987**, 66(1), 128-140.

65.   Burstedt, M. K. O., Flanagan, J. R. and Johansson, R. S. Control of grasp stability in humans under different frictional conditions during multidigit manipulation. *Journal of Neurophysiology* **1999**, 82(5), 2393-2405.

66.   Persson, B. N. J. Theory of rubber friction and contact mechanics. *Journal of Chemical Physics* **2001**, 115(8), 3840-3861.

67.   O'Meara, D. M. and Smith, R. M. Static friction properties between human palmar skin and five grabrail materials. *Ergonomics* **2001**, 44(11), 973-988.

68.   Hendriks, C. P. and Franklin, S. E. Influence of surface roughness, material and climate conditions on the friction of human skin. *Tribology Letters* **2010**, 37(2), 361-373.

69.   van Kuilenburg, J., Masen, M. A., Groenendijk, M. N. W., Bana, V. and van der Heide, E. An experimental study on the relation between surface texture and tactile friction. *Tribology International* **2012**, 48, 15-21.

70.   Tomlinson, S. E., Carre, M. J., Lewis, R. and Franklin, S. E. Human finger contact with small, triangular ridged surfaces. *Wear* **2011**, 271(9-10), 2346-2353.

71.   Tomlinson, S. E., Lewis, R., Liu, X., Texier, C. and Carre, M. J. Understanding the Friction Mechanisms Between the Human Finger and Flat Contacting Surfaces in Moist Conditions. *Tribology Letters* **2011**, 41(1), 283-294.

72.   Nonomura, Y. *et al.* . Tactile impression and friction of water on human skin. *Colloids And Surfaces B-Biointerfaces* **2009**, 69(2), 264-267.

73.   Andre, T., Lefevre, P. and Thonnard, J.-L. A continuous measure of fingertip friction during precision grip. *Journal Of Neuroscience Methods* **2009**, 179(2), 224-229.

74.   Buchholz, B., Frederick, L. J. and Armstrong, T. J. An investigation of human palmar skin friction and the effects of materials, pinch force and moisture *Ergonomics* **1988**, 31(3), 317-325.

75.   Liu, X., Lu, Z., Lewis, R., Carré, M. J. and Matcher, S. J. Feasibility of using optical coherence tomography to study the influence of skin structure on finger friction. *Tribology International* **2012**, Article in press, 10.1016/j.triboint.2012.1008.1020.

76.   Deleau, F., Mazuyer, D. and Koenen, A. Sliding friction at elastomer/glass contact: Influence of the wetting conditions and instability analysis. *Tribology International* **2009**, 42(1), 149-159.

77.   Forster, T. *Cosmetic Lipids and the Skin Barrier.* Vol. 24 Taylor & Francis, 2001.

78.   Iwai, I. *et al.* . The human akin barrier is organized as stacked bilayers of fully extended ceramides with cholesterol molecules associated with the ceramide sphingoid moiety. *Journal of Investigative Dermatology* **2012**, 132(9), 2215-2225.

79. Loden, M. Role of topical emollients and moisturizers in the treatment of dry skin barrier disorders. *American Journal of Clinical Dermatology* **2003**, 4(11), 771-788.

80. Knowles, A. M. Aspects of physicochemical methods for the detection of latent fingerprints. *Journal of Physics E: Scientific Instruments* **1978**, 11(8), 713-721.

81. Kucken, M. and Newell, A. C. Fingerprint formation. *Journal of Theoretical Biology* **2005**, 235(1), 71-83.

82. Maeno, T., Kobayashi, K. and Yamazaki, N. Relationship between the structure of human finger tissue and the location of tactile receptors. *Jsme International Journal Series C-Mechanical Systems Machine Elements and Manufacturing* **1998**, 41(1), 94-100.

83. Cartmill, M. The volar skin of primates: Its frictional characteristics and their functional significance. *American Journal of Physical Anthropology* **1979**, 50(4), 497-510.

84. Spurr, R. T. Fingertip friction *Wear* **1976**, 39(1), 167-171.

85. Warman, P. H. and Ennos, A. R. Fingerprints are unlikely to increase the friction of primate fingerpads. *Journal Of Experimental Biology* **2009**, 212(13), 2015-2021.

86. Wandersman, E., Candelier, R., Debrégeas, G. and Prevost, A. Texture-induced modulations of friction force: The fingerprint effect. *Physical Review Letters* **2011**, 107(16), 164301.

87. Mate, M. C. and Carpick, R. W. A sense for touch. *Nature* **2011**, 480(7376), 189-190.

88. Purves, D. *et al.* . *Neuroscience*. Second edition edn, Sinauer Associates, Inc, 2001.

89. Johansson, R. S. and Vallbo, A. B. Tactile sensory coding in the glabrous skin of the human hand *Trends In Neurosciences* **1983**, 6(1), 27-32.

90. Johnson, K. O. The roles and functions of cutaneous mechanoreceptors. *Current Opinion in Neurobiology* **2001**, 11(4), 455-461.

91. Vallbo, A. B. and Johansson, R. S. Properties of cutaneous mechanoreceptors in the human hand related to touch sensation *Human Neurobiology* **1984**, 3(1), 3-14.

92. Bruce, M. F. The realtion of tactile thresholds to histology in the fingers of elderly people *Journal of Neurology Neurosurgery and Psychiatry* **1980**, 43(8), 730-734.

93. Bruce, M. F. and Sinclair, D. C. The relationships between tactile thresholds and histology in the human finger. *Journal of Neurology Neurosurgery and Psychiatry* **1980**, 43(3), 235-242.

94. Johnson, K. O., Yoshioka, T. and Vega Bermudez, F. Tactile functions of mechanoreceptive afferents innervating the hand. *Journal of Clinical Neurophysiology* **2000**, 17(6), 539-558.

95. Bolanowski Jr, S. J., Gescheider, G. A., Verrillo, R. T. and Checkosky, C. M. Four channels mediate the mechanical aspects of touch. *Journal Of The Acoustical Society Of America* **1988**, 84(5), 1680-1694.

96. Fagiani, R., Massi, F., Chatelet, E., Berthier, Y. and Akay, A. Tactile perception by friction induced vibrations. *Tribology International* **2011**, 44(10), 1100-1110.

97. Lederman, S. J. and Klatzky, R. L. Haptic perception: A tutorial. *Attention Perception & Psychophysics* **2009**, 71(7), 1439-1459.

98. Hatwell, Y. *Touching for knowing. Cognitive psychology of haptic manual perception* John Benjamins Publishing Company, 2003.

99. Katz, D. The world of touch. *Edited and translated by Lester E. Krueger* **1989**(Lawrence Erlbaum Associates, Hillsdale, New Jersey), Original work published 1925.

100. Schiff, W. and Foulke, E. *Tactual Perception: A Sourcebook*. Cambridge University Press, 1982.

101. Gescheider, G. A. *Psychophysics: The fundamentals*. 3rd edn, Lawrence Erlbaum Associates, 1997.

102. Stevens, S. S. The direct estimation of sensory magnitudes-loudness. *The American journal of psychology* **1956**, 69(1), 1-25.

103. Berglund, B., Rossi, G. B. B., Townsend, J. T. T. and Pendrill, L. R. R. *Measurements with Persons*. Taylor & Francis, 2012.

104. Friedman, R. M., Hester, K. D., Green, B. G. and LaMotte, R. H. Magnitude estimation of softness. *Experimental Brain Research* **2008**, 191(2), 133-142.

105. Srinivasan, M. A. and Lamotte, R. H. Tactual discrimination of softness. *Journal of Neurophysiology* **1995**, 73(1), 88-101.

106. Hollmark, H. Evaluation Of Tissue Paper Softness. *Tappi Journal* **1983**, 66(2), 97-99.

107. Smith, A. M. and Scott, S. H. Subjective scaling of smooth surface friction. *Journal of Neurophysiology* **1996**, 75(5), 1957-1962.

108. Smith, A. M., Chapman, C. E., Deslandes, M., Langlais, J. S. and Thibodeau, M. P. Role of friction and tangential force variation in the subjective scaling of tactile roughness. *Experimental Brain Research* **2002**, 144(2), 211-223.

109. Lawrence, M. A., Kitada, R., Klatzky, R. L. and Lederman, S. J. Haptic roughness perception of linear gratings via bare finger or rigid probe. *Perception* **2007**, 36(4), 547-557.

110. Bergmann Tiest, W. M. and Kappers, A. M. L. Haptic and visual perception of roughness. *Acta psychologica* **2007**, 124(2), 177-189.

111. Klatzky, R. L., Lederman, S. and Reed, C. Haptic integration of object properties - texture, hardness, and planar contour. *Journal pf Experimental Psychology-Human Perception and Performance* **1989**, 15(1), 45-57.

112. Chapman, C. E., Tremblay, F., Jiang, W., Belingard, L. and Meftah, E. M. Central neural mechanisms contributing to the perception of tactile roughness. *Behavioural Brain Research* **2002**, 135(1-2), 225-233.

113. Ekman, G., Hosman, J. and Lindstrom, B. Roughness, smoothness, and preference: A study of quantitative relations in individual subjects. *Journal of Experimental Psychology* **1965**, 70(1), 18-26.

114. Lederman, S. J. Tactile roughness of grooved surfaces: The touching process and effects of macro- and microsurface structure. *Perception & Psychophysics* **1974**, 16(2), 385-395.

115. Taylor, M. M. and Lederman, S. J. Tactile Roughness Of Grooved Surfaces - Model And Effect Of Friction. *Perception & Psychophysics* **1975**, 17(1), 23-36.

116. Blake, D. T., Hsiao, S. S. and Johnson, K. O. Neural coding mechanisms in tactile pattern recognition: The relative contributions of slowly and rapidly adapting mechanoreceptors to perceived roughness. *Journal of Neuroscience* **1997**, 17(19), 7480-7489.

117. Connor, C. E., Hsiao, S. S., Phillips, J. R. and Johnson, K. O. Tactile roughness: Neural codes that account for psychophysical magnitude estimates. *Journal of Neuroscience* **1990**, 10(12), 3823-3836.

118. Connor, C. E. and Johnson, K. O. Neural coding of tactile texture: Comparison of spatial and temporal mechanisms for roughness perception. *Journal of Neuroscience* **1992**, 12(9), 3414-3426.

119. Miyaoka, T., Mano, T. and Ohka, M. Mechanisms of fine-surface-texture discrimination in human tactile sensation. *Journal Of The Acoustical Society Of America* **1999**, 105(4), 2485-2492.

120. Hollins, M. and Risner, S. R. Evidence for the duplex theory of tactile texture perception. *Perception & Psychophysics* **2000**, 62(4), 695-705.

121. Bensmaia, S. J. and Hollins, M. The vibrations of texture. *Somatosensory and Motor Research* **2003**, 20(1), 33-43.

122. Bensmaia, S. and Hollins, M. Pacinian representations of fine surface texture. *Perception & Psychophysics* **2005**, 67(5), 842-854.

123. Bensmaia, S., Hollins, M. and Yau, J. Vibrotactile intensity and frequency information in the Pacinian system: A psychophysical model. *Perception & Psychophysics* **2005**, 67(5), 828-841.

124. Craig, J. C. and Johnson, K. O. The two-point threshold: Not a measure of tactile spatial resolution. *Current Directions in Psychological Science* **2000**, 9(1), 29-32.

125. Lamotte, R. H. and Whitehouse, J. Tactile detection of a dot on a smooth surface - peripheral neural events *Journal of Neurophysiology* **1986**, 56(4), 1109-1128.

126. Picard, D., Dacremont, C., Valentin, D. and Giboreau, A. Perceptual dimensions of tactile textures. *Acta psychologica* **2003**, 114(2), 165-184.

127. Hollins, M., Faldowski, R., Rao, S. and Young, F. Perceptual dimensions of tactile surface texture - A multidimensional-scaling analysis. *Perception & Psychophysics* **1993**, 54(6), 697-705.

128. Bergmann Tiest, W. M. and Kappers, A. M. L. Analysis of haptic perception of materials by multidimensional scaling and physical measurements of roughness and compressibility. *Acta psychologica* **2006**, 121(1), 1-20.

129. Hollins, M., Bensmaia, S., Karlof, K. and Young, F. Individual differences in perceptual space for tactile textures: Evidence from multidimensional scaling. *Perception & Psychophysics* **2000**, 62(8), 1534-1544.

130. Lyne, M. B., Whiteman, A. and Donderi, D. C. Multidimensional-scaling of tissue quality. *Pulp & Paper-Canada* **1984**, 85(10), 43-50.

131. Yoshioka, T., Bensmaia, S. J., Craig, J. C. and Hsiao, S. S. Texture perception through direct and indirect touch: An analysis of perceptual space for tactile textures in two modes of exploration. *Somatosensory and Motor Research* **2007**, 24(1-2), 53-70.

132. Gescheider, G. A., Bolanowski, S. J., Greenfield, T. C. and Brunette, K. E. Perception of the tactile texture of raised-dot patterns: A multidimensional analysis. *Somatosensory and Motor Research* **2005**, 22(3), 127-140.

133. Soufflet, I., Calonnier, M. and Dacremont, C. A comparison between industrial experts' and novices' haptic perceptual organization: a tool to identify descriptors of the handle of fabrics. *Food Quality and Preference* **2004**, 15(7-8), 689-699.

134. Schiffman, S. S., Young, F. W. and Reynolds, M. L. *Introduction to multidimensional scaling: theory, methods, and applications* Academic Press 1981.

135. Borg, I. and Groenen, P. *Modern multidimensional scaling: Theory and applications.* Springer Verlag New York 1997.

136. Worldatlas. *http://www.worldatlas.com/travelaids/flight_distance.htm*.

137. Okamoto, S., Nagano, H. and Yamada, Y. Psychophysical Dimensions of Tactile Perception of Textures. *Haptics, IEEE Transactions on* **2012**, PP(99), 1-1.

138. Hollmark, H. and Ampulski, R. S. Measurement of tissue paper softness: A literature review. *Nordic Pulp & Paper Research Journal* **2004**, 19(3), 345-353.

139. Binnig, G., Quate, C. F. and Gerber, C. Atomic Force Microscope. *Physical Review Letters* **1986**, 56(9), 930-933.

140. Thomas, T. R. *Rough Surfaces.* Imperial College Press, 1999.

141. Gustafsson, S. E. Transient plane source techniques for thermal-conductivity and thermal-diffusivity measurements of solid materials. *Review Of Scientific Instruments* **1991**, 62(3), 797-804.

142. Hulten, A. H., Basta, J., Larsson, P. and Ernstsson, M. Comparison of different XPS methods for fiber surface analysis. *Holzforschung* **2006**, 60(1), 14-19.

143. Helgesson, M. http://www.forceboard.com.

144. Soneda, T. and Nakano, K. Investigation of vibrotactile sensation of human fingerpads by observation of contact zones. *Tribology International* **2010**, 43(1-2), 210-217.

145. Ulman, A. *An Introduction to Ultrathin Organic Films: From Langmuir-Blodgett to Self-Assembly.* Academic Press, 1991.

146. Chung, J. Y., Nolte, A. J. and Stafford, C. M. Surface wrinkling: A versatile platform for measuring thin-film properties. *Advanced Materials* **2011**, 23(3), 349-368.

147. Schweikart, A. and Fery, A. Controlled wrinkling as a novel method for the fabrication of patterned surfaces. *Microchimica Acta* **2009**, 165(3-4), 249-263.

148. Lee, Y. L., Du, Z. C., Lin, W. X. and Yang, Y. M. Monolayer behavior of silica particles at air/water interface: A comparison between chemical and physical modifications of surface. *Journal of Colloid and Interface Science* **2006**, 296(1), 233-241.

149. Tsai, P. S., Yang, Y. M. and Lee, Y. L. Fabrication of hydrophobic surfaces by coupling of Langmuir-Blodgett deposition and a self-assembled monolayer. *Langmuir* **2006**, 22(13), 5660-5665.

150. Hansson, P. M. *et al.* . Robust Hydrophobic Surfaces Displaying Different Surface Roughness Scales While Maintaining the Same Wettability. *Langmuir* **2011**, 27(13), 8153-8159.

151. Stafford, C. M. *et al.* . A buckling-based metrology for measuring the elastic moduli of polymeric thin films. *Nature Materials* **2004**, 3(8), 545-550.

152. Chung, J. Y., Youngblood, J. P. and Stafford, C. M. Anisotropic wetting on tunable micro-wrinkled surfaces. *Soft Matter* **2007**, 3(9), 1163-1169.

153. Bowden, N., Brittain, S., Evans, A. G., Hutchinson, J. W. and Whitesides, G. M. Spontaneous formation of ordered structures in thin films of metals supported on an elastomeric polymer. *Nature* **1998**, 393(6681), 146-149.

154. Stafford, C. M., Guo, S., Harrison, C. and Chiang, M. Y. M. Combinatorial and high-throughput measurements of the modulus of thin polymer films. *Review Of Scientific Instruments* **2005**, 76(6)

155. Stafford, C. M., Vogt, B. D., Harrison, C., Julthongpiput, D. and Huang, R. Elastic moduli of ultrathin amorphous polymer films. *Macromolecules* **2006**, 39(15), 5095-5099.

156. Wilder, E. A., Guo, S., Lin-Gibson, S., Fasolka, M. J. and Stafford, C. M. Measuring the modulus of soft polymer networks via a buckling-based metrology. *Macromolecules* **2006**, 39(12), 4138-4143.

157. Rand, C. J. and Crosby, A. J. Friction of soft elastomeric wrinkled surfaces. *Journal of Applied Physics* **2009**, 106(6), 064913.

158. Kim, Y. S., Lee, N. Y., Lim, J. R., Lee, M. J. and Park, S. Nanofeature-patterned polymer mold fabrication toward precisely defined nanostructure replication. *Chemistry of Materials* **2005**, 17(23), 5867-5870.

159. Chan, E. P., Smith, E. J., Hayward, R. C. and Crosby, A. J. Surface wrinkles for smart adhesion. *Advanced Materials* **2008**, 20(4), 711-716.

160. Bowden, N., Huck, W. T. S., Paul, K. E. and Whitesides, G. M. The controlled formation of ordered, sinusoidal structures by plasma oxidation of an elastomeric polymer. *Applied Physics Letters* **1999**, 75(17), 2557-2559.

161. Volynskii, A. L., Bazhenov, S., Lebedeva, O. V. and Bakeev, N. F. Mechanical buckling instability of thin coatings deposited on soft polymer substrates. *Journal of Materials Science* **2000**, 35(3), 547-554.

162. Huang, R. Kinetic wrinkling of an elastic film on a viscoelastic substrate. *Journal of the Mechanics and Physics of Solids* **2005**, 53(1), 63-89.

163. Chung, J. Y., Chastek, T. Q., Fasolka, M. J., Ro, H. W. and Stafford, C. M. Quantifying Residual Stress in Nanoscale Thin Polymer Films via Surface Wrinkling. *Acs Nano* **2009**, 3(4), 844-852.

164. Chung, J. Y., Lee, J.-H., Beers, K. L. and Stafford, C. M. Stiffness, Strength, and Ductility of Nanoscale Thin Films and Membranes: A Combined Wrinkling-Cracking Methodology. *Nano Letters* **2011**, 11(8), 3361-3365.

165. Skedung, L. *et al.* . Finger friction measurements on coated and uncoated printing papers. *Tribology Letters* **2010**, 37(2), 389-399.

166. Skedung, L. *et al.* . Tactile friction of controlled, fine surface textures: Mechanism of real contact area and adhesion. *Submitted* **2012**, October

167. Westergaard, H. M. Bearing pressures and cracks. *Journal of Applied Mechanics - Transactions of the ASME* **1939**, 6

168. Dandekar, K., Raju, B. I. and Srinivasan, M. A. 3-D finite-element models of human and monkey fingertips to investigate the mechanics of tactile sense. *Journal of Biomechanical Engineering-Transactions of the Asme* **2003**, 125(5), 682-691.

169. Raveh Tilleman, T., Tilleman, M. M. and Neumann, M. H. A. The elastic properties of cancerous skin: Poisson's ratio and Young's modulus. *Israel Medical Association Journal* **2004**, 6(12), 753-755.

170. Skedung, L. *et al.* . Tactile perception: Finger friction, surface roughness and perceived coarseness. *Tribology International* **2011**, 44(5), 505-512.

171. Johansson, A., Fellers, C., Gunderson, D. and Haugen, U. Paper friction - influence of measurement conditions. *Tappi Journal* **1998**, 81(5), 175-183.

172. Garoff, N., Fellers, C. and Nilvebrant, N. O. Friction hysteresis of paper. *Wear* **2004**, 256(1-2), 190-196.

173. Sato, J., de Silveira, G. and Hutchings, I. M. Measurement of the friction of paper by the strip-on-drum method. *Tribology International* **1997**, 30(9), 633-640.

174. Williams, D. K., Schwartz, R. L. and Bartick, E. G. Analysis of latent fingerprint deposits by infrared microspectroscopy. *Applied Spectroscopy* **2004**, 58(3), 313-316.

175. Clarys, P. and Barel, A. Quantitative evaluation of skin surface lipids. *Clinics in Dermatology* **1995**, 13(4), 307-321.

176. Day, J. S., Edwards, H. G. M., Dobrowski, S. A. and Voice, A. M. The detection of drugs of abuse in fingerprints using Raman spectroscopy I: latent fingerprints. *Spectrochimica Acta Part a-Molecular and Biomolecular Spectroscopy* **2004**, 60(3), 563-568.

177. Karlsson, D. and Tranberg, R. On skin movement artefact-resonant frequencies of skin markers attached to the leg. *Human Movement Science* **1999**, 18(5), 627-635.

178. Tang, W. and Bhushan, B. Adhesion, friction and wear characterization of skin and skin cream using atomic force microscope. *Colloids And Surfaces B-Biointerfaces* **2010**, 76(1), 1-15.

179. Tang, W., Bhushan, B. and Ge, S. Friction, adhesion and durability and influence of humidity on adhesion and surface charging of skin and various skin creams using atomic force microscopy. *Journal of Microscopy* **2010**, 239(2), 99-116.

180. Bhushan, B., Tang, W. and Ge, S. Nanomechanical characterization of skin and skin cream. *Journal of Microscopy* **2010**, 240(2), 135-144.

181. Wakefield, G. and Stott, J. Photostabilization of organic UV-absorbing and anti-oxidant cosmetic components in formulations containing micronized manganese-doped titanium oxide. *Journal of Cosmetic Science* **2006**, 57(5), 385-395.

182. Bhushan, B. and Tang, W. Surface, Tribological, and Mechanical Characterization of Synthetic Skins for Tribological Applications in Cosmetic Science. *Journal Of Applied Polymer Science* **2011**, 120(5), 2881-2890.

183. Turner, R. B. *et al.* . Efficacy of organic acids in hand cleansers for prevention of rhinovirus infections. *Antimicrobial Agents and Chemotherapy* **2004**, 48(7), 2595-2598.

184. Borne, J., Nylander, T. and Khan, A. Phase behavior and aggregate formation for the aqueous monoolein system mixed with sodium oleate and oleic acid. *Langmuir* **2001**, 17(25), 7742-7751.

185. Lopes, L. B. *et al.* . Reverse hexagonal phase nanodispersion of monoolein and oleic acid for topical delivery of peptides: in vitro and in vivo skin penetration of cyclosporin A. *Pharmaceutical Research* **2006**, 23(6), 1332-1342.

186. Shah, J. C., Sadhale, Y. and Chilukuri, D. M. Cubic phase gels as drug delivery systems. *Advanced Drug Delivery Reviews* **2001**, 47(2-3), 229-250.

187. Carr, M. G., Corish, J. and Corrigan, O. I. Drug delivery from a liquid crystalline base across Visking and human stratum corneum. *International Journal of Pharmaceutics* **1997**, 157(1), 35-42.

188. Arvidsson, M. *et al.* . Haptic perception of fine surface texture: Psychophysical interpretation of the multidimensional space. *Submitted to Attention, Perception and Psychophysics* **2012**, July

189. Skedung, L. *et al.* . Feeling small: Exploring the tactile perception limits. *Submitted* **2012**, October

190. Carroll, J. D. and Chang, J. J. Analysis of individual differences in multidimensional scaling via an n-way generalization of "Eckart-Young" decomposition. *Psychometrika* **1970**, 35(3), 283-319.

191. Makous, J. C., Friedman, R. M. and Vierck, C. J. A critical band filter in touch *Journal of Neuroscience* **1995**, 15(4), 2808-2818.